

154- 26008

CR. 171 789
c.2

DEVELOPMENT OF LIMB VOLUME MEASURING SYSTEM

by

Pramode K. Bhagat
Principal Investigator

Prasad K. Kadaba
Co-Investigator

Project Number - NAS9-15452 - Final Report
Project Period - November 1, 1977 - September 30, 1983

University of Kentucky
Wenner-Gren Biomedical Research Laboratory
Department of Mechanical Engineering
Lexington, Kentucky

October 1983

TABLE OF CONTENTS

Acknowledgements.....	i
Abstract.....	v
Introduction.....	1
Background.....	1
Plethysmography.....	1
Relationship of Orthostatic Tolerance to Limb volume changes.....	3
Requirements for a Space Qualified Plethysmograph.....	5
Ultrasonic Plethysmography.....	6
Single Chord Ultrasonic Plethysmograph.....	8
Two Chord Ultrasonic Limb Volume System.....	31
Ambulatory Ultrasonic Plethysmography.....	44
Transducer Development.....	50
Summary and Conclusions.....	66
Theses, Dissertations and Publications.....	67
Appendix A - Background Data on Transducers.....	70
Appendix B - Test Procedure and Results Using Prototype ULP..	81
Appendix C - Description of Individual Circuit Blocks of Two Transmitter ULVS.....	108
References.....	142

ACKNOWLEDGEMENTS

The development of ultrasonic plethysmography from a technical concept to a flight certified unit capable of measurements in space (zero G) environment has been the result of long term collaborative between the principal investigator and his associates with the National Aeronautic and Space Administration (NASA) personnel. This project was interdisciplinary in nature and required contributions from a variety of individuals.

NASA personnel with direct responsibility for technical monitoring of the project are gratefully acknowledged. In particular, Drs. Wayland Hull and Carter Alexander supported the initial development of the instrumentation detailed here. The continuous encouragement and long term support of Mr. Cletis Booher and his associates are sincerely appreciated.

The principal investigator is indebted to Dr. J. F. Lafferty, Director, Wenner-Gren Research Laboratory, for his continued support in terms of personnel, equipment and facilities for this project. The efforts of Mr. Tom Patrick, in the redesign and implementation of his pinger and receiver circuit electronics are gratefully acknowledged. It is a pleasure to acknowledge the assistance of Don Bowman, Charles Lewis, Dr. M. P. Kadaba, and Ms. Vicky Ruszczyk in the development and evaluation of the single transmitter ULVS. Ms. Cindy Green assisted in the development of two transmitter transducer holder.

Also acknowledged is the support of Dr. W. T. Nickell, Mark Shafer, Dave Brewer and Ms. Julie Skidmore in the development and evaluation of two transmitter ULVS.

The principal investigator is deeply indebted to the chief project engineer, Mr. V. C. Wu, for his participation in all phases of the reported work and his abilities to carry out all the needed tasks in a timely manner.

The assistance and support of the technical group at Denver Research Institute led by Whitney Patten towards the development of prototype flight certified ULVS is sincerely acknowledged.

LIST OF FIGURES

- Figure 1 - Schematic of Single Transmitter ULVS
- Figure 2 - System Timing and D/A Converter Schematic
- Figure 3 - Avalanche Pulse Generator (Pinger) Circuit
- Figure 4 - Ultrasonic Receiver Amplifier and Comparator
- Figure 5 - Static Measurements of Dimensional Changes on the Lower Leg Using ULVS
- Figure 6 - Cross Section View of Lower Limb at the Level of Plethysmograph Application
- Figure 7 - Schema of System for Inducing Venous Occlusion in Lower Limbs
- Figure 8 - Relative Placement of Ultrasonic Transducer and Whitney Strain Gauge
- Figure 9 - Photograph Showing Actual Locations of Ultrasonic Transducers and Whitney Strain Gauge
- Figure 10 - Calibration Curve for Whitney Strain Gauge as Recorded on Chart Recorder
- Figure 11 - Dynamic Comparison of Whitney Gauge and ULVS Measurements
- Figure 12 - Computation of Arterial Flow and Compliance Level
- Figure 13 - Correlation Between Initial Slope of Ultrasonic and Whitney Strain Gauge Plethysmograph
- Figure 14 - Average Initial Slopes (Ultrasound and Strain Gauge) as a Function of Cuff Pressure
- Figure 15 - Compliance Time Versus Cuff Pressure
- Figure 16 - Computation of Cross-Sectional Area from Two Chord Length Measurements
- Figure 17 - Two Transmitter ULVS
- Figure 18 - Block Diagram of ULVS Electronics
- Figure 19 - System Electrode Placement
- Figure 20 - Comparison of ULVS and Whitney Dimension Measurement Under Venous Occlusion
- Figure 21 - Design of Flat and Hemispherical Transducers

Figure 22 - Construction of Receiver and Transmitter Elements

Figure 23 - The Developed Ultrasonic Transducers

Figure 24 - Off Axis Performance of Transducers

Figure 25 - Directional Characteristics of Ultrasonic Transducers

Figure 26 - Comparison of Performance of Different Transducer Combinations

Figure 27 - Domain Alignment in Ferroelectric Materials

Figure 28 - The Ultrasonic Field of Circular Disk Transducer

Figure 29 - Data Collection and Analysis Block Diagram

Figure 30 - Mechanical System

Figure 31 - ULP Transducer Output Pulse Shape

Figure 32 - Digital Output in EDI Mode (2400 Baud)

Figure 33 - Output Pulse with 50 Ω Termination

Figure 34 - Amplitude Spectrum of the Output Pulse

Figure 35 - Pulse Shape with Transducer Load

Figure 36 - Tape Recorded Signal Played Back with 1K Load and Captured by Biomation A/D Converter

Figure 37 - Time Course of Dimension Changes Under 50 mm Hg Venous Occlusion Procedure

Figure 38 - Time Course of Limb Dimension Changes Under 50° Head Up Tilt

Figure 39 - ULP Data Played Back From the Recorded Venous Occlusion (50 mm Hg) Data

Figure 40 - Passive Monitoring of Data Through a Tilt Table Experiment

Figure 41 - Schematic of Processor and Memory for the Two Transmitter ULVS

Figure 42 - Schematic of Controller Logic, Transmitter Select and Counter for Two Transmitter ULVS

Figure 43 - Schematic of Power Supply Circuits Used in Two Transmitter ULVS

Figure 44 - Flow Graph of Software Implementation

Figure 45 - Subroutine "NOTYET"

ABSTRACT

The mechanisms underlying the reductions in orthostatic tolerance associated with weightlessness are not well established. Contradictory results from measurements of leg volume changes suggest that altered venomotor tone and reduced blood flow may not be the only contributors to orthostatic intolerance. It is felt that a more accurate limb volume system which is insensitive to environmental factors will aid in better quantification of the hemodynamics of the leg. Of the various limb volume techniques presently available, the ultrasonic limb volume system has proven to be the best choice. The system as described herein is free from environmental effects, safe, simple to operate and causes negligible radio frequency interference problems. The segmental ultrasonic plethysmograph is expected to provide a better measurement of limb volume change since it is based on cross sectional area measurements. Limb volume change is computed from the two cross-sectional areas measured at different sites (fixed length apart) using an equivalent right circular cylinder geometry. A space qualified version of our device has been built by Denver Research Institute and is expected to be used in a future space shuttle mission.

I. INTRODUCTION

The study and evaluation of cardiovascular deconditioning during space flight impose unique requirements on the limb volume measuring system (LVMS). The LVMS must operate, in both earth and zero gravity environments, be simple to calibrate and respond to both small and large changes in limb volume and be largely insensitive to humidity, ambient temperature and pressure variations.

The objective of this project was to develop a new technique for real time measurement of lower limb volume changes in space. The technique developed in this study, the ultrasonic plethysmograph, is based on transit time measurement of an acoustic pulse propagating through tissue. A microprocessor based ultrasonic lower limb volume measuring system was developed as a prototype system for use in space flight applications. It is based on the assumption that the cross section of the lower limb can be approximated by a circle. On this basis two independent chord length measurements using ultrasonic through transmission technique are made at a given site on the lower limb. This data is used by the microprocessor to compute the area of a circle passing through the measured chord lengths.

This report details the development of the ultrasonic limb volume measuring system in to a flight certified unit which is expected to be used in a future space flight mission.

II. Background

A. Plethysmography

Plethysmography is the recording of variations in the volume of a liquid or undissolved gas in biological tissue. Studies of

peripheral circulation have been carried out through a variety of methods which record/measure the volume of blood content in a limb (plethysmography).

The principle of plethysmography was first introduced by Glissonio (1677) who used water displacement for limb volume measurement (1). Variations of this method, some using air as the displaced fluid, are still used for the measurement of arterial flow into segments or distal portions of limbs. Another frequently used plethysmograph is the Whitney strain gage, introduced in 1953 (2). The Whitney, or mercury-in-rubber, strain gage is attached around the limb segment in question and any relative change in the electrical resistance of the strain gage is used as a measure of a change in circumference of that limb segment. The accuracy of this method of plethysmography was compared to that of water displacement plethysmography by Paulev, et al.(1). They found that "the accuracy of the water and strain-gage plethysmograph is identical, and the two instruments closely follow random variations in blood flow." However, they further state that "The results of the strain-gage plethysmograph are dependent on the actual location of the strain gage."

Other methods of plethysmography include impedance and capacitance plethysmography. Impedance plethysmography (rheography) makes use of the fact that the electrical impedance of a limb segment varies with its blood content. Capacitance plethysmography involves the use of the skin as one plate of a capacitor. An electrode attached to a band around the limb segment completes the capacitor. Assuming a purely radial expansion with increased limb volume, the change in capacitance between the skin and the electrode is proportional to the change in volume of the limb segment. These and

other currently used methods of plethysmography are discussed more thoroughly by Sigdell (3). A comparative analysis of their feasibility for space flight applications may be found in an earlier report from this laboratory (4).

B. Relationship of Orthostatic Tolerance to Limb Volume Changes

Reductions in orthostatic tolerance due to exposure to zero G environment were first reported during the late flights of Mercury when tilt table tests conducted post-flight revealed moderate orthostatic hypotension. These findings were also observed during the Gemini program (flight duration 3-14 days). However, responses to the 70 degree upright tilt usually returned to normal within fifty hours after splash down (5,6).

During the Apollo program (7), a new test procedure, lower body negative pressure (LBNP) was used to study orthostatic tolerance. LBNP has several advantages over tilt table testing, some of which are:

1. No movement of subject is required which leads to simplified instrumentation and stable physiological signals.
2. Ease of application of controlled stress (magnitude and duration) to the cardiovascular system.
3. Suitability of use in the weightless condition.

LBNP studies were performed for most Apollo crews, and the response of cardiovascular system during weightlessness was inferred from pre-flight and post-flight data. The results demonstrated reduced orthostatic tolerance, which returned to normal within 48 hours. Supine measurements of maximal calf circumference were also performed, before and after flight, of 24 crewmen. During post-flight evaluation 67% of crewmembers showed significantly reduced calf circumference, and this was not totally regained approximately 120

hours after splash down (7,8).

During the Skylab Program, the LBNP experiments were performed during missions 2,3 and 4 to determine the extent and time course of changes in orthostatic tolerance during weightlessness (9). An additional objective was to determine whether the inflight data can be used for prediction of post-flight orthostatic tolerance status. LBNP produced exaggerated blood pressure and heart rate responses during the first inflight test of Skylab 2 crew, but did not show a trend towards the pre-flight levels during the 28-day flight. It was observed that cardiovascular responses to LBNP tended to become more stable after six to eight weeks of flights, but no trend toward pre-flight levels could be seen. Johnson et al (9) suggest that total blood volume may already have been reduced by the time first inflight LBNP tests were performed, and that a significant fraction of fluids previously located in the legs was now accommodated by veins and interstitial tissues of the upper part of the body. Thornton and Hoffler (10) conducted studies of lower limb during the Skylab 4 mission to test the hypotheses that changes in hemodynamics of legs with increased blood pooling and reduction in cardiac output is the most probable cause of orthostatic intolerance following spaceflight. In spite of the individual variability, the data showed increased blood flow above pre-flight and post-flight levels. Vascular compliance changes were high for both the scientist pilot and pilot whereas for the commander there was little change, and post-flight data showed return to pre-flight values of compliance. Based on scant data from three crew members, the authors were unable to further prove their hypothesis. However, their findings support the need for

careful assessment of pressure flow relationship in the lower limb.

Measurement techniques used in these redistribution studies include estimates of leg volume using multiple tape measurements of limb circumference, standard and infrared photography, and center of mass measurement (7,8). During the Skylab 3 and 4 missions, limb volume measurements were made using a space qualified version of the capacitance limb volume system developed by Barnett et al (11). This system represented the best available at that time for measurement of limb volume, although it is affected by environmental factors, such as humidity and temperature variations. In addition, all of these techniques suffer from the difficulty that considerable crew effort is required to obtain data, or that the transducers are bulky and cannot be used during launch or normal activities. For this reason, no experiments could be performed during the first hours and days of zero-gravity.

C. Requirements for a Space Flight Qualified Plethysmograph

Based on previous research (4) it is felt that an ideal space flight plethysmograph should have the following characteristics:

1. Operation in both zero and earth gravity environment.
2. Insensitive to humidity.
3. Insensitive to ambient temperature and pressure variation.
4. Compatible in size and operation with LBNP test procedures.
5. Simplicity of operation and calibration.
6. Reliable and safe.
7. Nonconfining and non-restrictive of limb dimensional changes.
8. Insensitive to limb movement.
9. Must respond to both small and large changes in limb volume.

III. ULTRASONIC PLETHYSMOGRAPHY

Ultrasonic plethysmography is based on measurement of transit time required for an ultrasonic pulse to propagate from one given point to another. If the velocity of the propagating sound wave in the medium under study is known, then measurement of transit time leads to computation of the pulse traversed distance, d :

$$d = c.t \quad (1)$$

where c = velocity of sound in the medium (m/sec)

t = measured transit time (sec)

Velocity of propagation of acoustic waves have been measured and reported in selected animal tissues using pulse echo techniques. Goss et al (12) provide a comprehensive listing of published results on acoustic properties of mammalian tissues. For a given frequency and temperature, the velocity of propagation appears to be constant and the range of variation is quite small for soft tissues. The average velocity of sound in soft tissues (excluding fat tissue) is 1560 ± 20 m/sec at 2.25 MHz (Bhagat et al (12), Kadaba (13)). The temperature dependence of sound velocity in the range of 20-40 degrees C shows a variation of less than 2m/sec/degree C. Since the temperature within the living tissue is maintained constant by the body within very narrow limits, temperature related errors can be safely ignored.

The use of ultrasonic transit time measurements for biological studies was first reported by Rushmer et al (14) who monitored left ventricular dimensions in open chested laboratory animals. Stegall and colleagues (15,16) have reported the instrumentation and results associated with implementation of the transit time principles.

Stegall et al (17) in an abstract dealing with noninvasive diagnosis of peripheral vascular disease suggested the use of an

ultrasonic dimension gauge to measure changes in lower limb dimensions. However, we have been unable to find any details on its actual implementation. We were the first to demonstrate the feasibility of ultrasonic dimension gauge for noninvasive monitoring of lower limb dimensions (18). In this approach, two ultrasonic transducers (resonant at 2.25 MHz) are placed across the limb segment under study. One of the transducers is shock excited which causes it to vibrate at its natural frequency. This ultrasonic vibration is transmitted through the limb and is converted into an electrical signal by the receiving transducer. The time period between initiation of the shock pulse and its reception by the receiving transducer can, therefore, be accurately measured. With the knowledge of acoustic velocity in the lower limb, the segment dimension is easily obtained.

The most critical choice for ultrasonic plethysmography of lower limb segment is that of transducers' natural frequency. Ultrasonic waves are attenuated when propagating through biologic media. The amplitude of the propagating wave decreases by an exponential factor given by

$$P_o(f) = e^{-2\alpha(f)x} P_i(f) \quad (2)$$

where $P_o(f)$ is the amplitude at a distance x in the medium

$\alpha(f)$ is the attenuation coefficient of the medium (dB/cm)

$P_i(f)$ is the input wave

and f is the frequency of the wave.

Measurements in our laboratory (19) indicate that the attenuation coefficient $\alpha(f)$ is approximately linearly related to ultrasonic frequency ($\alpha(f) = af^b$; $b = 1.06$) for excised muscle tissue in

experimental animals. In light of this it is imperative that the ultrasonic frequency be kept as low as possible.

As the ultrasonic frequency is lowered two constraints come into play. In most transit time measurement systems arrival of the ultrasonic pulse is threshold detected with an amplitude comparator. Thus the maximum error due to threshold adjustment can be $\lambda/4$, where λ is the wavelength of ultrasound. Assuming an average velocity of 1,560 m/sec, and calf length of 15 cms, in the range of 2-3 MHz the maximum threshold error is approximately 0.2 mm.

Further as ultrasonic frequency is lowered the thickness of crystal increases. Higher shock voltages are required at lower frequencies to set the transducer into vibration, due to its increased inertia. While this is not critical in most applications since the excitation voltages are usually in the range of 100-200v and are of short duration (4 ns), the authors feel that from a safety viewpoint every attempt should be made to keep these voltages lower.

We, therefore, chose frequency range of 2-3 MHz for the plethysmographic applications.

SINGLE CHORD ULTRASONIC PLETHYSMOGRAPH

The single chord ultrasonic plethysmograph is schematically shown in Figure 1. The major components of this instrument are a pulse generator (Pinger) and receiver amplifier, a voltage comparator, a sync pulse generator and an elapsed time counter. The system is housed in a single unit, with the exception of the transmitting and receiving piezo-electric crystals. The crystals are cut from 1" square LZT-5 stock, resonant at 2 MHz, with approximately 3 mm diameter, and then wires are attached. The crystals are dipped in

clear epoxy to maintain the integrity of the transducer material over a period of time. The crystals are positioned on a limb such that the ultrasonic pulse will travel from the transmit crystal to the receiver crystal. The wave propagation time between crystals is measured by counting the number of cycles generated by a time base oscillator. Output from the system is available as a 12-bit binary number or an analog signal derived from the binary number through a digital-to-analog converter (DAC).

The measurement cycle begins on the leading edge of a 40 ns wide negative-going pulse. This pulse is generated by a monostable multivibrator (IC6, Fig. 2) triggered by a crystal controlled oscillator and frequency divider at a repetition rate of 1 KHz. This pulse induces a 150-V signal across a piezoelectric crystal. Due to this shock excitation, the crystal vibrates at its natural frequency, 2 MHz, resulting in the transmission of an ultrasonic signal across the limb.

The pinger circuit (Figure 3) works as follows:

When the trigger level is high (+15V) the base to emitter junction in transistor Q_1 , is non conductive, therefore, no current flows through it. This also implies that transistor Q_2 will also be off and no signal is available across the transformer to the ultrasonic crystal. However, when the trigger level is lowered to zero, Q_1 and therefore Q_2 are turned on. With Q_2 in the operating mode a 200V signal is induced through the 1:1 transformer to excite the transmitting transducer. The transformer is included in the pinger circuit to provide isolation of 200V source from the test media (usually human subjects). The 200V signal is derived from a commercially available module (ERG) which is a dc to dc inverter with

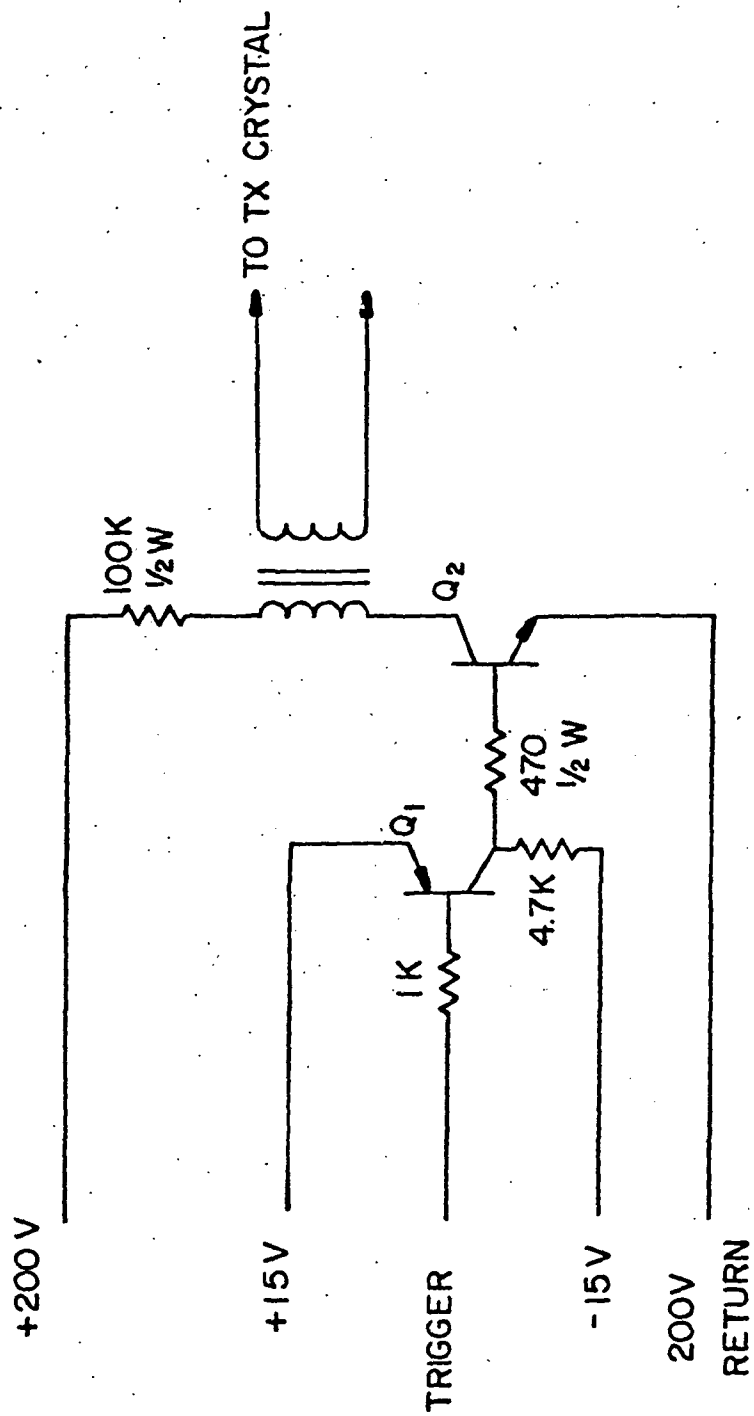


FIGURE 3
 AVALANCHE PULSE GENERATOR (PINGER) CIRCUIT

input of 15V.

Simultaneous to the triggering of the transmitter circuit, the elapsed time counter (IC's 10-13, Fig. 2) is cleared and the time base signal (32 MHz) is gated to the input (IC 10) of the counter. The count accumulates until the voltage comparator senses a signal from the ultrasonic receiver which exceeds the operator controlled threshold voltage.

The input signal to the ultrasonic receiver (Fig. 4) comes from a piezoelectric receiving crystal attached to the limb. the receiving crystal is connected to the primary winding to T_2 which is balanced by a 1 kohm potentiometer and a 220 μ f capacitor to provide common mode rejection. Transformer T_2 also provides electrical isolation for the subject. The signal induced in the secondary of T_2 is then amplified by a factor of 1,000 with two cascaded RF amplifier (LM371). The resulting signal serves as input to the voltage comparator (LM306).

Once the comparator senses the received signal, the time base signal being input to the counter is halted. After a short delay, allowing for propagation delays in the counter, the final count is latched in a separate register. The digital-to-analog converter changes the 12-bit register output to a proportional voltage which is recorded by an analog recorder. The register output can also be input into a computer system for data storage and analysis. A portion of the output can be suppressed by dialing in a number on a set of thumbwheel switches. The negative value of this number is loaded into the counter at the beginning of each measurement cycle thereby subtracting the number from every measurement. This feature allows



FIGURE 4
ULTRASONIC RECEIVER-AMPLIFIER AND COMPARATOR

the operator to record only the variations from a baseline reading. The distance resolution of this system using a 32 MHz clock is given by $\text{resolution} = (\text{sound velocity}/\text{clock frequency}) = 0.049 \text{ mm}$. This system has been described in literature (18).

Extensive experimentation was carried out using human subjects to investigate the reliability, accuracy and repeatability of the developed instrument. Experimental protocols are defined below:

a) Static tests

With the subject in a supine position on a tilt-table, the instrument was tested by inducing a small precise changes in leg diameter. A 2 MHz transducer was mounted on each tip of a 5 in. micrometer. With the micrometer rigidly clamped, the leg of the subject was positioned so the micrometer spanned the major chord length from near the crest of the tibia to the back of the gastrocnemius. The micrometer head was advanced until the crystals made firm contact with the skin. The chord length was then varied by advancing the micrometer head in steps of 0.025 in (0.635 mm). The change in the chord length as measured by the ultrasonic system is shown in Figure 5. As can be seen from the figure the system response to discrete step changes from 11.74 cm diameter to 11.30 cm diameter is repeatable as well as accurate.

b) Dynamic tests

A comparative study using Whitney Strain Gauge, (WSG), "Mercury in rubber" plethysmograph, was carried out to establish the dynamic performance of the system. If the limb segment involved in the plethysmographic measurement is assumed to be circular and the path between the ultrasonic transducers is assumed to be its diameter, then the cross-section area or volume per unit length of the limb

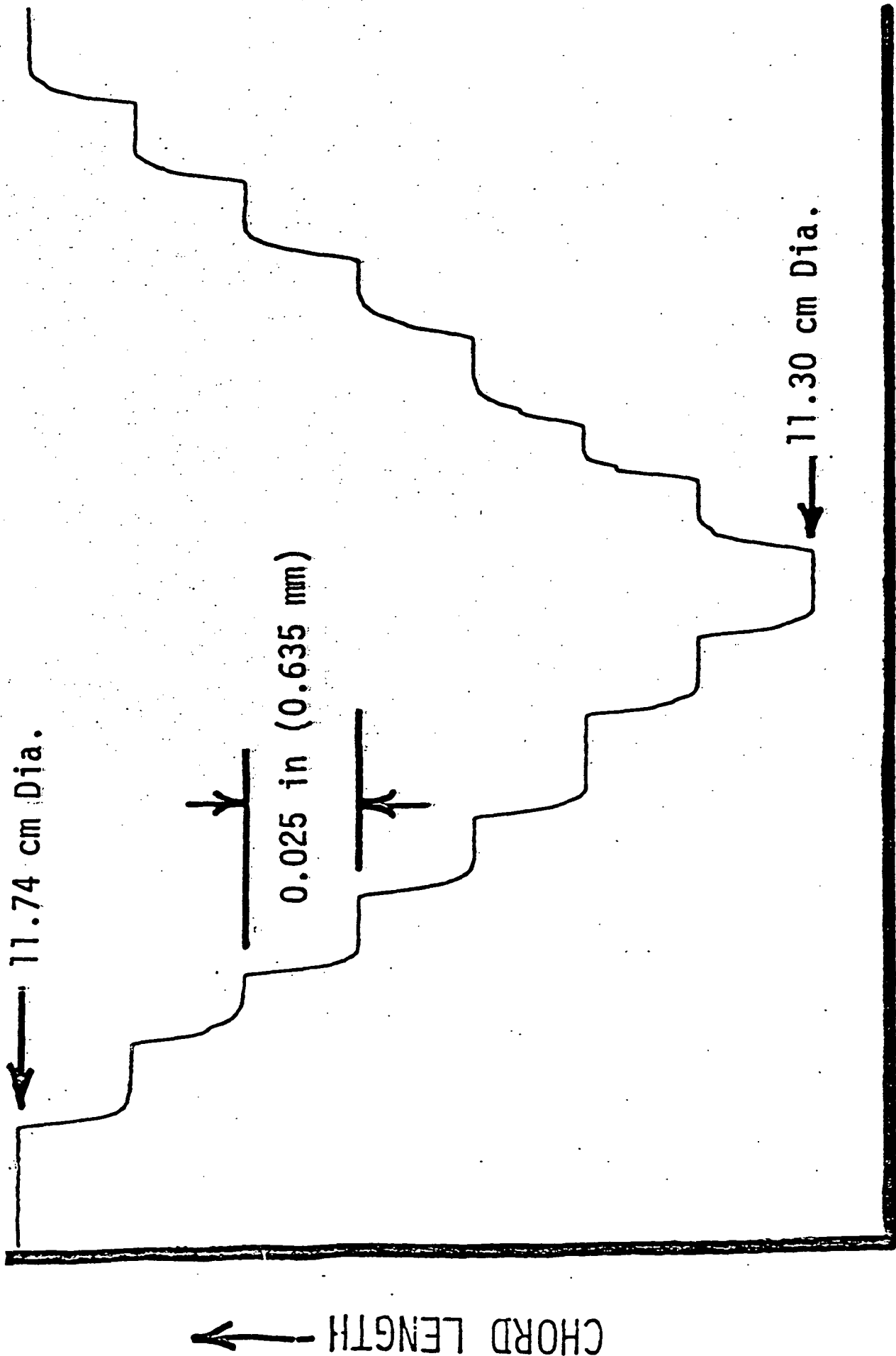


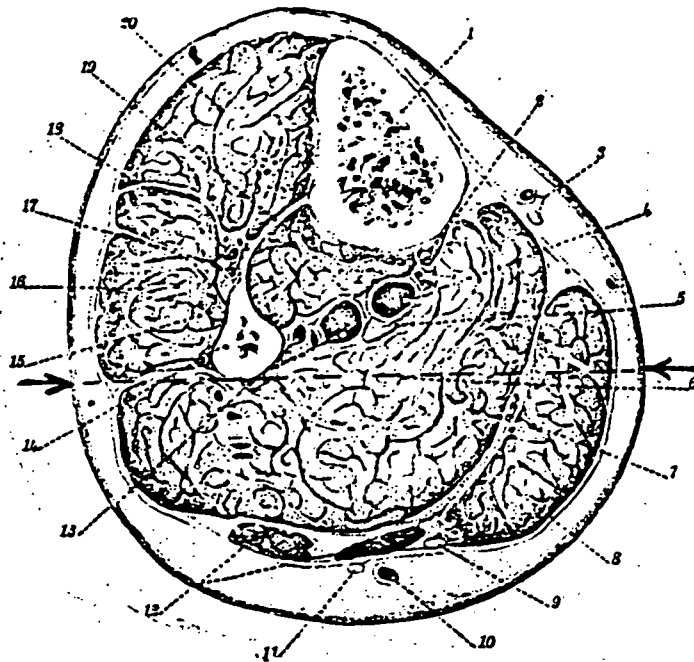
FIGURE 5

STATIC MEASUREMENTS OF DIMENSIONAL CHANGES ON THE LOWER LEG USING ULVS

segment is directly proportional to the measured distance. Any change in volume is, therefore, reflected in a change in travel time of the ultrasonic pulse. The Whitney Strain Gauge measures changes in circumference of the limb. Based on this hypothesis the plethysmographic measurements by the WSG and the ultrasonic plethysmograph, placed over the same limb segment, should be linearly related.

A typical cross-section of the lower leg in a healthy adult, at the level of limb segment normally involved plethysmography studies, is shown in Fig. 6 with approximate transducer locations. As can be seen from the figure, the ultrasonic distance measured is more like a chord of the limb segment. However, the ultrasonic output and the Whitney Strain Gauge output should still be related by a constant.

In this experiment, venous occlusion was used to produce a discrete change in limb volume. A pressure cuff was applied to the proximal portion of the limb and the pressure in the cuff was increased above the venous pressure but below the diastolic arterial pressure (usually between 20-60 mm Hg). Because the arterial inflow of blood was not stopped, there would be a net increase in the volume of the limb below the cuff due to a pooling of blood in the segment. The rate of volume change with respect to time immediately after occlusion can be used to determine the rate of blood flow in the arteries. The volume will stabilize when the pressure in the veins reaches the cuff pressure. This is known as the compliance level and, along with the initial rate of volume change, is one of the important parameters in venous occlusion plethysmography. A more thorough discussion of the mechanisms of venous occlusion plethysmography is



SECTION 96

(→) Approximate position of transducers

1. Tibia
2. M. flexor digitorum longus
3. V. saphena magna et n. saphenus
4. V. et a. tibialis posterior
5. N. tibialis
6. M. soleus
7. Tendo m. plantaris
8. M. gastrocnemius
9. N. cutaneus surae medialis
10. V. saphena parva
11. N. cutaneus surae lateralis
12. M. gastrocnemius
13. A. et v. peronaea
14. Fibula
15. N. peronaeus superficialis
16. Mm. peronaei longus et brevis
17. N. peronaeus profundus
18. Mm. extensores longi digitorum et hallucis
19. Membrana interossea cruris
20. M. tibialis anterior

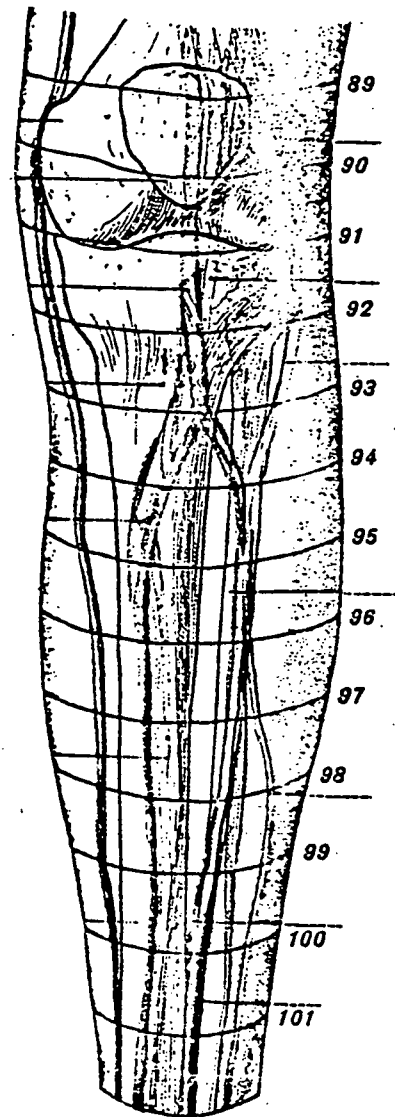


FIGURE 6

Cross sectional view of lower limb at the level of plethysmograph application.

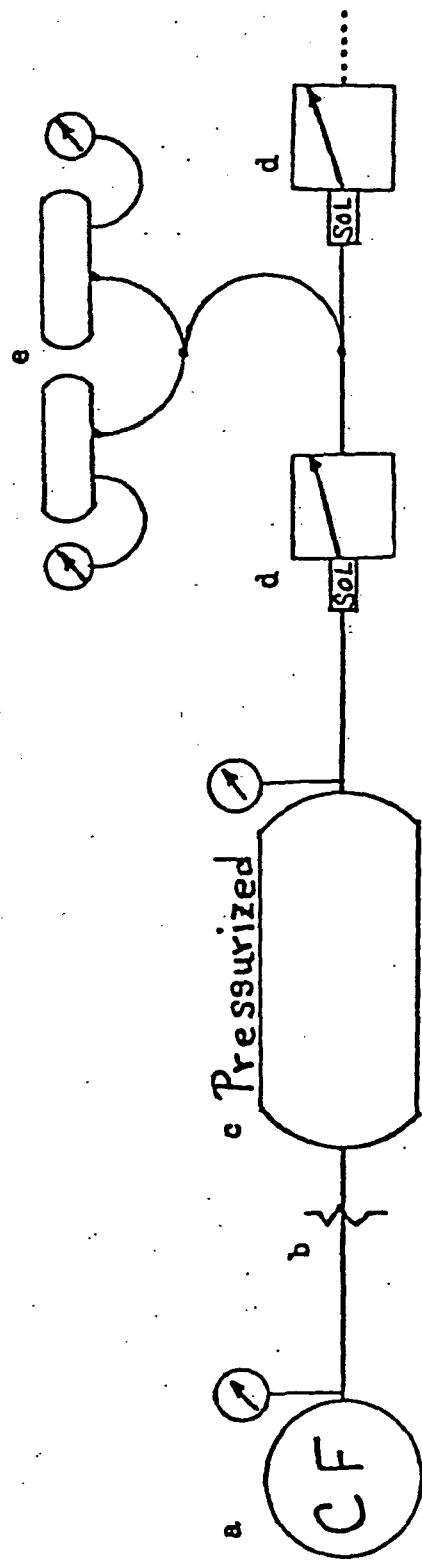
given by Sigdell (3).

The apparatus used for this study includes two ultrasonic transducers, a Whitney strain gauge, a system for obtaining venous occlusion of the lower limbs, and the single chord ultrasonic plethysmograph.

The venous occlusion system, shown in Figure 7, consists of a twelve gallon fixed displacement air compressor (a), a pressure attenuator (b) for limiting the pressure in a small pressurized tank (c), two normally closed solenoids (d), and standard thigh cuffs equipped with sphygmomanometers. Upon activation of the first solenoid in the system, the pressure in the thigh cuffs is increased in approximately a stepwise matter. The amount of pressure in each cuff is determined from the sphygmomanometers. Once the first solenoid is deactivated the pressure in the thigh cuffs remains constant until the second, release, solenoid is activated.

With the subject relaxed in a supine position, the ultrasonic transducers are positioned on the lower leg at the level shown in Figure 6, using the oscilloscope to determine the position corresponding to maximum signal. Once the optimum position is determined, the transducers are taped in place using the smallest piece of tape necessary for secure placement. The Whitney strain gauge is then placed over the same limb segment as shown in Fig. 8 schematically and a photograph is shown in Fig. 9. The leg is, then, elevated slightly to eliminate pressure on the calf muscle and to prevent drag on the strain gauge. The thigh cuffs are applied to both legs above the knee.

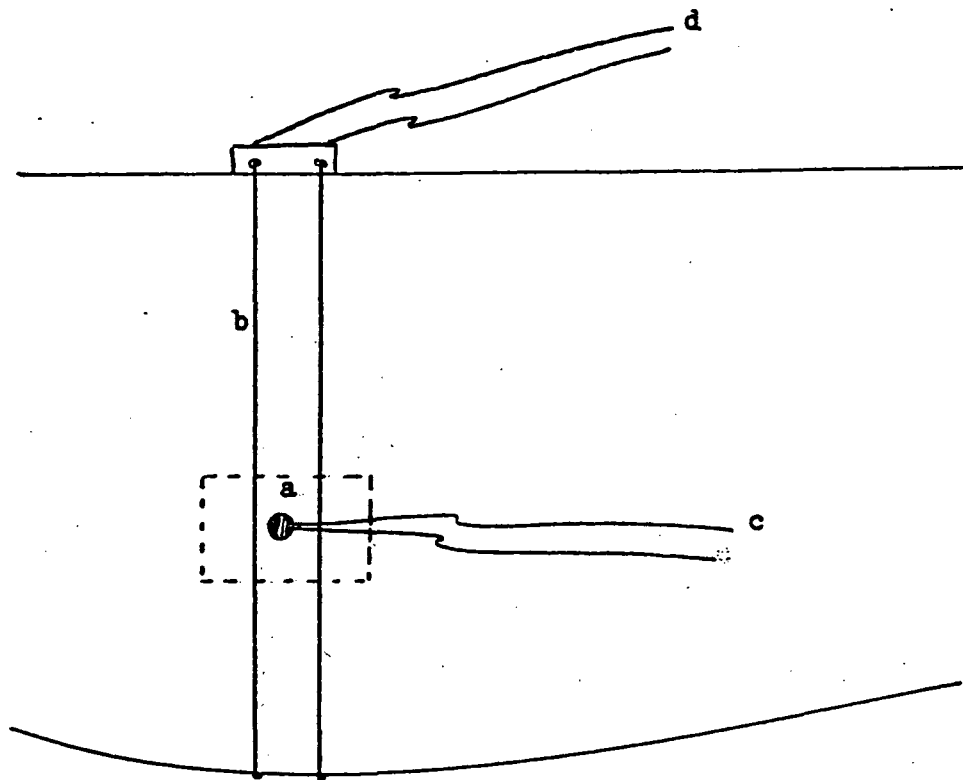
After a stable base line is obtained on both channels of the chart recorder, the initial readings of the ultrasonic digital display



- a) 12 gallon fixed displacement air compressor
- b) Pressure attenuator
- c) Small pressure tank
- d) Normally closed ASCO solenoids electrically controlled by a two-way switch
- e) Standard thigh cuffs with sphygmomanometers

FIGURE 7

Schema of system for inducing venous occlusion in lower limbs.



- a. Ultrasonic transducer taped in place
- b. Whitney strain gage
- c. Ultrasound connection wires-- to oscilloscope, digital display, and chart recorder
- d. Strain gage connection wires--to gage display and chart recorder

FIGURE 8

Relative placement of ultrasonic transducer and Whitney strain gage

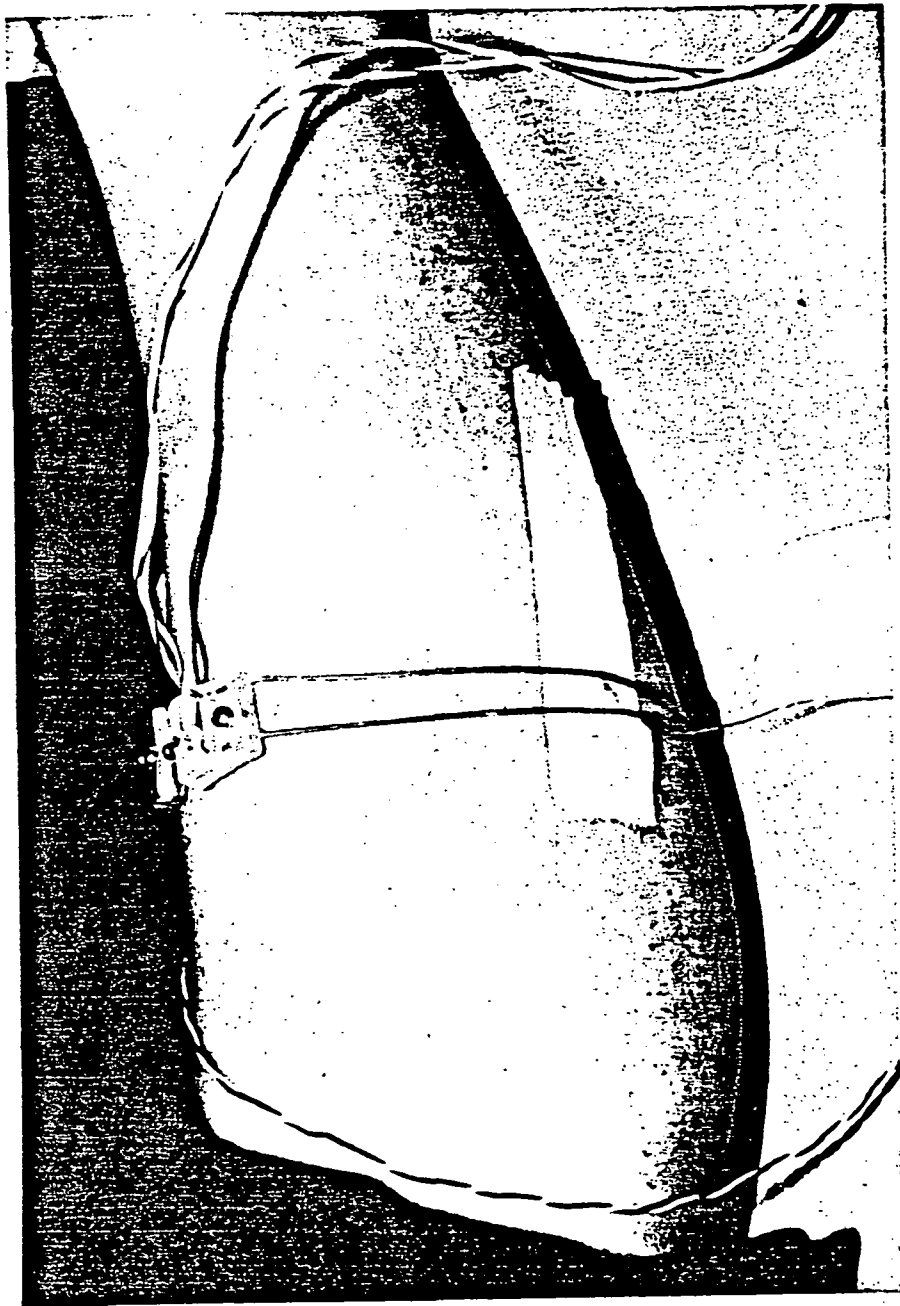


FIGURE 9

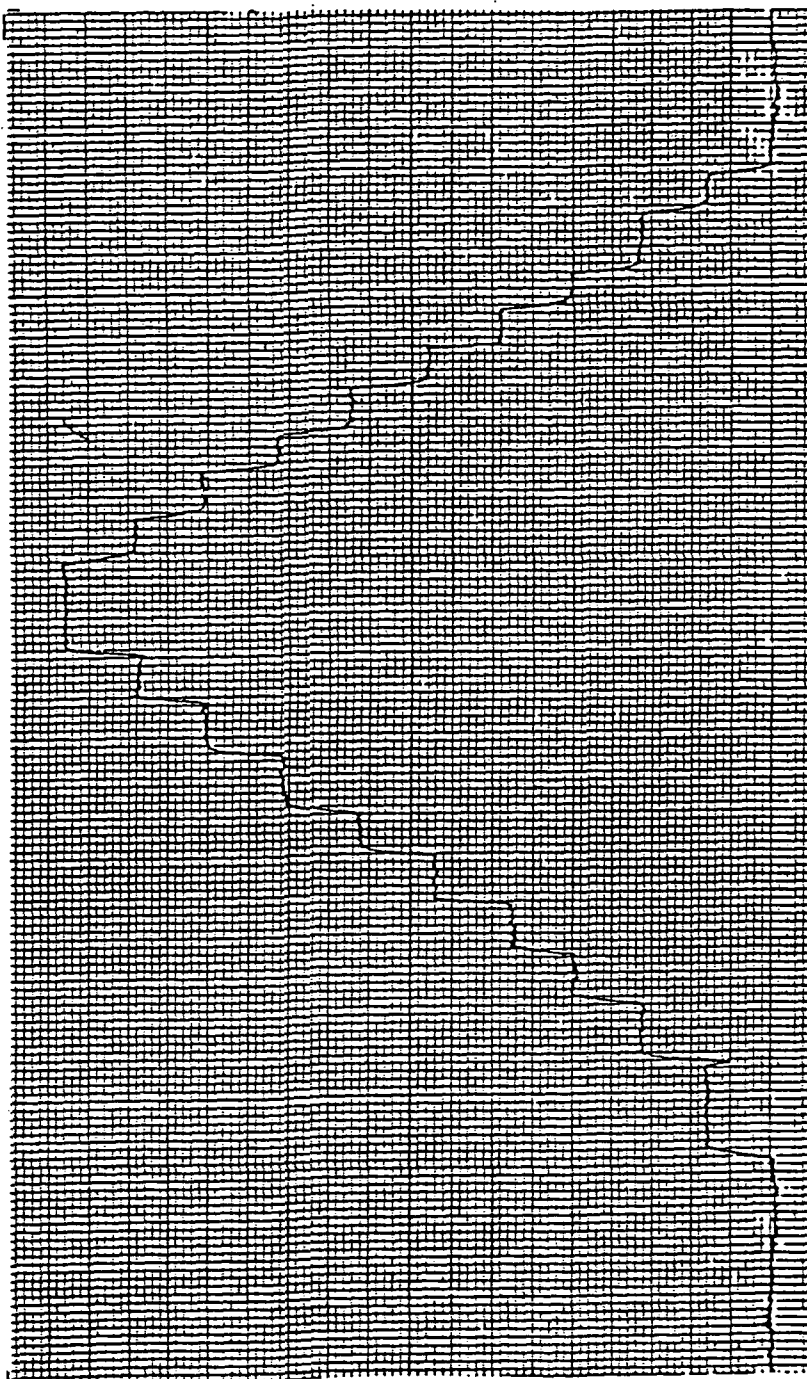
PHOTOGRAPH SHOWING ACTUAL LOCATIONS OF ULTRASONIC TRANSDUCERS AND WHITNEY STRAIN GAUGE

and the strain gauge display are recorded. The thigh cuff pressure is then increased to 20 mm Hg and held constant until the chart recorder graph reaches a maximum (compliance level). Readings are again recorded for the strain gauge display and the ultrasonic digital display. The pressure is then released and the system allowed to stabilize. This procedure is repeated for pressures of 30, 40 and 50 mm Hg. In this project at least three complete sets of data (i.e. pressures of 20-50 mm Hg) were taken during each session. Data sets were taken for each leg under the conditions of bilateral and unilateral venous occlusion. However, the equipment did not permit collection of data from both legs simultaneously.

To facilitate the interpretation of chart recorder data in terms of physical parameters (i.e. change in length per unit time and percent change in length at compliance), it was necessary to perform calibration experiments for the Whitney strain gauge and the ultrasonic system. The calibration of the ultrasonic system has been described under static test.

The calibration procedure for the Whitney strain gauge was as follows: One end of the strain gauge was fixed and the other end attached to a vernier device. The system was adjusted to an initial position with the strain gauge straight but not extended. The strain on the strain gauge was then incremented in 1 mm steps to a total of 10 mm strain. The gauge reading was recorded at each increment to check the linearity of the readings. The strain gauge was then returned to its initial length in steps of 1 mm and the readings were again recorded. Figure 10 shows the static data for Whitney strain gauge.

A typical venous occlusion record is shown in Figure 11. Cuff



L incremented by 1 mm
Gain = 5 volts full scale

FIGURE 10
Calibration curve for Whitney strain gage
as recorded on chart recorder

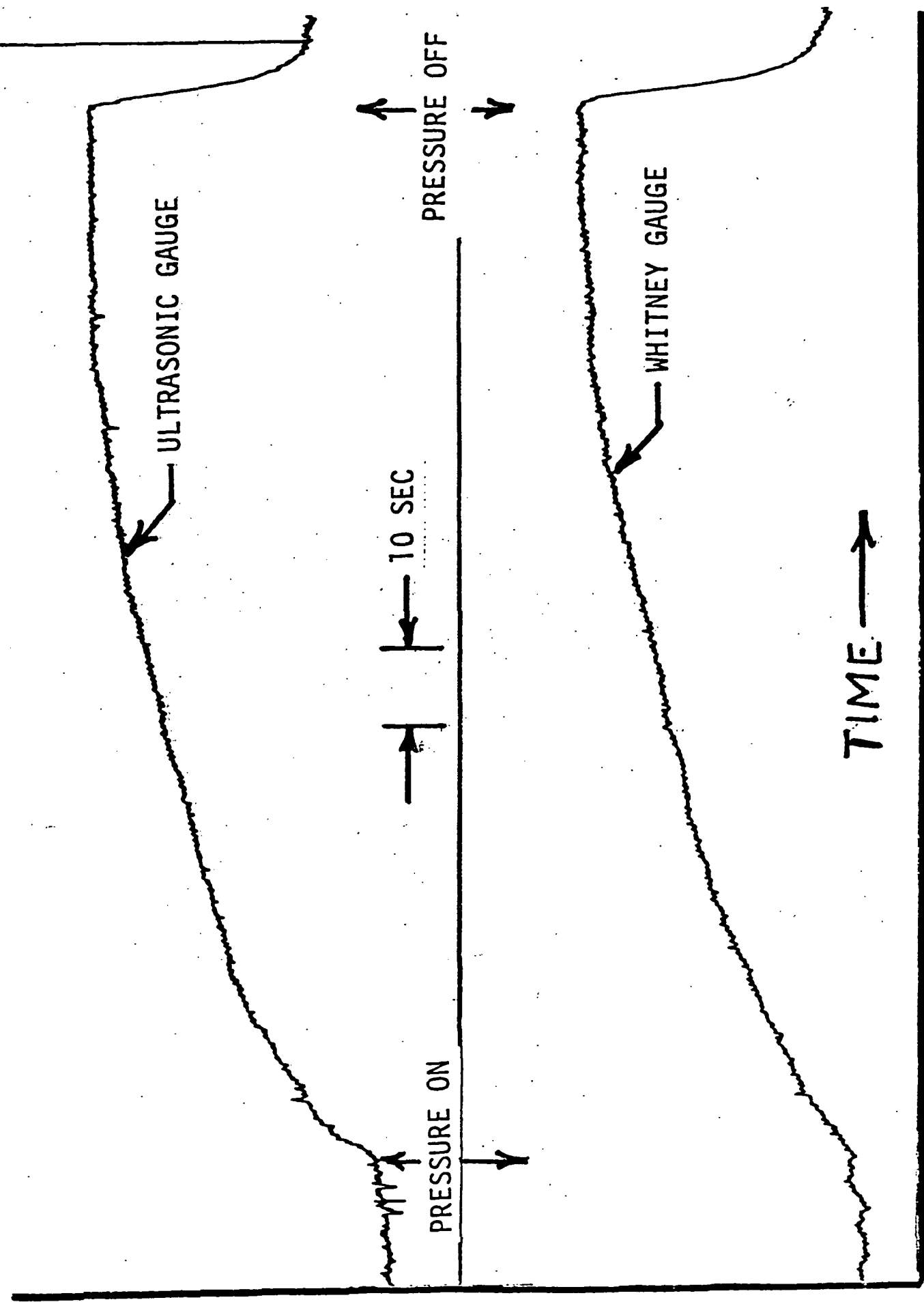


FIGURE 11: DYNAMIC COMPARISON OF WHITNEY GAUGE AND ULVS MEASUREMENTS

occluding pressure of 50 mm Hg was applied to the subject identified by pressure on arrow on the graph. The occlusion was maintained for a time period of approximately 2 minutes when the ultrasonic plethysmograph output reached steady state. The occluding pressure was released then and the record indicates a rapid emptying of the pooled blood followed by a slower decline to baseline values. Calculations of maximal blood flow and compliance levels can be made and the procedure is illustrated in Figure 12.

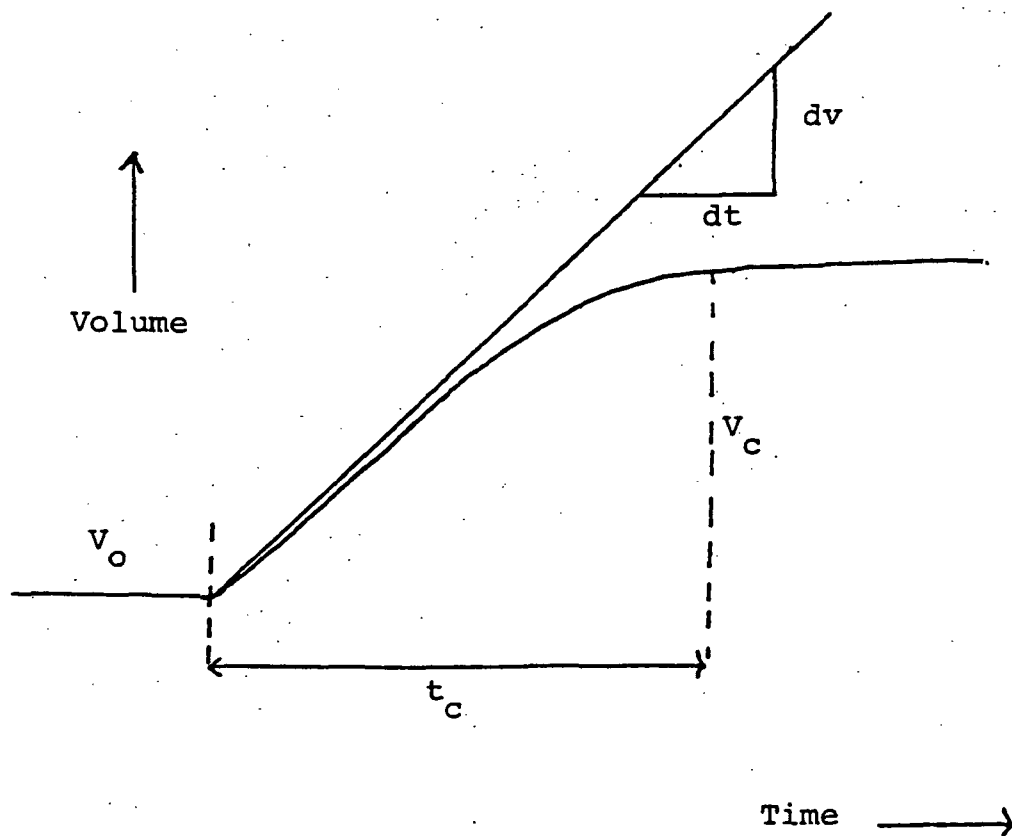
Figure 13 shows initial slope of the ultrasonic plethysmograph plotted against initial slope obtained using the Whitney strain gauge. The equation of the line shown in this figure, as determined by the least square error method, is

$$W = 2.235 u + 0.176$$

The above equation was derived using data from 30 independent experiment runs. The correlation is quite good ($r = 0.9077$).

Figure 14 shows the average initial slope as a function of cuff pressure. As can be seen, the initial slope remains approximately constant for pressures of 20-40 mm Hg and drops off slightly when the cuff pressure is 50 mm Hg. One possible explanation is that 50 mm Hg occluding pressure may have caused occlusion of some arterial vessels and thus decreasing the inflow rate.

The compliance level showed a direct dependence on the applied cuff pressure. Both the ultrasonic plethysmograph and the Whitney strain gauge outputs leveled off around the same time frame. Figure 15 shows a plot of compliance time versus cuff pressure for two subjects. As expected time to reach final compliance level increased with the applied occluding pressures.



$$\text{Arterial inflow} = \frac{dv}{dt}$$

$$\text{Compliance level} = V_c$$

Figure 12 Computation of arterial flow and compliance level

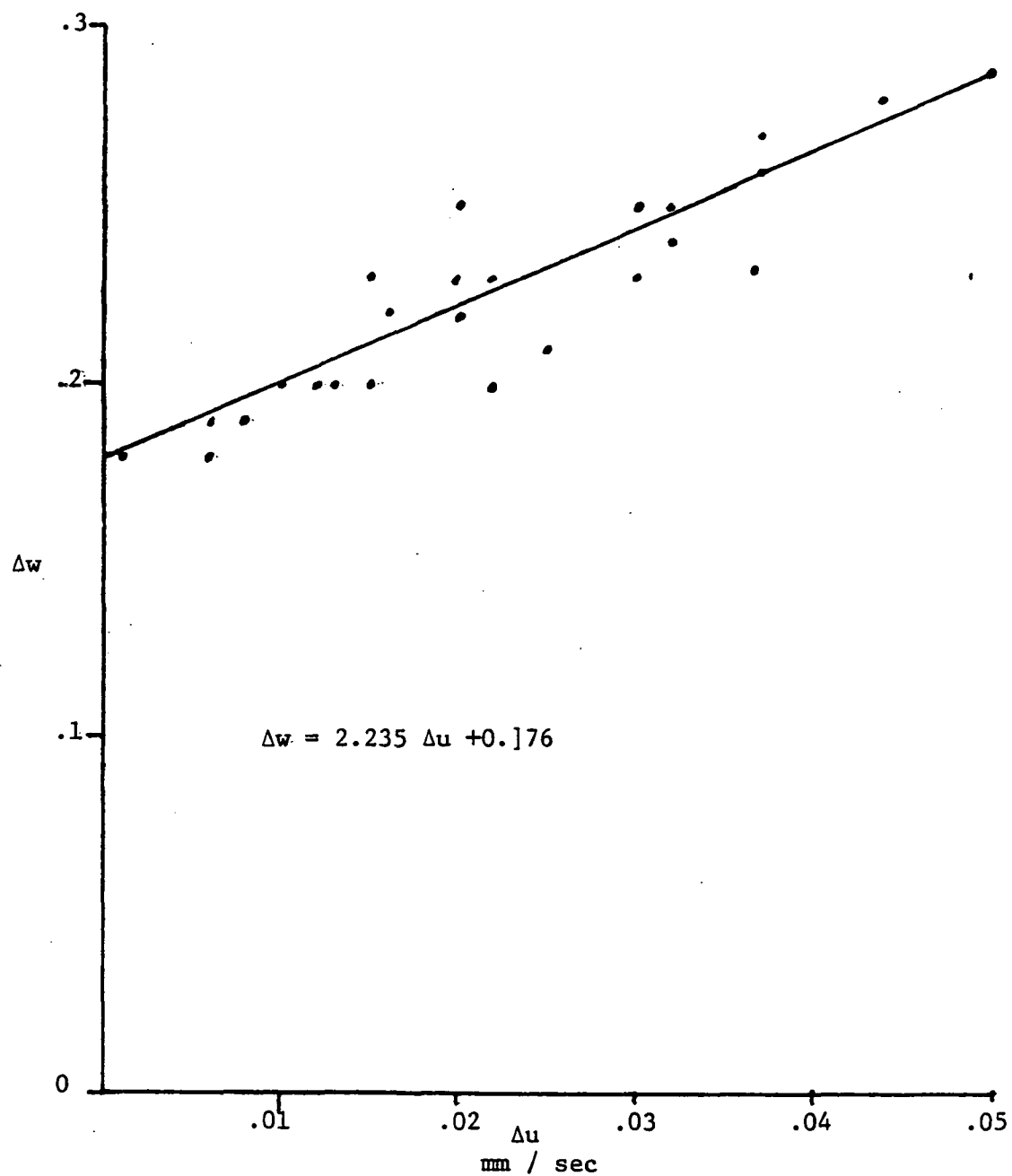


FIGURE 13: Correlation between initial slope of ultrasonic and Whitney strain gage plethysmographs

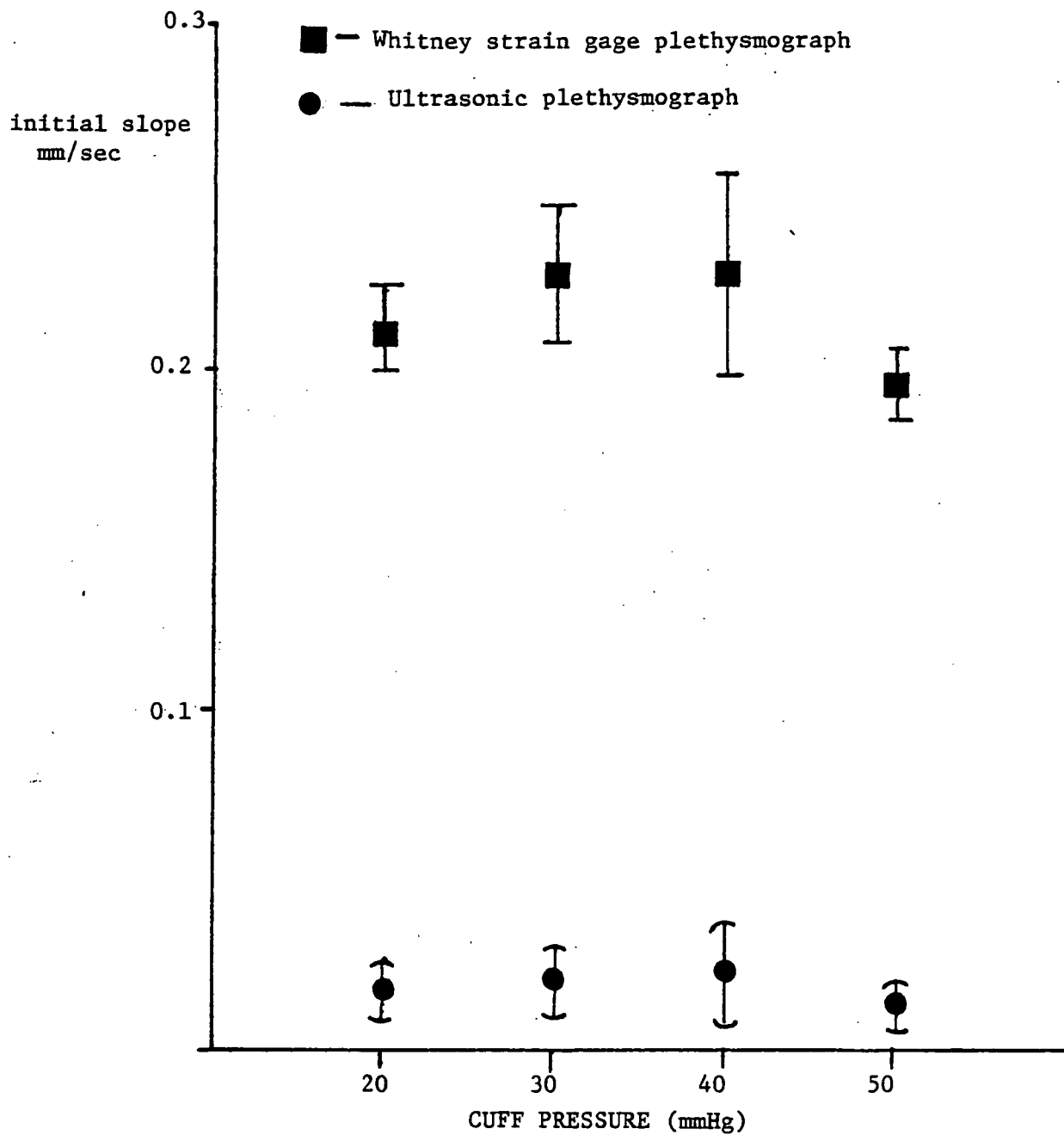


FIGURE 14: Average initial slopes (ultrasound and strain gage) as a function of cuff pressure

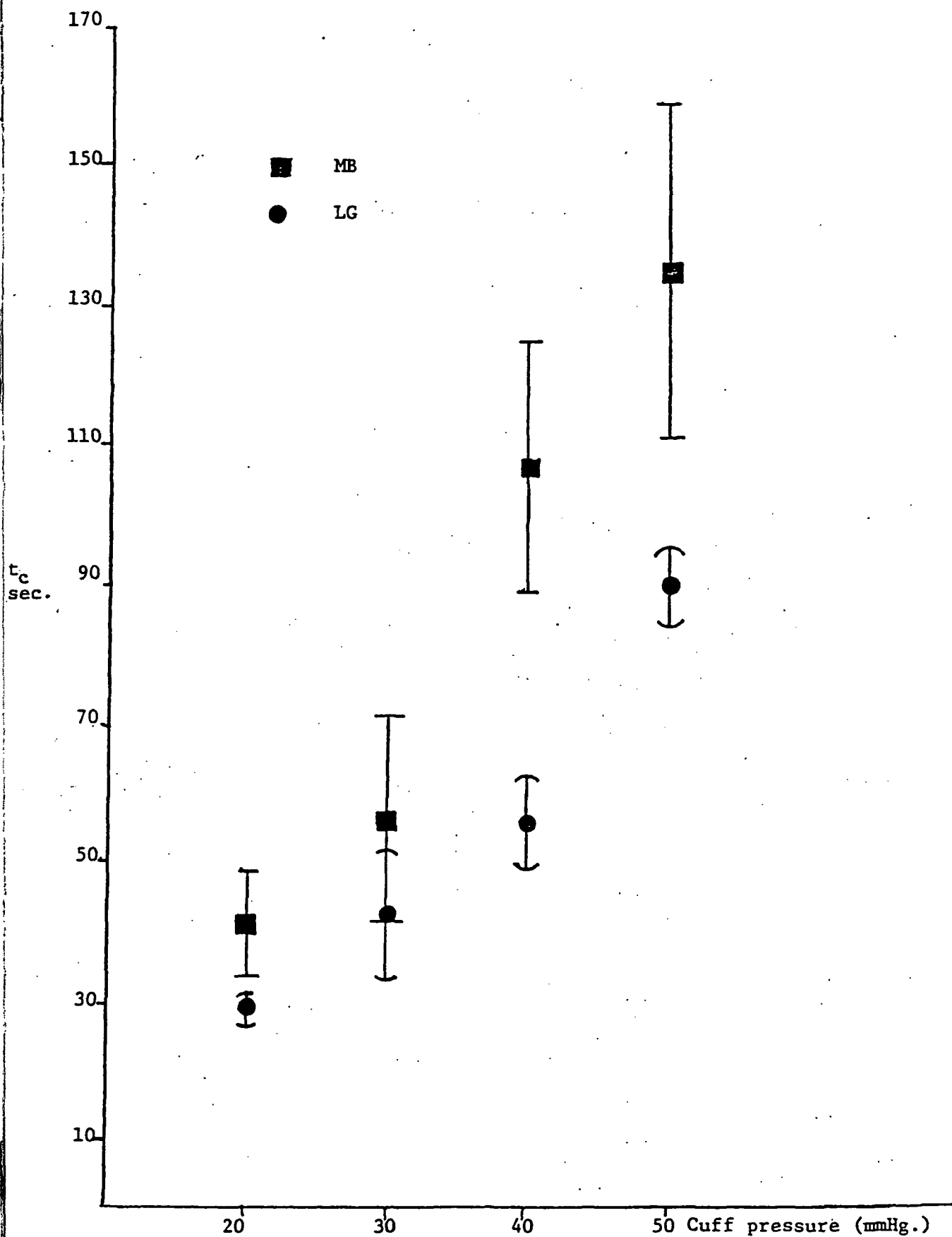


FIGURE 15: Compliance time versus cuff pressure

TWO CHORD ULTRASONIC LIMB VOLUME SYSTEM

A single dimension measurement is not a true indicator of the volume change in the lower limb. It was felt that a more accurate measure of limb volume could be obtained through computation of a cross-sectional area from two independent chord length measurements. The independent chord lengths are measured ultrasonically through placement of ultrasonic transducers around the circumference of the limb. We exploit the well known concept from analytic geometry that three points in a plane can define a unique circle. Our implementation of this concept uses three transducers, located on the limb. Two of these transducers, kept a fixed distance apart and located on one side of the limb act as transmitters of ultrasonic energy. This energy is received by the third transducer which is located on the opposite side of the limb. Thus, two independent transit time measurements can be made at any given site on the limb. With the knowledge of ultrasonic propagation velocity, the chord lengths can be computed as described earlier in this report. It may be noted that this computation also provides a sort of "averaging" of the ultrasonic chord length measurements, whenever the tissue expansion is approximately isotropic even when the cross-section is noncircular. A microprocessor was incorporated into the system to provide real time computations of limb cross-section, as well as to control the entire measurement process. Further the use of a microprocessor makes it easy to change the computational and control routines thus facilitating subsequent refinements of the design.

Theoretical details:

The following mathematical scheme defines the procedure for computation of the cross-sectional area from chord length

measurements:

Consider Figure 16 where OA and OB are the chord length obtained from the measured transit times using transmitters (located at A and B respectively) and receiver transducer (located at O). The distance, AB, between the transmitters is fixed and known = D_3 cm and

$$OA = t_{OA}$$

$$OB = t_{OB}$$

Where t_{OA} and t_{OB} are times required for the ultrasonic pulse to be received at O from the sites at A and B respectively.

Without any loss of generality we can assumed that OA defines the x axis. Hence the x-coordinate of the center

$$x_C = D_1/2 \quad (1)$$

The equation of the circle passing through O, A and B with center (x_C, y_C) is given by:

$$(x-x_C)^2 + (y-y_C)^2 = r^2 \quad (2)$$

Where 'r' is the radius of the circle.

At the point O(0,0) the equation is

$$(D_1/2)^2 + y_C^2 = r^2 \quad (3)$$

and at the point B (x_2, y_2)

$$(x_2 - D_1/2)^2 + (y_2 - y_C)^2 = r^2 \quad (4)$$

also

$$D_3^2 = D_1^2 + D_2^2 - 2D_1D_2 \cos\theta \quad (5)$$

solving equations 3, 4 and 5 for radius, r, we obtain

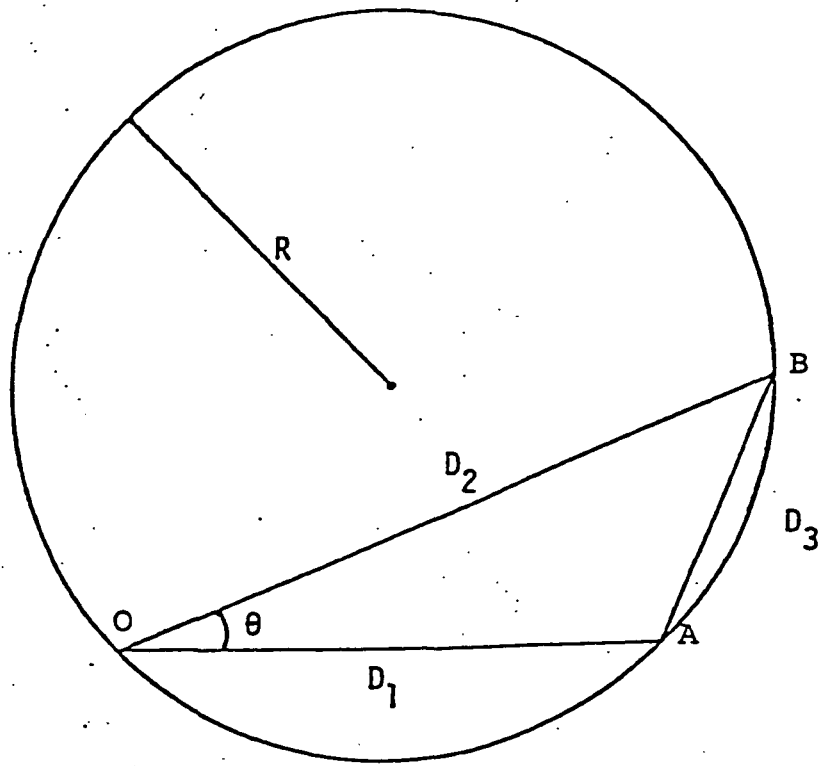


FIGURE 16. Computation of cross-sectional area from two chord length measurements

$$\begin{aligned}
r^2 &= x_c^2 + y_c^2 \\
&= D_1^2 D_2^2 D_3^2 / (D_1 + D_2 - D_3) (D_1 + D_2 + D_3) (D_1 + D_3 - D_2) (D_1 - D_2 - D_3) \quad (6)
\end{aligned}$$

Area of the circle passing through O, A and B is

$$\pi r^2$$

which can be easily computed with knowledge of radius, r .

Equation 6 was simulated on both a minicomputer and a microcomputer for computational accuracy using several chord length sizes. All calculations were carried out in floating point arithmetic. The program, written in assembly language using Intel 8080 microprocessor chip, took approximately 1.5 k memory space. The accuracy of microprocessor computations was compared with that obtained using a DEC PDP-11/10 minicomputer and the results were in excellent agreement with each other. The truncation error in area computations using $D_1 = 6.54$ cm; $D_2 = 7.55$ cm and $D_3 = 1.85$ cm was $5 \times 10^{-3}\%$, an insignificant error. It should be noted that these computations are affected by accuracy in measurement of D_3 (which must be accurate to within 0.1 mm). A large D_3 provides very accurate computations but leads to practical problems in implementation of the concept since the bony tissue, tibia, must not be in path of ultrasonic transmission. In addition, operational difficulties with actual placement of transducers dictate the transmitters be mounted on the same assembly. We have determined that D_3 of the order of 2.5 cm provides a good compromise between computational accuracy requirements and operational ease. (21).

Details of the developed instrument:

A. Hardware Description:

The developed instrument (Fig. 17) is housed in a Tektronix TM 515 Mainframe. An SC 502 oscilloscope is included to monitor the quality of received signals. The instrument is modular with transmitters, receiver, and processor circuits housed in separate compartments. Transmitter and receiver circuits are identical to those described earlier for the single chord ultrasonic plethysmograph. Two separate transmitter (pinger) circuits are provided. Either of these pinger circuits can be selected by the processor, providing independent measurement of the two chord lengths. The piezoelectric transducer elements, which are mounted in specially-molded housings for attachment to the limb, are connected to the instrument by unshielded twisted pair cables.

Processor and Memory: A block diagram of the implemented circuits is shown on Figure 18. The system uses one Intel 8080 CPU with a clock generator (8224), which provides 18 MHz for the counter and the timing frequency of 2 MHz for the CPU. 256 byte random access memory (RAM) is used for storage of generated data and a 2kb read only memory (ROM) is available for storage of software codes and constants needed for computation of cross-sectional area. The data lines from CPU are latched through a data bus and control status bus driver in order to increase the drive capacity of the CPU. Two peripheral interface adapters (PIA) are used: one connects the data bus to LED display through four BCD to seven segment decoder/drivers while the other interfaces the counter to the CPU. Due to the available number of lines on the PIA chosen the output display is limited to less than 200 cm² (The 5th digit of the display is wired so that it will show

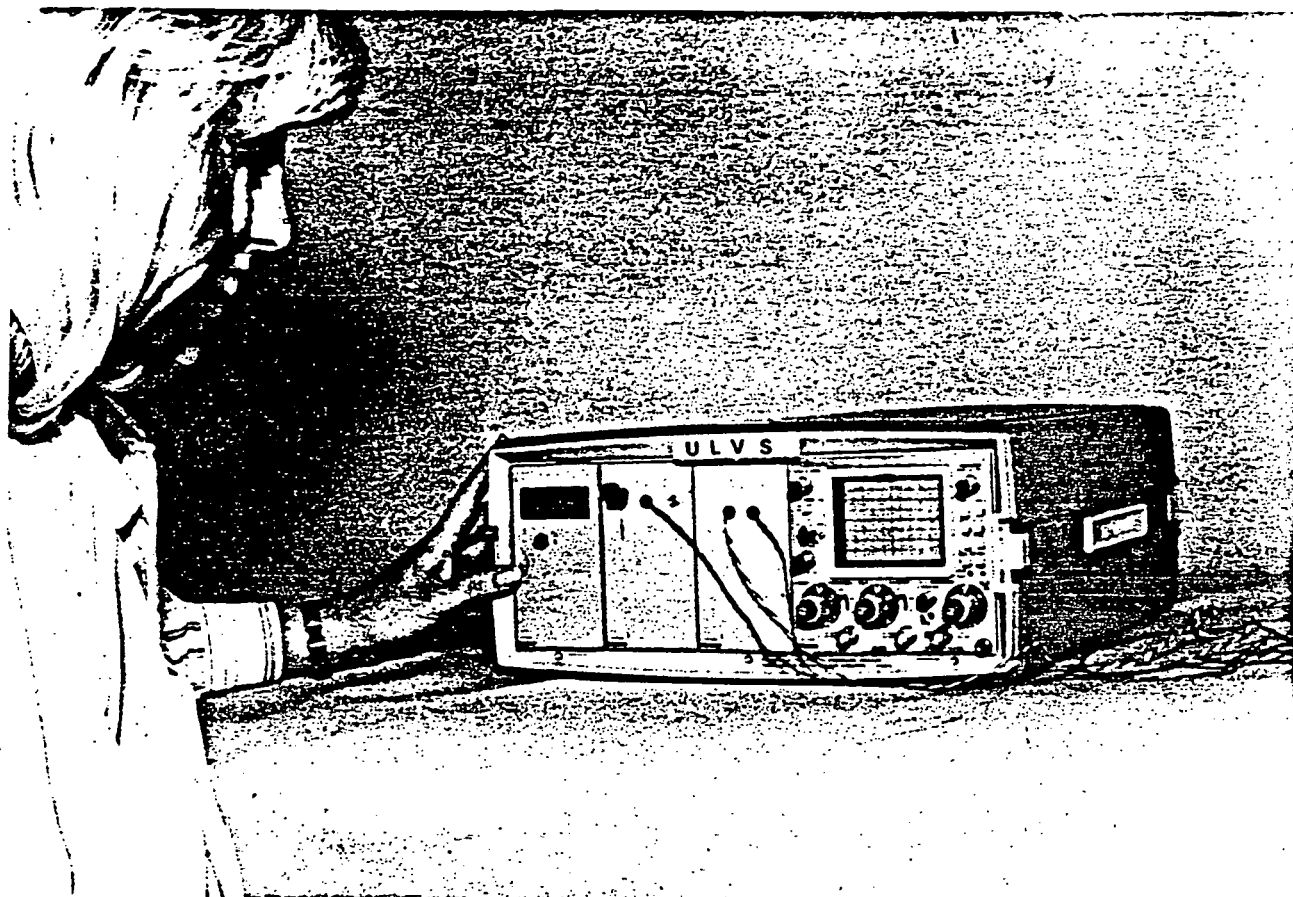


FIGURE 17: Two transmitter ULVS

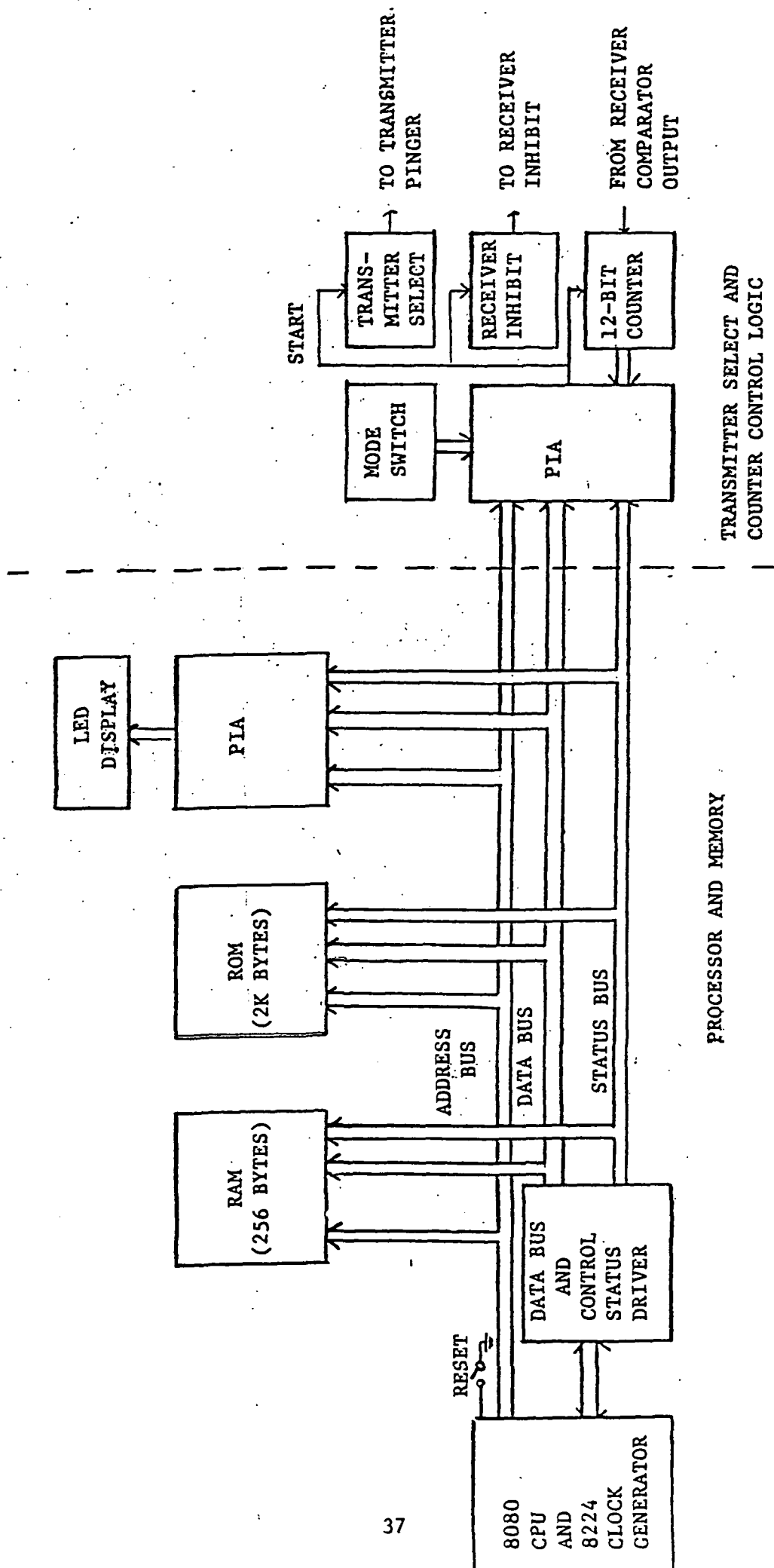


FIGURE 18. BLOCK DIAGRAM OF ULVS ELECTRONICS.

blank or "1" only). This restricts the maximum calf diameter to less than 16.5 cms. For the normal adult population this is not a serious limitation. The power for all the units is derived from the TM 515 power module with suitable regulators to obtain ± 12 V and ± 5 V.

Transmitter Select and Counter Control Logic: The 12-bit binary counter is interfaced with the CPU through PIA as shown. The 18-MHz clock frequency provides 56 ns resolution for time measurements. Following transmitter activation, the comparator output is inhibited for 10 μ s to allow electrical interference from the transmitting pulse to decay. This block also contains transmitter select and level conversion circuitry necessary for producing a pulse from one of the two transmitters. The command pulse which fires the selected transmitter also starts the counter. The counter continues to count until it is stopped by a level change signal from comparator.

A three-position switch (mode switch) is used to select the modes of operation of the unit. Each of the first two positions causes one of the two transmitters to be "pinged" at a 2-KHz rate. The receiver amplifier and comparator outputs are displayed on the oscilloscope so that the quality of the received signal can be assessed. The pinger and receiver amplifier circuits are shown in Figures 3 and 4 of this report.

Transducer Assembly: The two transmitting crystals are mounted in a plexiglass assembly which is curved to fit the shape of the leg. The distance between the two crystals is set at approximately 2.5 cm. This spacing was selected as a compromise between computational accuracy and ease of fabrication. Crystals are cut from sheets of lead zirconium titanate transducer material (LTZ-2), with a resonant

frequency of approximately 2 MHz. The transmitting crystals are relatively large (5 mm diameter), in order to ensure an adequate signal level at the receiver. The receiving crystal is smaller (2 mm). Use of a small crystal makes the receiver less directional, but does not seriously reduce signal amplitude. All the crystals are fitted with lenses which produce a wider beam width than would be provided by the crystal alone.

B. Software Description:

The instructions necessary to operate the instrument are contained within the 2K ROM. This ROM contains, in addition to operating instructions, subroutines for floating point arithmetic and for conversion of floating point numbers into a code suitable for output to the LED display. Computations are carried to five significant figures.

The operating routines are designed to make use of the instrument as simple as possible. When the three-position selector switch is in the OPERATE position, pushing RESET causes the instrument to output a series of voltage levels on the analog output. These voltage levels produce a calibration record for the strip chart recorder.

The instrument next measures two chords and computes a baseline value for the cross-sectional area. Chords are then measured at a rate of about 10/s. Simultaneous with the analog output, the computed cross-sectional area is sent to the display. The analog output is scaled so that full scale deflection of the recorder represents +6% to -2% volume change.

Two digital filters are used to improve the appearance of the analog output. A slew rate filter serves to limit the effect of

occasional false comparator triggers. This filter functions by limiting to three steps the maximum change allowed in the 8-bit D/A convertor in one sampling interval. Thus, very large and sudden deviations are not passed to the output.

A one pole low-pass filter is used to reduce the effect of digitization and other noise on the analog output. This filter requires storage of one previous value of the output and one multiplication. Implementation, therefore, requires only a minimum of processor time and memory. In the current version of the software, the time constant of the filter is set at about 3 s.

Additional details regarding actual hardware and software implementation can be founded in Appendix C.

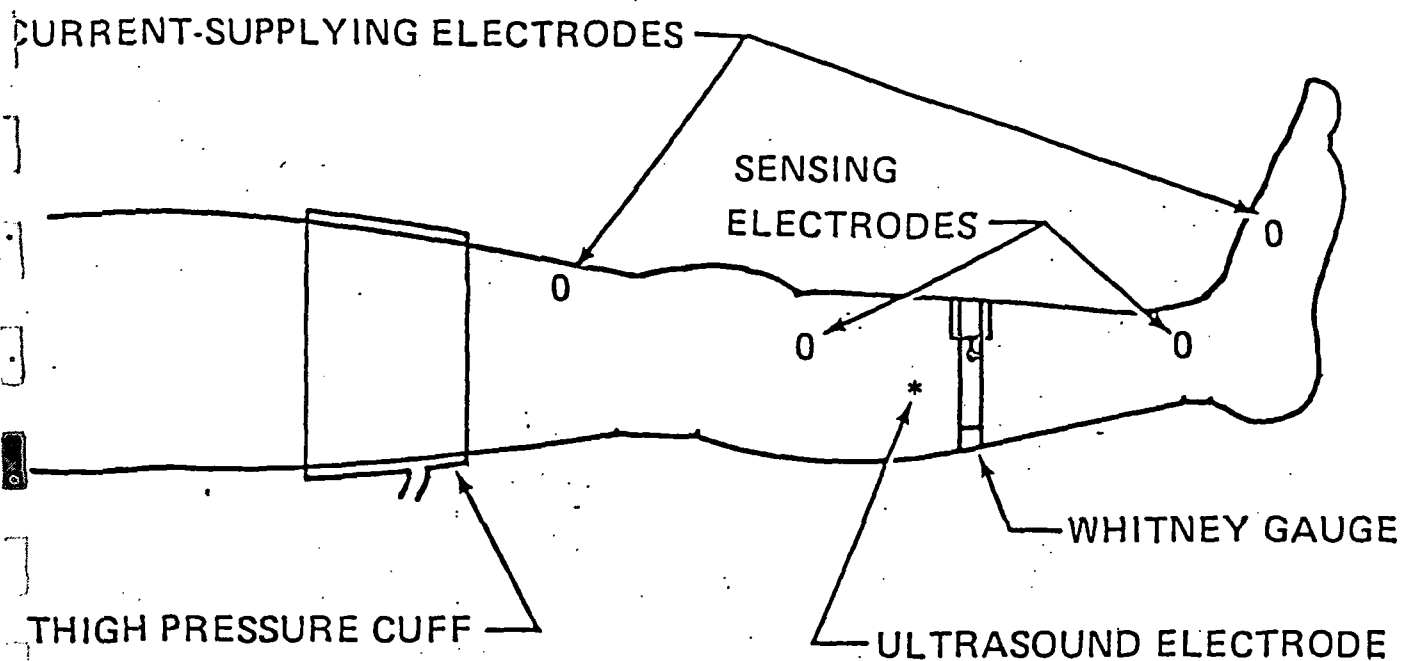
C. Operation of the Instrument:

To use the instrument, ultrasonic transducers must be properly attached to the subject's leg. Transducers are mounted using exercise EKG adhesive collars (Beckman). The transducers are attached first at midcalf level in such a way as to avoid passing the ultrasonic pulse through the bones of the leg. This is conveniently accomplished by placing the received transducer just to the inside of the tibia. The transmitter assembly is then moved around the rear half of the calf until adequate signals are obtained. By use of the three-position selector switch, the signal from either of the two transmitting crystals can be displayed on the oscilloscope screen. The position of the receiving transducer is adjusted until an acceptable signal is obtained from both transmitters. When such a position is found, the selector switch is set to the OPERATE position. Pushing RESET causes the instrument to produce a series of calibration levels before beginning to measure and output fractional changes in leg volume. The

analog output of the ULVS should be connected to a strip-chart recorder with ± 2.5 V full scale sensitivity.

Comparison of ULVS with other plethysmographic techniques:

The developed two transmitter ULVS was used in a study by NASA (22) to compare the sensitivity and accuracy of our methodology. A population of thirty subjects (50% male) was used. These subjects were non-paid volunteers (age 18-45), in good health with no evidence of varicosity. Tests were carried out in an environmental chamber with controlled temperature and humidity. The Whitney Strain Gauge was used as a standard and compared against our ULVS and an impedance plethysmograph. Figure 19 shows the system electrode placements and the results of a 50 mm Hg venous occlusion are shown in Figures 20. The correlation coefficient between the WSG and ULVS for the computed limb volume was 0.996. The maximum volume indicated by the ULVS was consistently higher than the corresponding WSG output. The impedance plethysmograph gave similar results when compared against WSG (22).



SITE OF ONE ULTRASOUND ELECTRODE IN WHITNEY/ULTRASOUND TESTING, SECOND ELECTRODE APPROXIMATELY 135° AROUND BELLY OF GASTROCNEMIUS MUSCLE.

= SITE OF IMPEDANCE ELECTRODES IN WHITNEY/IMPEDANCE TESTING.

FIGURE 19. SYSTEM ELECTRODE PLACEMENT

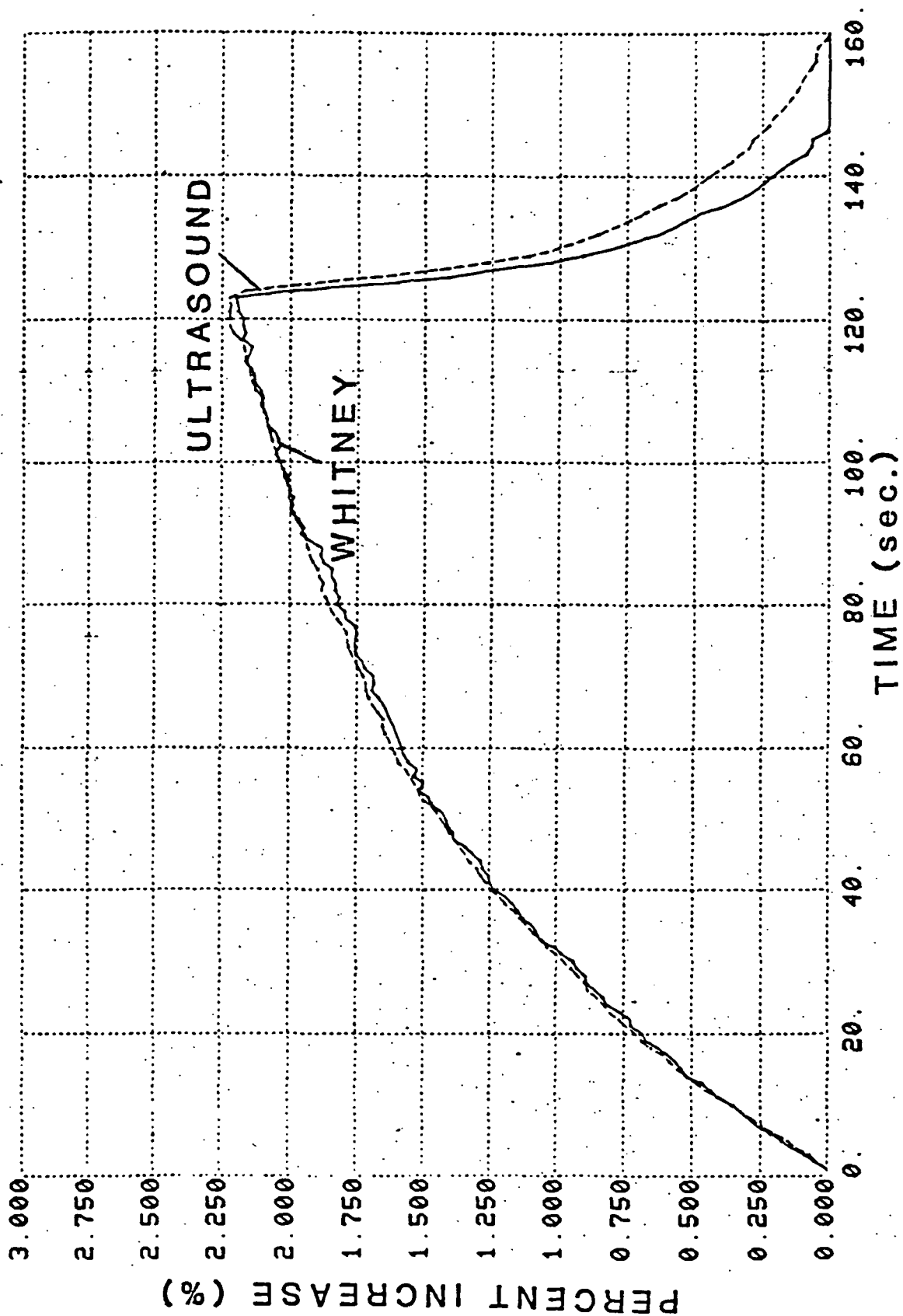


FIGURE 20. COMPARISON OF ULVS AND WHITNEY DIMENSION MEASUREMENT UNDER VENOUS OCCLUSION

AMBULATORY ULTRASONIC PLETHYSMOGRAPHY:

The following technical requirements were developed in consultation with responsible NASA personnel for fabrication of an ambulatory ultrasonic limb plethysmograph, ULP.

Overall System Requirement:

The contractor (equipment fabricator) shall be required to produce a flight qualified, portable four transmitter ultrasonic plethysmograph capable of measuring two limb cross sections simultaneously based on the designed two transmitter ultrasonic plethysmograph. The following additional constraints were also incorporated:

1. The ULP shall be capable of being attached to the crewmembers during launch and re-entry.
2. The ULP shall be capable of interfacing with the Experiment Data Interface (EDI) as specified.
3. The built-in Data Recording System (DRS) shall be capable of intermittantly recording ULP data during launch and re-entry.
4. The ULP shall operate on battery power.
5. The ULP shall be capable of operation from a DC power supply through an umbilical from the EDI.
6. The ULP shall be capable of operating continuously for 30 hours. One sample per second should be taken during this period.
7. The built-in DRS shall be capable of:
 - (a) Recording chord length sets determined at rates between one and ten times per second.
 - (b) Storing 1 to 4 megabits of data.
 - (c) Recording quiet period indications.
 - (d) Recording the 12 bit chord lengths generated by the ULP and the time associated with that data.
 - (e) Remotely turning on, taking data and then turning off.

General Design Requirements:

The total package for STS ULP shall be a portable, battery powered unit with dimensions not to exceed 2.5" x 5" x 8" including the batteries. The ULP shall not exceed .8 Kgs weight. The outputs of the ULP shall interface with the EDI. An on-off switch with an indicator light shall be provided on the ULP.

Data outputs from the ULP include:

1. An output of chord length D_1 digitally coded. This output interfaces the EDI.
2. An output of chord length D_2 digitally coded. Interfaces EDI and DRS.
3. Outputs of chord lengths D_1' and D_2' representing second leg cross-section, each digitally coded. These outputs interface the EDI and DRS.
4. Several outputs which can be accessed allowing internal parameters to be monitored. These outputs are defined under hardware test points (additional requirements).
5. Timing output and quiet period indications. These interface the EDI.

The ULP is made up of several subsystems which each perform a specified function. The subsystems should follow the specifications of the two transmitter ULVS developed at University of Kentucky and use minimization techniques to reduce size. Exceptions to these specifications are noted in the following:

Transducers

The ULP shall incorporate six piezoelectric crystals which are used as ultrasonic transducers. These transducers will be placed across the lower limb of the subject in two sets of three. Two of the transducers in each set act as transmitters of ultrasonic pulses, and the third transducer of each set acts as a receiver. The resonant frequency of these transducers is about 2.25 MHz.

Pinger Circuit

The pinger circuit shall provide the capability to excite a preselected ultrasonic transmitter by inducing a 100 to 150 volt, 10 nanosecond positive pulse. Modifications shall be made to eliminate the need for a -15V power supply.

Controller Logic, Transmitter Select and Counter

The function of this subsystem is to control the flow of information throughout the system, to select a transmitter for chord length measurement and to provide a count proportional to the measured ultrasonic transit time. The basic counter frequency shall be 18 MHz for this subsystem. This system supplies the following functions:

1. Provides interfacing to processor.
2. Provides mode selection for transducer placement and ultrasonic signal visualization.
3. Starts and stops counter.
4. Inhibits receiver section for an adjustable period of time to reduce the possibility of false output.
5. Selects the transmitter that is to be activated.

Receiver Circuit and Comparator

The ultrasonic signal receiving amplifier shall have a gain of 60 dB (min) and have standard wide band video capabilities. The receiver shall be transformer coupled to the ultrasonic transducer to provide high common mode rejection. The signal to noise ratio (SNR) shall be at least 40 dB. The comparator shall be a level detector at 0.2 ± 0.02 V measured at the output of the receiver amplifier.

Processor and Memory

This subsystem provides a timing signal for operation of the ULP. The timing signal shall be derived from a 18.0 MHz clock which will also be used for the binary count. A microprocessor, equivalent to

the 8080, shall be used for all command and store operations. The computational constants and instructions should be stored on permanent memory. Data output shall be interfaced through the processor. This subsystem shall drive a display on the ULP. The processor shall also provide command operations to the DRS.

Additional Requirements:

Hardware Tests Points

A connector shall be accessible which allows the following phenomena to be monitored:

1. The analog signals of the transmitters.
2. The analog signals of the receivers.
3. The comparator output. (digital)
4. The calculated cross sectional area measurement.
5. The 18 MHz time base. (digital)
6. The Pinger voltage

Self-Test Button

This button should be available to activate programmed inputs into the processor for calibration and check-out.

Quiet Period Indicator

An indicator for quiescent periods and sleep period shall be incorporated into the design of the ULP. These indications are to be imposed on the data.

Physical Configuration

Throughout the design phase of the program, weight, volume and power consumption minimization shall be a prime consideration within the measurement, operational and environmental constraints imposed herein. The ULP electronics shall be configured in one package. An

on-off switch shall be supplied on the electronics package. This package shall be two output connectors. One output shall provide chord transit time data, timing outputs and quiet period indications. The other output connector shall be able to provide all internal information which is required herein. The package shall be easily attached to the crewmembers and be comfortable to wear.

Range

The ULP shall have the capability to demonstrate the following characteristics:

1. Provide reliable measurements on calf lengths up to 18 cms corresponding to limb circumference of approximately 57 cms.
2. Duration of a single cross sectional area measurement shall not exceed 50 mseconds.
3. The chord length measurement must be accurate to within ± 0.6 mm for a nominal chord length of 14 cms.
4. The digital counter shall be 12 bits.

Calibration

The capability to inject appropriate calibration and test signals into the STS ultrasonic plethysmograph just prior to initiation of a data gathering sequence should be provided. This will be initiated whenever the self-test button is depressed.

Display

A four digit display shall be provided on the ULP which displays instantaneously to the crewmembers the measured chord length of the limb cross-sectional area. The display shall be visible to the crewmembers at all time during operation.

Battery Monitor

The ULP system shall have a battery check system and a warning if the battery power is low.

Optimum Signal Locator

A method of detecting transducer placement for the optimum signal without using an oscilloscope shall be incorporated. This method can be an envelope detector. A blinking display can be used to show that the optimum signal is not being received.

Ground Support Equipment

The Ground Support Equipment (GSE) to be developed in support of this program shall include as a minimum the following:

1. Playback equipment to allow playback of tapes recorded by the DRS.
2. ULP Data Interface Simulator (DIS). The DIS will be designed to emulate the ULP Data Interface with the EDI in amplitude, impedance, and format content to allow development and verification of hardware and software in, and down-stream of, the EDI. DIS electrical connectors need not be flight type.

The tape playback equipment should be supplied at the time of delivery of the first ULP prototype system containing a built-in DRS.

Delivery of the DIS will be required at least two months prior to delivery of the ULP prototype in order to allow timely development of the EDI and associated hardware and software.

Denver Research Institute, DRI, fabricated a prototype test unit for our evaluations in accordance with a test plan developed by us. Results of these tests are detailed in the "Appendix B".

TRANSDUCER DEVELOPMENT

The use of an ultrasonic micrometer in limb plethysmography has been described in this report (page 6). This technique, ultrasonic pulses are created through shock excitation of a piezo-electric transducer. After transit through the coupling medium, a second piezo-electric transducer converts the acoustic energy into an electrical signal. If the sound velocity in the medium is known and constant, the propagation time between the two crystals is an accurate measure of the separation distance. Arrival of the pulse at the receiver crystal is detected by the triggering of a comparator set just above the noise level of the receiver amplifier. In the usual situation the received signal level is very much larger than the noise level; changes in comparator firing time can then be confidently interpreted as changes in tissue dimension. If pulse amplitude is not much higher than the comparator level, however, small changes in signal amplitude or pulse shape will cause changes in comparator firing time. This will be falsely interpreted as a change in tissue dimension. Although these considerations are important in all applications of sonomicrometry, they are especially critical in plethysmographic applications, where very small dimension changes are measured.

To routinely obtain good signals, it is essential that well-designed transducers be available. The most critical requirement is that the beam pattern of the transducers must be sufficiently wide. Adequate signal amplitude can then be obtained with minimum care in placement of the transducers. In addition, small rotations of the transducers, which may occur during a limb expansion, will not affect

pulse shape substantially.

Two basic types of transducers for ultrasonic dimension measurements have been described in the literature, chiefly for use in cardiac dimension measurements. One type is constructed from a disk cut from flat stock piezo-electric ceramic. Size of the disk may vary from 2 mm to 5 mm in diameter, with the smaller diameters having the wider beamwidth. A convex plastic lens is added to diverge the beam [14,15,16]. This type of transducer has the advantage that it is inexpensive and simple to construct. The beamwidth of the transducers, however, is quite narrow, even with the addition of a diverging lens. Thus, careful orientation of the transducers is required. Small rotations of the transducers may produce relatively large changes in pulse amplitude and shape even after careful placement of the transducers on the tissue.

A second type of transducer has been more recently described [27]. This transducer uses a hemispherically shaped piezo-electric element which produces a broad beam pattern. A quarter wavelength matching layer between the ceramic and the tissue was used to maximize signal amplitude. With this approach, much less care in placement of the transducers is required. The hemispherical transducers are, however, quite expensive, and construction of the matching layer is somewhat difficult.

Although the problems encountered are similar, the transducers used in cardiometry are not ideal for use in plethysmography. In particular, transducers used for plethysmography require a rugged housing and a convenient means of attaching the housing to the skin. In this report we describe the design and construction of transducers specifically designed for plethysmographic applications, and provide

details on the performance of these units.

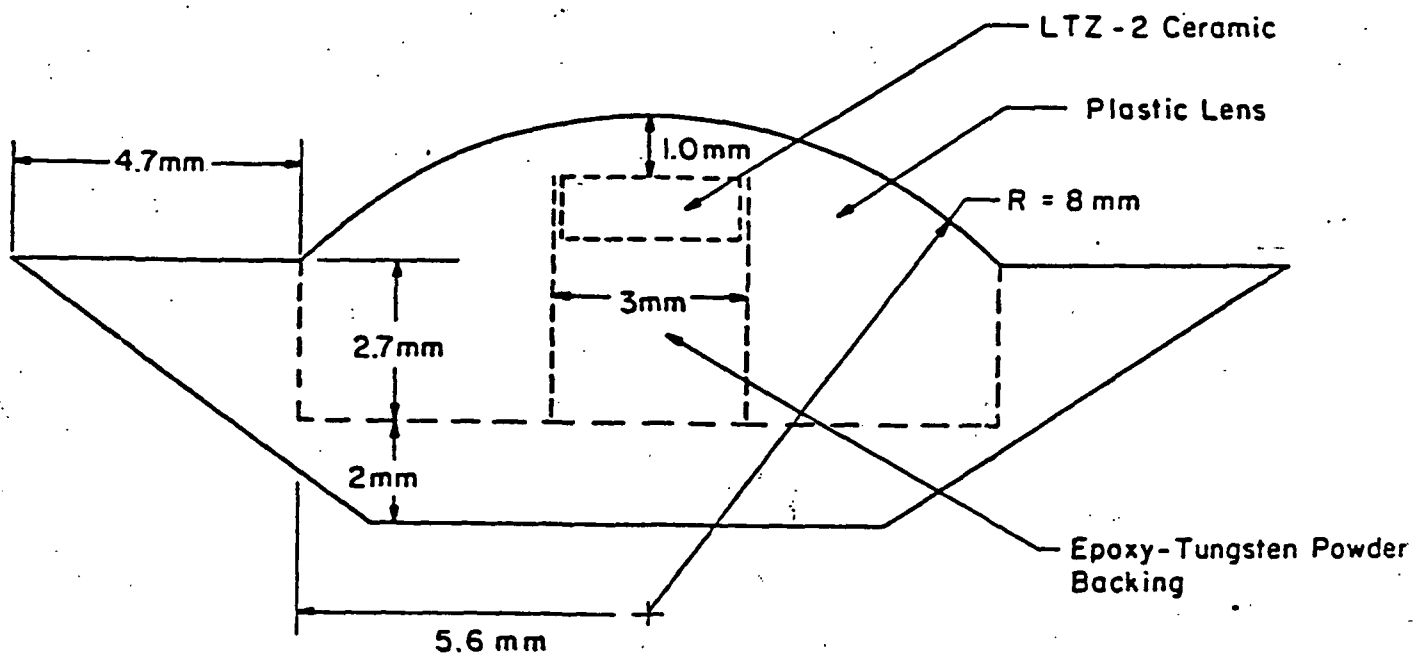
Design Considerations

For attaching the ultrasonic transducers to the skin, it is convenient to use a housing of the same size and shape as that used with exercise EKG electrodes. The transducers may then be very simply attached with double-sided adhesive collars. With the size of the external housing determined, it is necessary to consider the optimum design of the transducer mounting within the housing. Both the hemispherical and the flat plate transducer designs have been mounted within the housing. We will first consider the flat transducer.

Small flat-plate ultrasonic transducers produce a wider beam, and the electrical impedance of ceramic transducers is reasonably low even for small transducers. Thus, for this application flat plate transducers should be as small as possible. For measurements across the calf, a transducer frequency of 2 MHz offers a convenient compromise between signal attenuation, which increases with frequency, and transducer thickness, which decreases with frequency. At 2 MHz the ceramic material is approximately 1 mm thick; the smallest disc which can be reproducibly cut from this material is about 3 mm in diameter. These considerations determine the size of the transducer element.

Because addition of a convex lens will diverge the beam pattern somewhat, it is desirable to include a lens in the design. If the lens is allowed to protrude into the tissue slightly, it will also serve to provide good acoustic coupling between the transducer and the tissue. The implementation of this concept is shown in Fig.21A, where a 3 mm diameter transducer is shown mounted behind a lens which

A.



B.

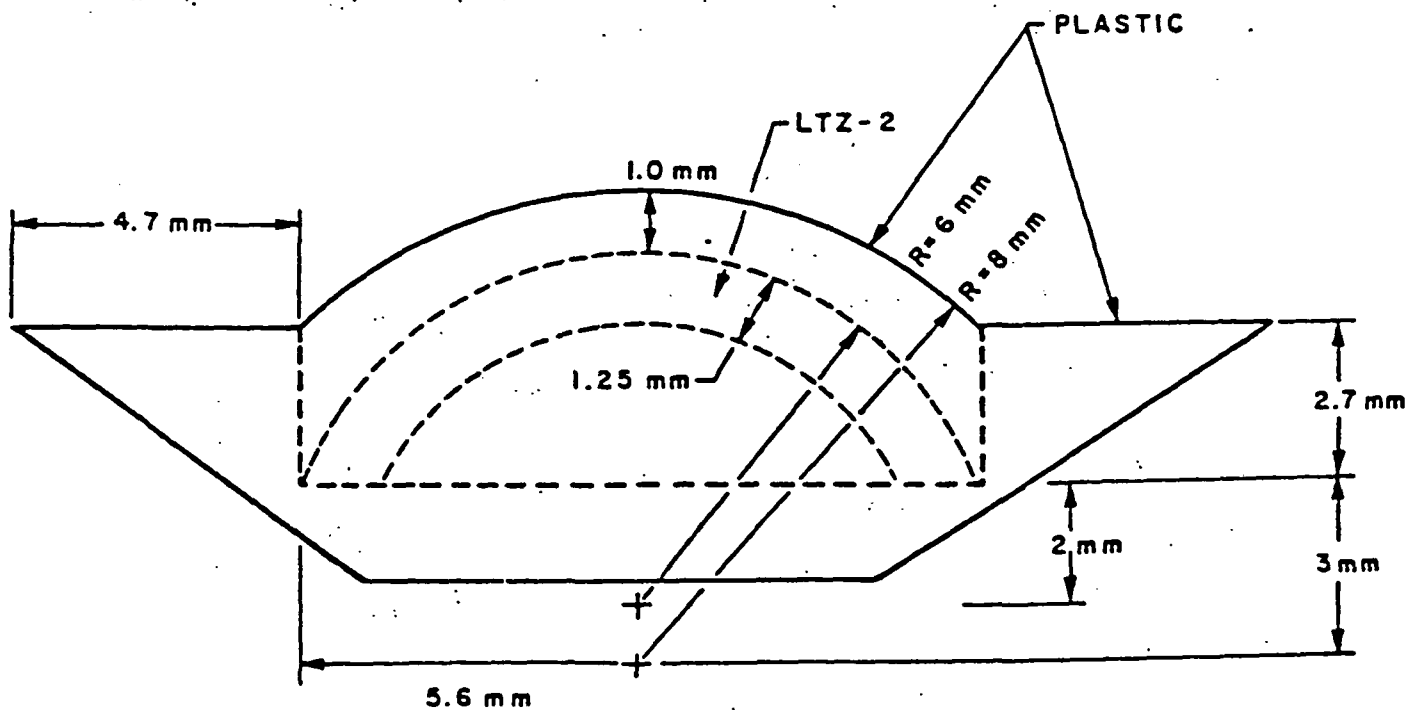


FIGURE 21. Design of Flat and Hemispherical Transducers

a 3 mm diameter transducer is shown mounted behind a lens which protrudes 3 mm into the tissue. The lens is mounted within the EKG housing to provide a space for attachment of the adhesive collars.

Hemispherical transducers may be mounted similarly within a housing of the same external shape as that used for the flat transducers. Because the hemisphere radiates in all directions, no lens is necessary; however, it is convenient to allow the transducer to protrude into the tissue to provide good acoustic coupling. Although hemispherical transducers are available in several diameters, there is no reason to expect significant differences in performance for different diameters. A more critical question is the design of the coupling layer between the crystal and the tissue.

Signal amplitude produced by an ultrasonic transducer may be increased somewhat by placing a quarter wavelength thick matching layer between the ceramic and the tissue [27]. This approach is routinely used in design of transducers for imaging applications [28]. In dimension gauges, however, signal levels are normally very high compared with those encountered in imaging; the wide beam pattern produced by hemispherical transducers enable strong signals to be obtained even when the crystals are badly misaligned. Thus, increasing the signal strength by several dB is of marginal value. The quarter wave length matching layer is very thin (<0.3 mm) and, thus, is difficult to fabricate and is subject to damage from abrasion. The capacitive coupling between the outer conductive coating of the crystal and the subject is large when a thin dielectric layer is used. The coupling can introduce high frequency noise into the system. For these reasons, the developed transducers use a coupling layer with a minimum thickness of 1 mm. Because this layer is more than one

wavelength thick, the second half-cycle of the received signal is not affected by reflections within the matching layer. Yet the layer is sufficiently thin so that attenuation within the layer is negligible. The implementation of this concept with a hemisphere of 12 mm diameter is shown in Fig. 21B.

Transducer Construction

Construction of the hemispherical receiver transducers is illustrated in Fig. 22. Three major elements are used to assemble the finished transducer. The plastic lens is molded from epoxy resin (STYCAST LN 78058, Emerson and Cuming, Canton, Mass.) in a machined teflon mold. After casting and curing, the back of this lens is machined with a ball mill to fit the hemispherical transducer. The transducer element is obtained commercially (Channel Industries, Santa Barbara, California) as a complete hemisphere. Teflon-insulated stainless steel leads (33 gauge, Cooner, Chatsworth, California) are carefully soldered to the inner and outer conductive coating of the crystal using a zinc chloride flux and ordinary solder. The crystal is then cemented into the plastic lens. A silastic tube is slipped over the leads. This assembly is mounted inside the pre-cast plastic exercise EKG electrode housing (Blackwell Plastics, Houston, Texas). The space between the plastic lens and the housing is sealed with non-corrosive silastic sealant (3140 RTV, Dow Corning Corp., Midland Mich).

Hemispherical transducers are available in several sizes, with the smallest being 6 mm in diameter with a resonant frequency of 3.8 MHz. Crystals resonant 2 MHz are available with a diameter of 12 mm and 9 mm. Any of these elements can be mounted within the lens

Receiver:

Receiver Lens



Receiver Crystal



Housing



Connecting Cable
(Stainless Wire in Silastic Tube)

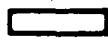


Transmitter:

Transmitter Lens



Transmitter Crystal



Housing



Connecting Cable
(Stainless Wire in Silastic Tube)



FIGURE 22. Construction of Receiver and Transmitter Elements

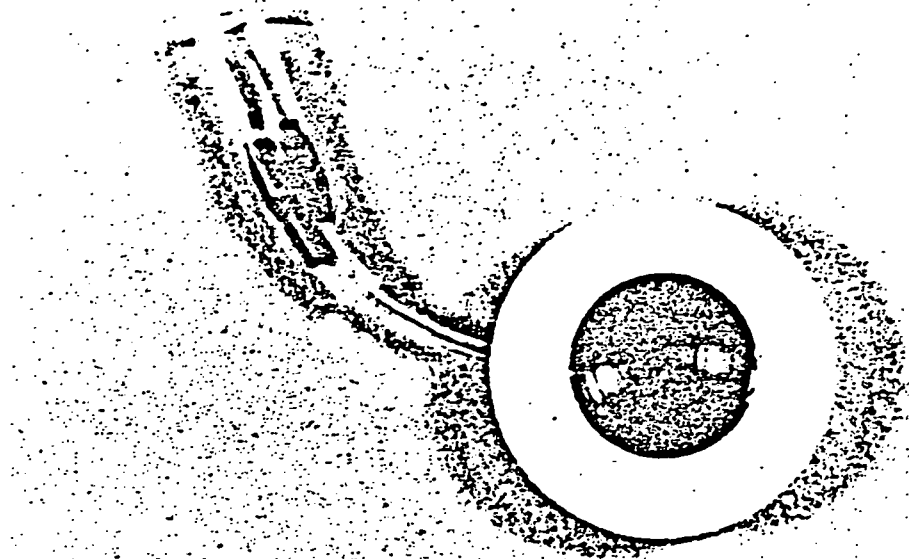
structure.

The housing of the flat transmitter transducer is accomplished in a similar manner. A 3 mm diameter disc is cut from a plate of LTZ-2 transducer material resonant at 2 MHz (Transducer Products, Inc., Gophen, Conn.). Leads are attached as before and the transducer is cemented into a cavity machined into the cast plastic lens. The assembly is then cemented into the plastic housing as before.

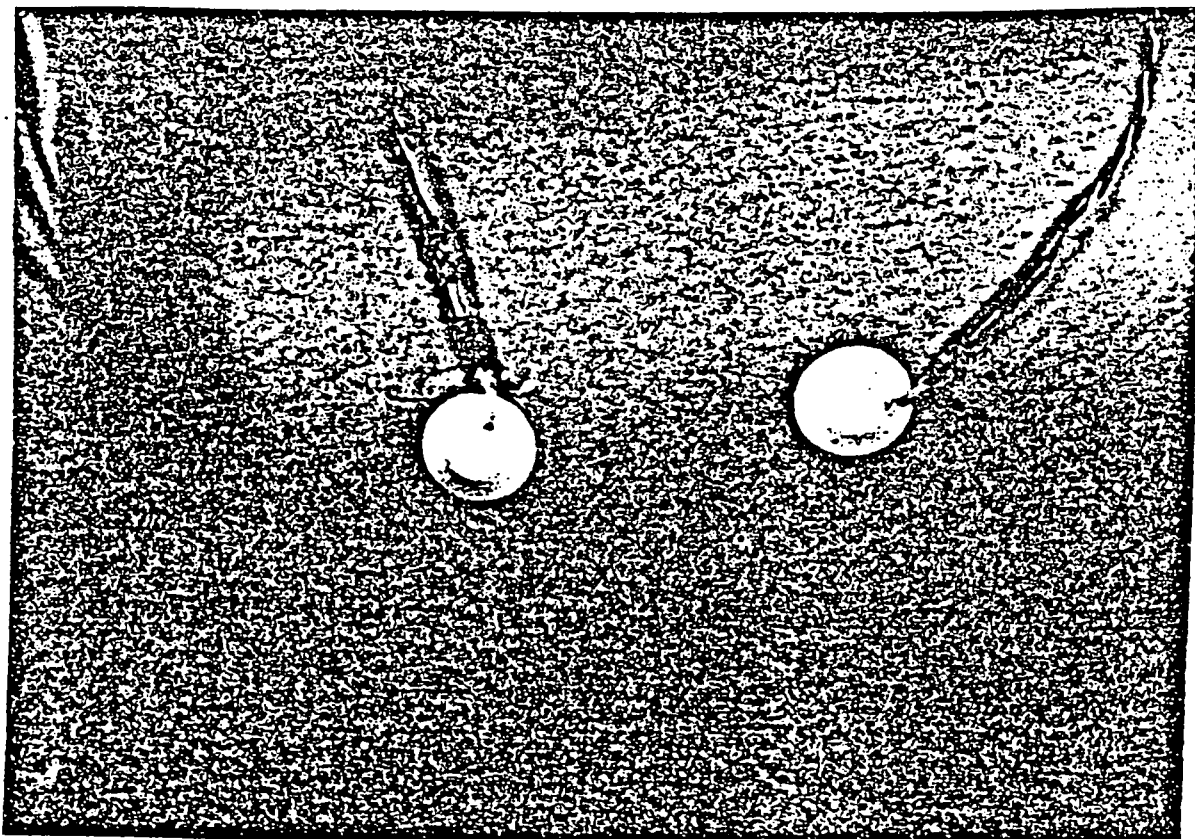
Transducer Performance

The external appearance of the developed transducers is depicted in Figure 23A. Fig. 23B shows the appearance of the transducers after attachment of the calf. Transducers are attached at two sites to allow simultaneous measurement of two chords. The adhesive collars provide a firm attachment which can be maintained for several days. Use of a very small quantity of acoustic coupling gel provides improved signal transmission in short-term attachment. For long-term experiments, gel is not necessary because normal skin secretions provide adequate coupling after several minutes attachment.

The most important characteristic of the transducer is the extent to which rotation off-axis reduces signal amplitude. Measured performance of the two transducer types is shown in Fig. 24. Two transducers were suspended in an acoustic test range, separated by 10 cm. In all tests a 3 mm diameter transducer was excited using a standard pulser to produce a constant acoustic signal. The transducer under test was connected to an amplifier having an input impedance of 50 ohms. The tested transducer was rotated in 5 degree increments and beam strength was determined by adjusting a calibrated attenuator to return the amplitude of the second half-cycle to the level obtained at



A. External Appearance



B. Attached to Mid-calf Region

FIGURE 23. The Developed Ultrasonic Transducers

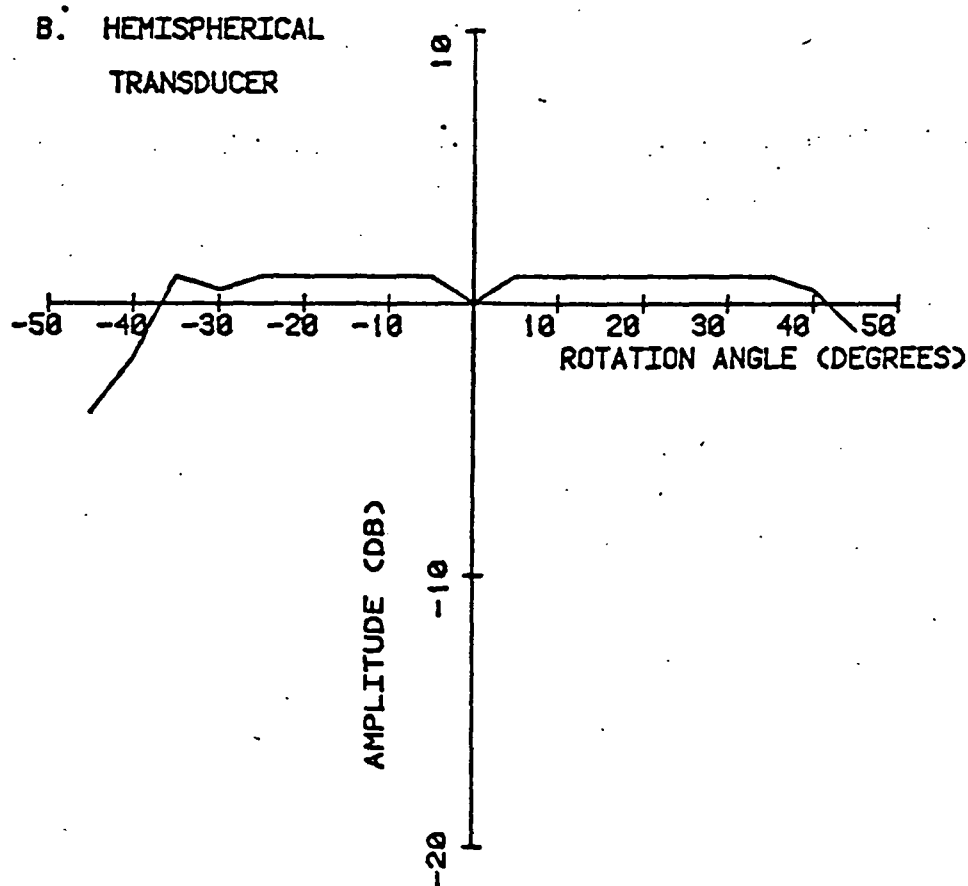
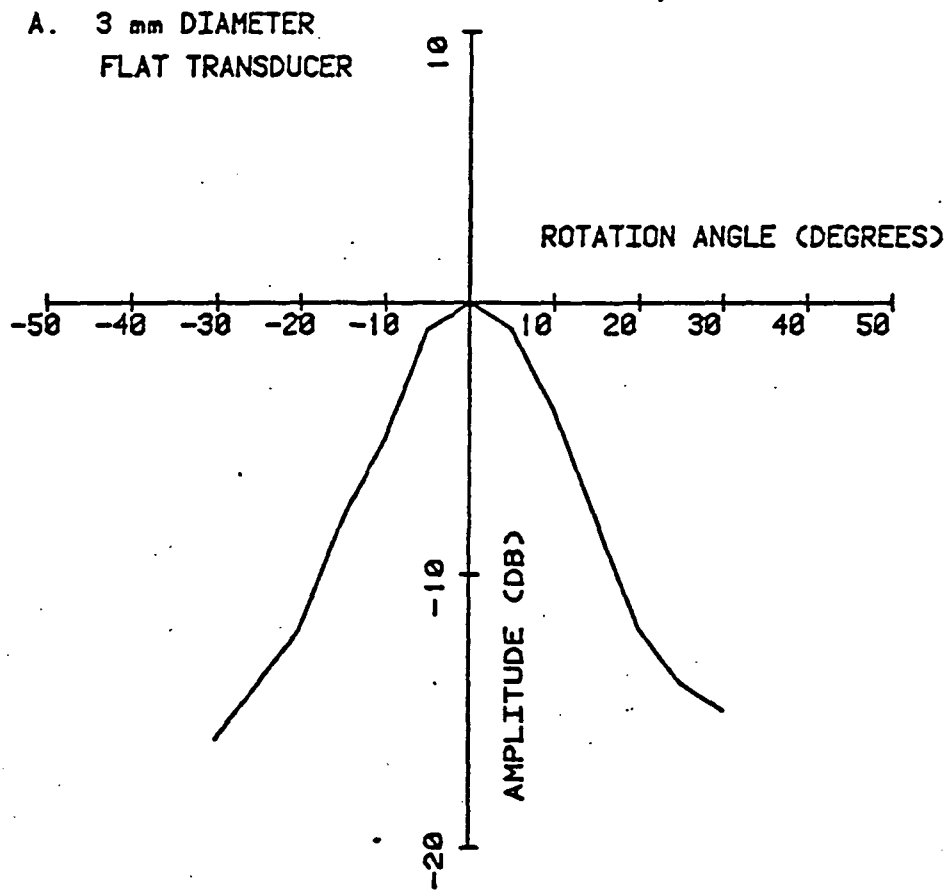


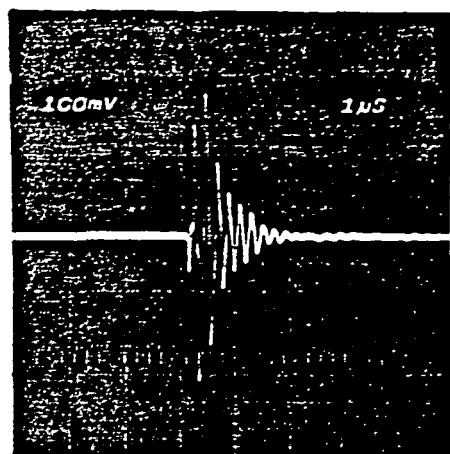
FIGURE 24. Off Axis Performance of Transducers

0 degrees. As expected the flat transducer is quite directional. The response of the hemispherical transducer is unaffected by rotation over the range of +40 to -40 degrees. Fall off of the response beyond this angle is probably due to interference within the plastic lens. The beam width of the hemisphere could be improved by protruding the lens further, but this would cause unnecessary distortion of the tissue and possible discomfort to the subject.

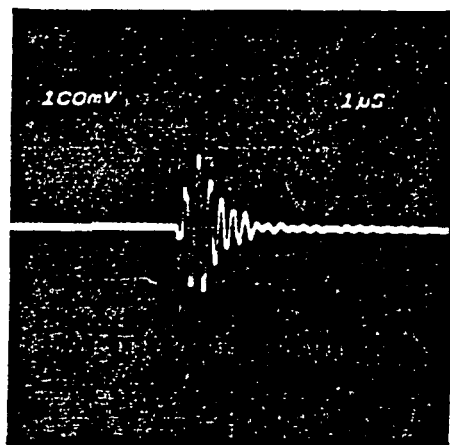
The directional characteristics of the transducers is further demonstrated in Fig. 25, where recorded pulses are shown. With the flat transducer the pulse shape remains unaltered with rotation, but the amplitude decreases sharply. The pulse shape of the hemispherical transducer is more complex, and changes with rotation; however, the amplitude and shape of the first cycle of the received pulse are almost unaffected by rotation. Because pulse arrival is determined by triggering a comparator on the second half-cycle of the received pulse, the remainder of the pulse is unimportant for plethysmographic applications.

In design of associated electrical circuitry, knowledge of the electrical behavior of the mounted transducers is necessary. Impedances of the two transducer types were measured in air, using an impedance meter (HP model 4815A). The flat transducer, because of its smaller size, presents a relatively large impedance (approximately 800 ohms at resonance) and behaves as a much more reactive (capacitive) load. The hemispherical transducer displays an impedance of only 80 ohms and behaves as a nearly resistive load at resonance. At very high frequencies the impedance of both transducers decreases sharply due to the parallel capacitance of the crystal.

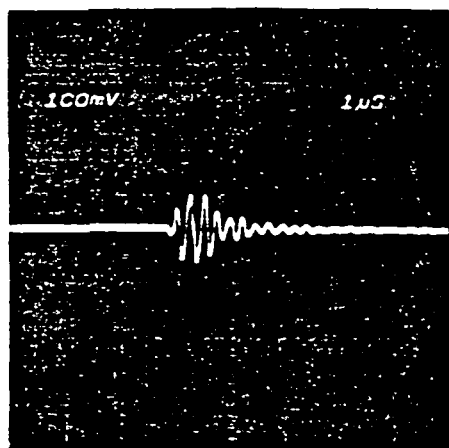
FLAT TRANSDUCER



0°

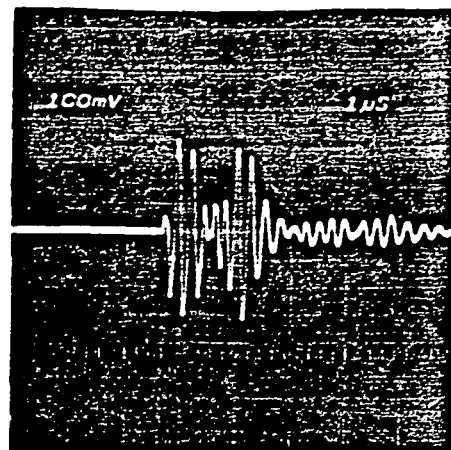


10°

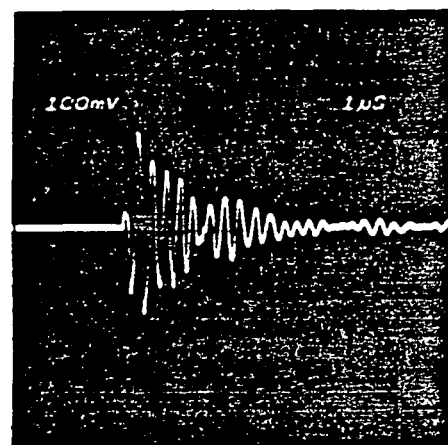


20°

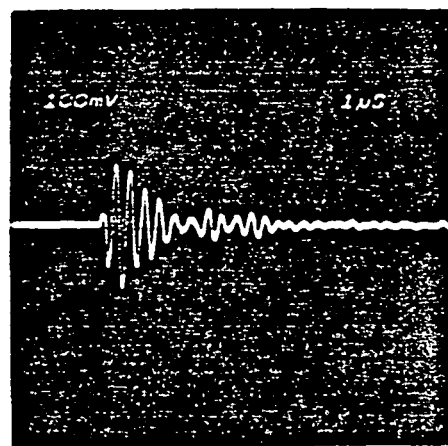
3/8 INCH DIAMETER HEMISPHERICAL TRANSDUCER



0°



20°



40°

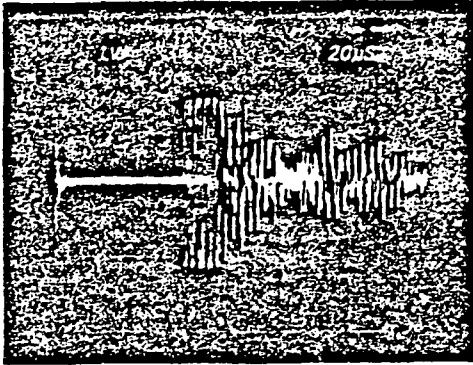
FIGURE 25. Directional Characteristics of Ultrasonic Transducers

Use of the Transducers

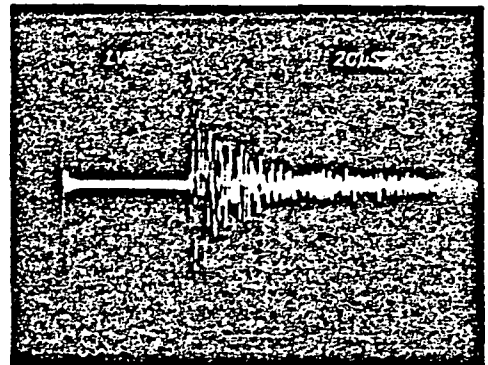
Although these transducers may be used interchangeably as receiver and transmitter, when the two are used in combination it is often convenient to use the flat transducer as a transmitter and the hemisphere as a receiver. Because of the high voltage and current required, changing impedance and voltage levels in the pulser requires extensive redesign of the circuit. The low impedance of the hemispherical transducer at high frequencies may load the pulser of some dimension gauges excessively. The flat transducer, however, will produce negligible loading. On the other hand, when the hemisphere is used as a receiver, the low impedance of the hemisphere can easily be matched to the higher impedance of the RF amplifier by use of the step-up transformer, producing a higher voltage input. The low impedance of the hemisphere allows use of the relatively long cable without significant capacitive loading of the transducer.

The use of two hemispheres provides most freedom in placement of transducers when a sufficiently low-impedance pulser is used. This is illustrated in Fig. 26A, where signals passed though a calf of 38 cm girth are reproduced. To provide a reference for location of the transducer, the zero point of a cloth tape measure was attached to the leg at the sharp point of the tibia with the numbers increasing toward the inside of the leg. The tape was then wrapped loosely about the calf, and attached with adhesive tape. Positions of transducers were determined by recording the tape number nearest the transducer. Positions were then computed as angular deflections as if the cross-section of the calf were circular.

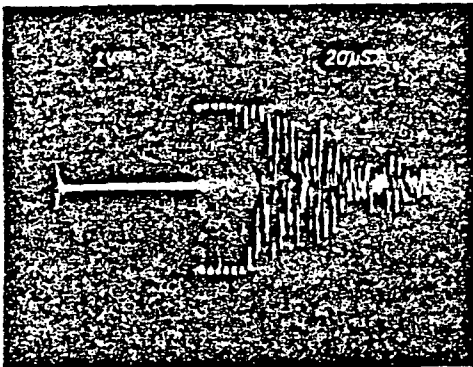
A hemispherical transducer was attached to the calf at 76 degrees



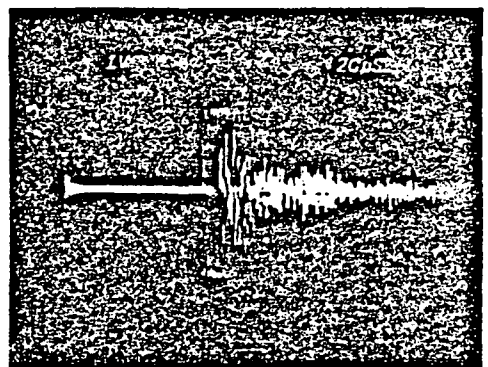
76/208



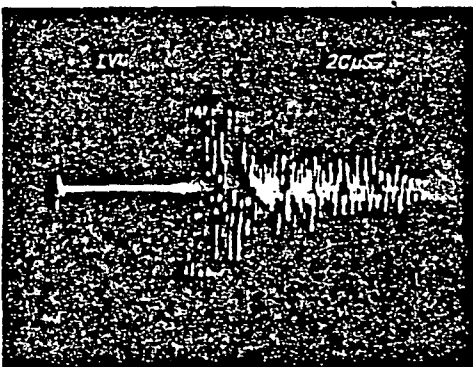
76/208



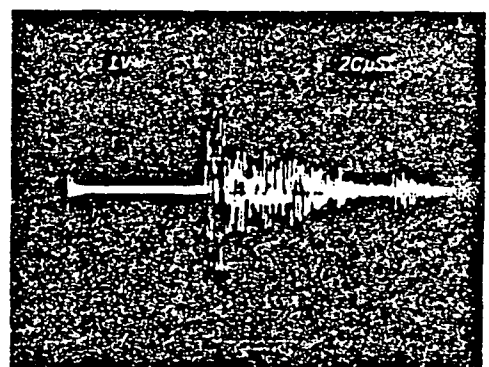
76/246



76/237



76/293



76/246

HEMISPHERE/HEMISPHERE

HEMISPHERE/FLAT

FIGURE 26. Comparison of Performance of Different Transducer Combinations

the lower edge of the tibia by palpation and then moving several cm down the calf. This location is optimum for the plethysmographic measurement: Placing the transducer further down the calf forces passage of the signal through the fibula; placing the transducer nearer to the tibia causes transducer movement to be restricted by the bone. The transmitting transducer was then placed at selected locations, as indicated in the Figure 26. Excellent signal quality was obtained as one of the transducers was moved over an 85 degree arc on the calf. The receiver amplifier is saturated on the second half-cycle of the received signal in each photograph.

In most situations the combination of a hemisphere as receiver with a flat crystal as transmitter provides very good results, although the range from which adequate signals can be obtained is smaller (Fig. 26B). Performance of this combination is due to the anatomy of the calf and the attachment procedure used. The receiver crystal (hemisphere) is first attached; the transmitter (flat) crystal is then placed against the opposite side of the leg and adjusted until maximum signal level is obtained. Thus, the directional transducer is adjusted until it is aimed at the receiver. This procedure is far simpler than would be the simultaneous adjustment of two directional transducers.

When flat transducers are used as both receiver and transmitter, signal quality is found to vary dramatically with small changes in transducer location. Small rotations of the transducer will also produce significant changes in the shape of the received pulse. These pulse shape changes are due to the narrow beam width of the flat transducers.

Both the combinations illustrated in Fig. 26 have been tested extensively both in short term physiological experiments and in long term attachment tests. Good signal quality is routinely obtained with minimal training of operators. In long-term attachment tests of up to 7 days no discomfort has been noted; signal quality is maintained so long as the transducers are firmly attached.

Summary and Conclusions:

The development of ultrasonic dimension measurement principles into a laboratory instrument providing plethysmographic data has been detailed in this report. The developed instrument has been compared with the Whitney strain gauge and an impedance measuring device and shown to yield consistent and reliable results.

In human subjects undergoing provocative maneuvers such as venous occlusion and tilt experiments the results have been shown to be repeatable and reliable. The major aim of this project was to develop instrumentation which freed the investigator from the transducer related problems of the capacitance plethysmograph and this was achieved. Since the developed plethysmograph uses transducers on opposite sides of the limbs, the integrity of movement is not compromised and also individualized transducer configurations are not required.

The transformation of the above instrument into a flight certified unit was carried out by Denver Research Institute. This unit has been fabricated and tested in accordance with the procedures developed in the report and is a part of NASA supplied LSLE item.

Theses, Dissertations and Publications:

The following theses, dissertations and publications resulted from the support derived from this research contract.

- i. Murali P. Kadaba
"Tissue characterization using ultrasonic transmission and scattering parameters." Ph.D., 1978, Co-director - Dr. J. F. Lafferty.
- ii. An ultrasonic plethysmograph, P. K. Bhagat, J. F. Lafferty and M. P. Kadaba, Aerospace Medical Association 1979 Meeting, Washington, D. C., May, 1979.
- iii. A microprocessor based ultrasonic data acquisition and analysis system, P. K. Bhagat, M. P. Kadaba and V. Wu, AAMI 14th Annual Meeting, Las Vegas, May, 1979.
- iv. Utility of acoustic parameters for remote characterization of tissues, P. K. Bhagat and M. P. Kadaba, Fourth Midwest Biomedical Engineering Conference and Workshop, Columbus, Ohio, May 4-5, 1979.
- v. A microprocessor based system for ultrasonic tissue characterization, P. K. Bhagat, M. P. Kadaba, V. N. Gupta, and V. Wu, Medical Instrumentation, 14(4), 220-224, 1980.
- vi. Attenuation and backscattering of ultrasound in freshly excised animal tissues, M. P. Kadaba, P. K. Bhagat, and V. Wu, I.E.E.E. Transactions on Biomedical Engineering, BME-27(2), 76-83, 1980.
- vii. An ultrasonic plethysmograph for space flight applications, P. K. Bhagat, J. F. Lafferty, D. Bowman, and M. P. Kadaba, Aviation, Space and Environmental Medicine, 51(2), 185-188, 1980.
- viii. Ultrasonic characterization of aging in skin tissue, P. K. Bhagat, W. Kerrick, and R. W. Ware, Ultrasound in Medicine and Biology, 6, 369-375, 1980.
- ix. Estimating ultrasound propagation velocity in tissue using unwrapped phase spectra, V. N. Gupta, P. K. Bhagat, and A. M. Fried, Ultrasonic Imaging, 2, 223-231, 1980.
- x. Significance of phase of an ultrasonic pulse in tissue characterization, V. N. Gupta, P. K. Bhagat and A. M. Fried, Fifth Midwest Biomedical Engineering Conference and Workshop, Columbus, Ohio, May 30-31, 1980.

- xi. A two transmitter ultrasonic plethysmograph, P. K. Bhagat, V. C. Wu, W. T. Nickell and P. K. Kadaba. Fifth Midwest Biomedical Engineering Conference and Workshop, Columbus, Ohio, May 30-31, 1980.
- xii. Ultrasonic pulse broadening due to tissue inhomogeneities, V. N. Gupta, P. K. Bhagat, A. M. Fried, and M. P. Kadaba. Fifth International Symposium on Ultrasonic Imaging and Tissue Characterization, Gaithersburg, Maryland, June 1-4, 1980.
- xiii. Vic C. Wu
"A microprocessor based ultrasonic limb volume measurement system." MSEE, 1980, Co-advisor with Dr. T. L. Henderson.
- xiv. Vaikunth N. Gupta
"Ultrasonic tissue characterization via homomorphic transform." Ph.D., 1980.
- xv. Ruth A. G. Dyer
"Classification and characterization of tissue pathology through ultrasonic signal analysis." Ph.D., 1980.
- xvi. A comparison of limb plethysmograph systems proposed for use on the space shuttle, B. M. Levitan, J. Zieglschmid, L. D. Montgomery and P. K. Bhagat, Aerospace Medical Association 1981 Meeting, San Antonio, Texas, May, 1981.
- xvii. Ultrasonic properties of normal and functionally impaired renal tissue, V. N. Gupta and P. K. Bhagat. Sixth International Symposium on Ultrasonic Imaging and Tissue Characterization, Gaithersburg, Maryland, June 1-4, 1981.
- xviii. Application of orthogonal transforms for classification of myocardial backscattered signals, R. A. G. Dyer, S. A. Dyer, W. O'Connor, and P. K. Bhagat. Sixth International Symposium on Ultrasonic Imaging and Tissue Characterization, Gaithersburg, Maryland, June 1-4, 1981.
- xix. Mark Shafer
"The application of homomorphic processing to ultrasonic signals." MSEE, 1981, Co-director, Dr. B. J. Leon.
- xx. Clinical applications of ultrasonic plethysmography, P. K. Bhagat, V. C. Wu, and W. T. Nickell, 17th annual meeting AAMI, San Francisco, California, May, 1982.
- xxi. Homomorphic processing of backscattered ultrasonic signals from normal and functionally impaired renal tissue, P. K. Bhagat, M. E. Shafer, W. T. Nickell, and V. N. Gupta, Seventh International Symposium on Ultrasonic Imaging and Tissue Characterization, Gaithersburg, Maryland, June, 1982.
- xxii. Ultrasonic quantification of skin and muscle hemodynamics, P. K. Bhagat, W. T. Nickell, and V. C. Wu, First Southern Biomedical Engineering Conference, Shreveport, Louisiana,

June, 1982.

- xxiii. Ultrasonic characterization of acute renal failure, V. N. Gupta, P. K. Bhagat, C. E. Ott, and A. M. Fried, Ultrasound in Medicine and Biology, 8, 249-261, 1982.
- xxiv. A practical ultrasonic plethysmograph, V. C. Wu, W. T. Nickell, and P. K. Bhagat, Aviation, Space and Environmental Medicine, 53(4), 375-388, 1982.
- xxv. Transducers for ultrasonic plethysmography, W. T. Nickell, V. C. Wu and P. K. Bhagat, Aviation, Space and Environmental Medicine, 54(5), 458-463, 1983.
- xxvi. Ultrasonic quantification of skin and muscle hemodynamics. P. K. Bhagat, W. T. Nickell and V. C. Wu, Proceedings First Southern Biomedical Engineering Conference, Shreveport, Louisiana, June, 1982.
- xxvii. A comparison of limb plethysmograph systems proposed for use on the space shuttle, B. M. Levitan, L. D. Montgomery, P. K. Bhagat and J. F. Zieglschmid, Aviation, Space and Environmental Medicine, 54(1), 6-10, 1983.

APPENDIX A

Background Data on Transducers

A. Piezoelectric material properties

Ferroelectric crystals are among the ceramic materials which do not have identical centers of positive and negative charges. A necessary but not sufficient condition for a solid to be ferroelectric is the absence of a center of symmetry of electrical charges. This type of material such as quartz, either elongates or contracts upon the application of an electric field. This dimensional change is due to the effect of the applied electric field on the dipole length. Such behavior in the ferroelectric material provides a means of converting electrical energy into mechanical energy. The crystal vibrates with the frequency of applied alternating field and in proportion to the voltage differential. This property of ferroelectric materials of dimensional changes upon the application of an electric field has led to the electro-mechanical transducer devices, which are commonly used for the production of high frequency sound waves.

In piezoelectric material the converse effect exists, i.e., upon the application of mechanical stress to the crystal, an electric potential is produced which is proportional to the applied stress. There are 21 classes of crystals which can be classified as ferroelectric material (24). Twenty of these materials are piezoelectric, i.e., they exhibit the converse effect too. Some commonly used piezoelectric ceramics are barium titanate (BaTiO_3) and lead zirconate (PbZrO_3).

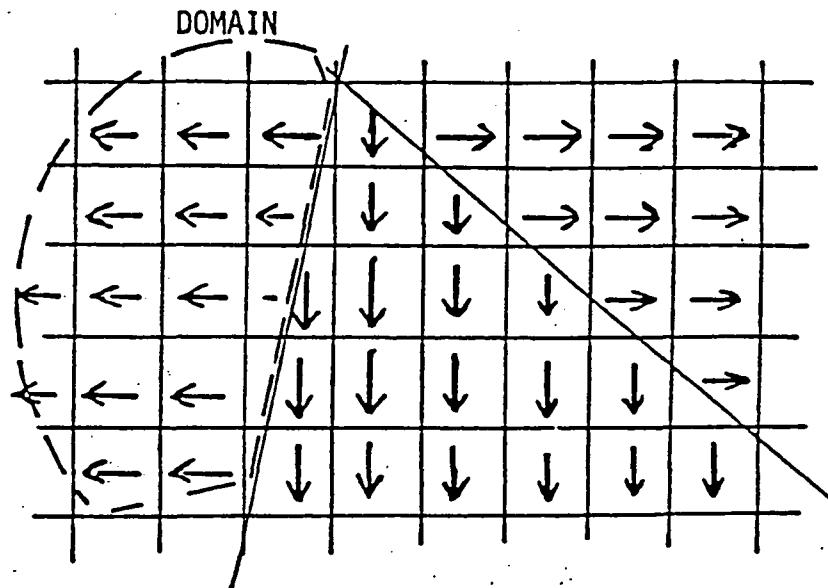
Ferroelectric ceramics are spontaneously polarized material.

This polarization is dependent on the temperature at which the material exists. The transition from ferroelectric to nonferroelectric occurs at a temperature called the "Curie point". Barium titanate (BaTiO_3) has a stable cubic structure above 120°C . At room temperature it changes to a tetragonal structure, thus producing a polarization due to the movement of the titanium ion (Ti^{+4}). Such movement of the titanium ion (Ti^{+4}) introduces an electrical charge imbalance into the unit cell. There is the probability that the titanium ion would be located in one of two locations along one of the major axis (x,y, or z). Since neither location is at the center of the unit cell the center of negative and positive charges are not coincidental and an electrical dipole must exist. The movement of the titanium ion to the second location by a neighboring polarized unit cell is possible, since the energy barrier between the two possible sites along one axis is low. This is known as the cooperative alignment of unit cells, which gives rise to electrical domain in the ferroelectric material as shown in Figure 27.

Upon application of an external electrical field the ferroelectric material domain, will follow the polarization of the applied field, and dimensional changes in the material will occur due to a change in the dipole orientation in the unit cell. Therefore, if an alternating electrical field was applied, vibration of the crystal will take place and ultrasound waves will be generated.

Mason (25) noted that dimensional changes in piezoelectric crystals are dependent on the polarity of the applied electric field and the crystal orientation. He deduced that the piezoelectric properties of a crystal are anisotropic and depend on its orientation.

Piezoelectric properties of a crystal are usually described by



a) Schematic Representation of Cooperative Alignment of Unit Cells

b) The Domain in Ferroelectric Materials

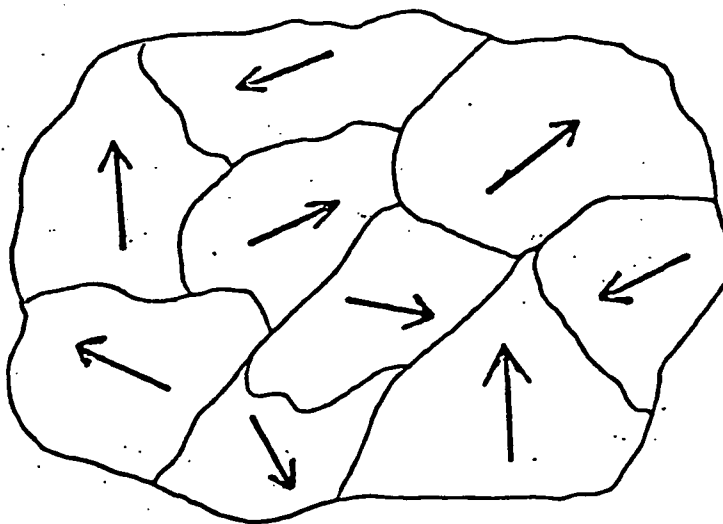


FIGURE 27. Domain Alignment in Ferroelectric Materials

certain parameters. Since these properties are direction-dependent, indices are usually used to specify each individual parameters. Some of the important parameters which pertain to the selection of a piezoelectric crystal for a specific application are listed below:

1. Transmitting Constant d_{ij}

Defined as the strain produced in a transducer by the application of a unit electric field, and has the unit of coulomb/newton.

2. Receiving Constant g_{ij}

Defined as the electromotive force produced in a crystal upon the application of a unit pressure input, and has the unit of

$$\frac{\text{volt/meter}}{\text{newton/(\text{meter})}^2} \cdot$$

3. Deformation Coefficient h_{ij}

Obtained by multiplying the receiving coefficient by Young's Modulus of the crystal for a specified direction. It has the unit of newton/coulomb.

4. Coupling Factor k_{ij}

Provides a measure of the crystal as a energy converter.

$$h = (h_{ij}d_{ij})^{1/2}$$

5. Permittivity Constant $\epsilon^{T,S}$

The dielectric constant representing the permittivity of the material, and how much current is flowing through for each volt. The units of $\epsilon^{T,S}$ are farad/meter. For this constant, the value of ϵ for the crystal is different in the clamped (ϵ^S) than the free (ϵ^T) state (25).

6. The Mechanical Factor Q_m

Determines the frequency characteristic of the crystal. This factor is independent of the geometry of the crystal, and is a

measure of the frequency band width:

$$Q_m = \frac{f_0}{f_2 - f_1}$$

f_0 = Resonance frequency

f_1 = frequency below resonance for a reduction in amplitude of 3 db.

f_2 = frequency above resonance for a reduction in amplitude of 3 db.

B. Ultrasonic Field

When an ultrasonic transducer is excited, waves are generated and travel in the immediate medium surrounding the transducer. A pressure distribution with maxima and minima is created in the medium. This is called an ultrasonic field. Fig. 28 is a schematic representation of the field for a circular disk transducer. Positions and amplitudes of the extrema in the ultrasonic field depend greatly upon the ratio of the surface dimensions of the source to the wave length produced.

There are two distinctive regions in the ultrasonic field which are of importance in the design of the transducer. The two regions are: The Fresnel Region (nearfield) and Fraunhofer Region (farfield).

1. The Fresnel Region

The Fresnel Region is also known as the near field. Its depth for circular transducer is given by:

$$x = d^2 / 4 \lambda$$

where:

d : disk diameter

λ : wave length.

x corresponds to the last axial maximum pressure which is the end of Fresnel zone and the beginning of Fraunhofer zone. For a complete mathematical treatment of this region, see Hueter and Bolt (26).

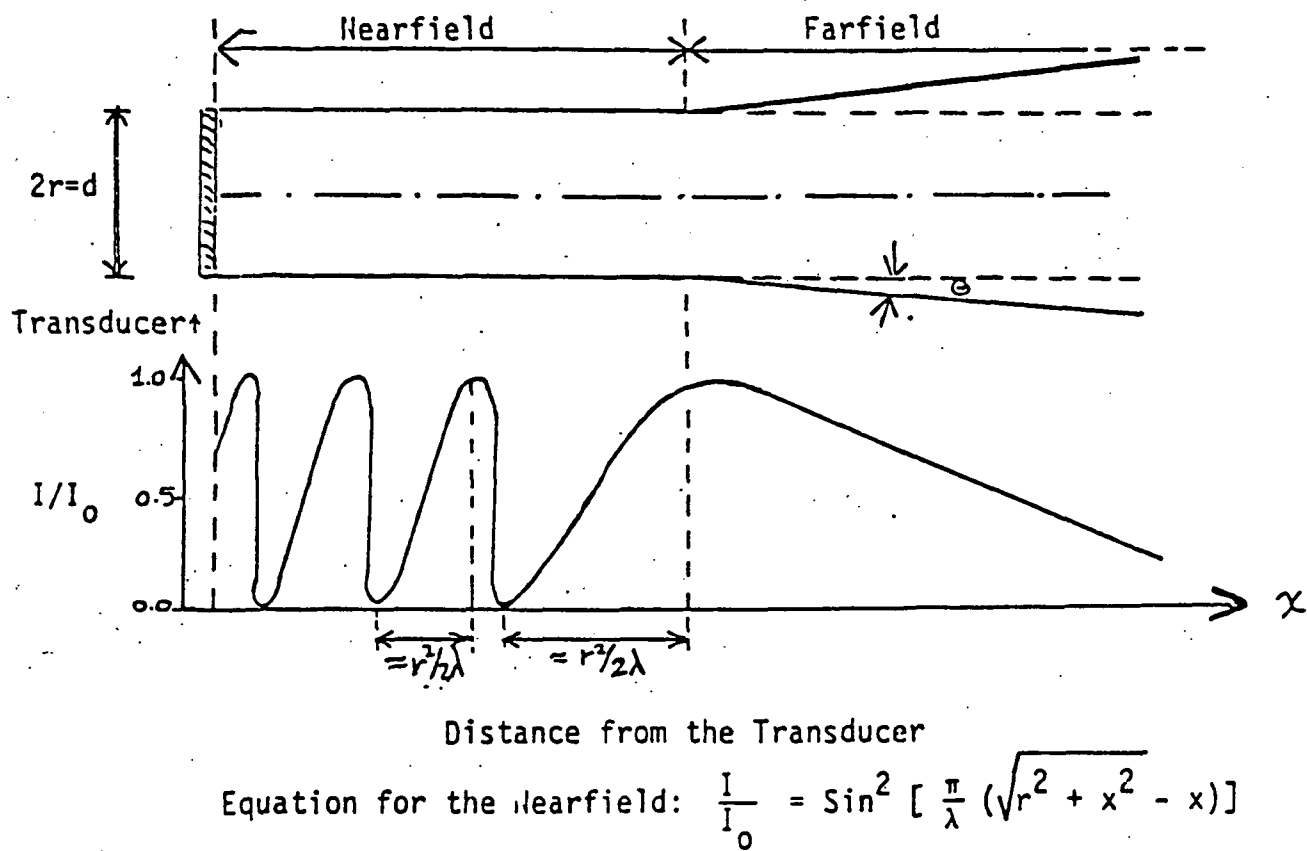


FIGURE 28. The Ultrasonic Field of Circular Disk Transducer

2. The Fraunhofer Region

The ultrasonic field generated by a circular disk transducer had the shape of a cylinder in the nearfield region. At the beginning of the farfield region the ultrasonic beam starts diverging from a uniform cylinder shape. The angle of the beam divergence from a cylindrical shape is given by:

$$\sin\theta = \frac{0.61(2\lambda)}{d} \quad (11)$$

And for a square transducer is given by:

$$\sin\theta = \lambda/t$$

Where (d) is the disk diameter and (t) is the width of the crystal. In this region the intensity of the wave is reduced sharply due to the divergence effect, and this will affect the attenuation measurement in the far field region.

C. Measurement System

We have developed a microprocessor based ultrasonic data acquisition and analysis system for measurement of acoustic parameters of a given sample (19,23). This system was used for measurement of transducer beam profile and central axis intensity as a function of distance.

Instrumentation details:

The main components of the developed pulse-echo system are shown in a block diagram in Fig 29. The system consists of a pulse generator, radio frequency (RF) receiver amplifier, calibrated attenuator, and a peak detector. A range gate enables the selection of a particular segment of the reflected signals for processing. All

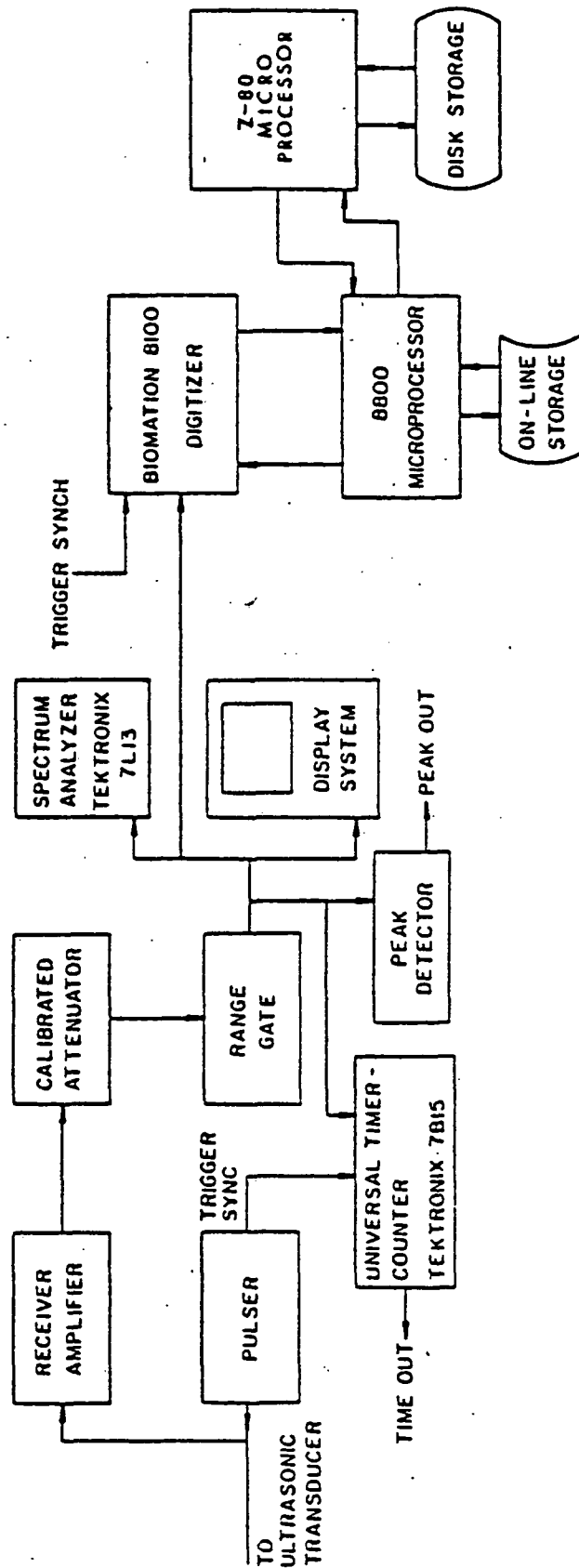


Figure 29. Data collection and analysis block diagram

of the above are housed in a single unit (Aerotech Labs,¹ UTA-3). The input receiver sensitivity is 5 mV with a frequency bandwidth of 24.6 MHz and a lower frequency cutoff at 400kHz. The receiver gain is 40dB with an output impedance of 50 Ω . A second set of pulser, receiver, and range gate (Metrotek, Inc.²) was utilized in some experiments primarily due to the higher value of excitation (adjustable up to 230V) delivered by the pulser. Acquisition of a microprocessor (Altair 8800), a high speed A/D convertor (Biomation 8100) and an off line minicomputer (PDP 11/34) facilitates digitization and storage of rf signals on a disk for further processing. Accurate transit time measurements can be accomplished using a 225 MHz universal counter timer (Textronix 7B15). Spectral analysis of data can be performed in analog fashion using spectrum analyzer (Tektronix 7L13) or digitally using standard Fast Fourier Transform (FFT) routines available on the DEC LAB applications package.

Mechanical Apparatus

The mechanical apparatus used in this project, shown in Figure 30, was designed and assembled in our laboratory. The acoustic test tank is made of clear, 1.25-cm thick plexiglass, and is lined with a sound-absorbing Styrofoam sheet to prevent any extraneous reverberations caused by multiple reflections. The test tank is filled with degassed distilled water, which acts as the coupling medium between the ultrasonic transducer and the specimen. The transducer holders are made out of plexiglass and are mounted on a sterotaxic positioning device, which provides several degrees of freedom for accurate positioning of the transducer. Thick plexiglass slabs of various geometries were

¹Subsidiary of KB-Aerotech, Lewistown, PA.

²Metrotek, Inc., Richland, WA

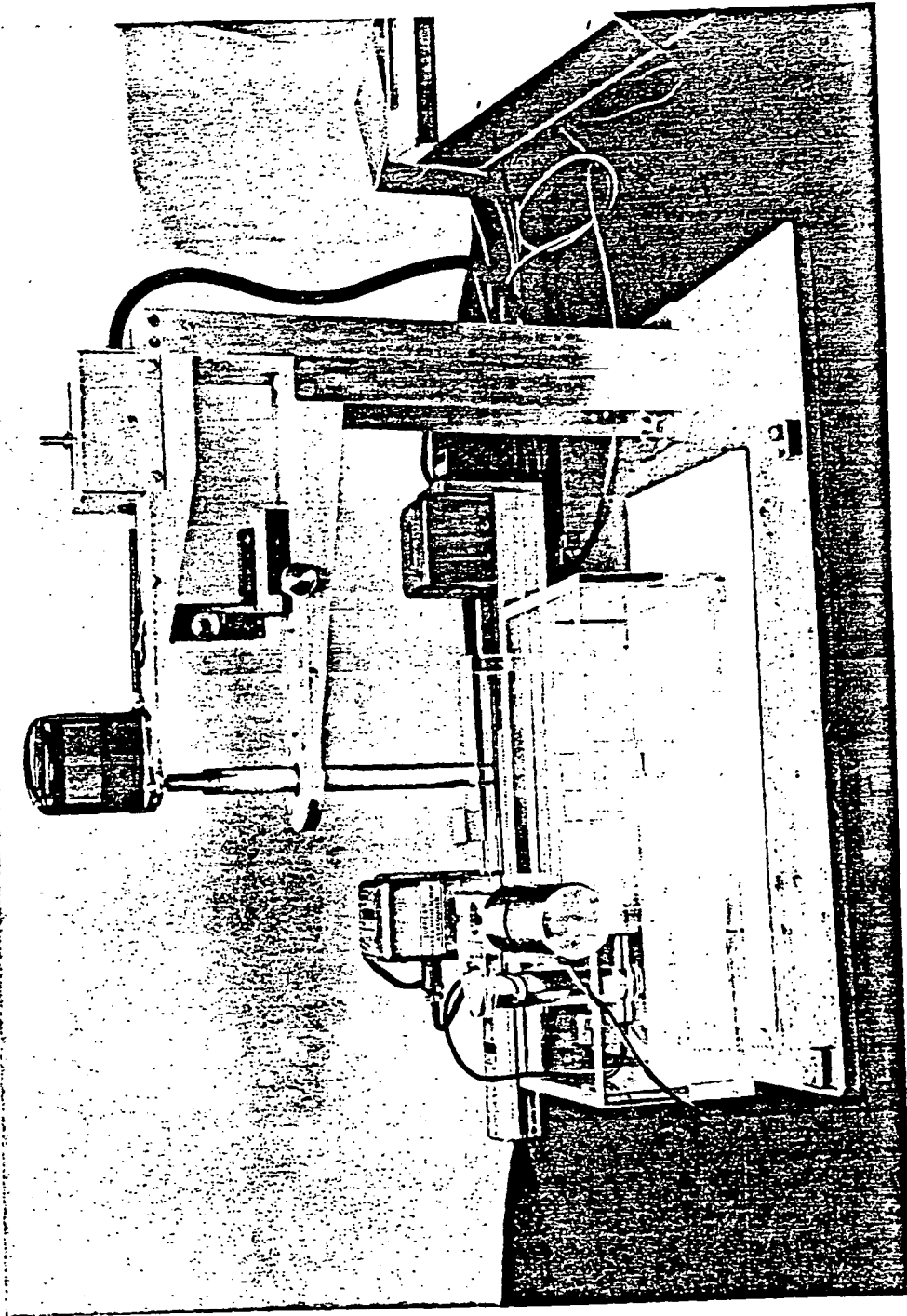


FIGURE 30. Mechanical System

used as reflectors. A 1-rpm synchronous motor is used to control the angular orientation of the transducer with respect to tissue sample.

The mechanical scanner consists of two motor-driven slide assemblies capable of movement in a longitudinal direction, as well as in a transverse direction. The linear velocity of the slides may be separately controlled. The slides have a maximum displacement of 30 cm in the longitudinal direction and 5 cm in the transverse direction. Analog position indicators were incorporated to indicate the position of the scanning transducer with respect to a reference coordinate frame. The whole assembly is made of Duralmin. A calibrated hydrophone (Mediscan, Inc.) with a crystal diameter of 0.7 mm is used as receiver to scan the beam. The scanning is carried out at various axial distances from the transmitting transducer and covers the entire transmitting cross section.

D. Piezoelectric transducer material used in this study.

The transducers used in this project were made from two types of piezoelectric material, LTZ-2 and LTZ-5. (Transducer Products, Inc.). The material is available in form of squares (1",1",t) where t is the thickness which varies to yield different resonance frequencies. The specification for the material are as follows:

<u>PROPERTY</u>	<u>LTZ-2</u>	<u>LTZ-5</u>
g_{33} volt/m/N/m ²	25.5×10^3	35.2
d_{33} m/volt	405×10^{12}	155×10^{12}
Q_m	75	500

For application in ultrasonic plethysmography either material type has been observed to be suitable.

APPENDIX B

Test Procedure and Results Using Prototype ULP

Introduction

The Ultrasonic Limb Plethysmograph, fabricated by Denver Research Institute, was received by the Wenner-Gren Research Laboratory (WGRL) on May 20, 1981. Tests were carried out in accordance with the test plan developed by WGRL in consultation with Clete Booher of NASA. Personnel involved in the testing program were: P. K. Bhagat, V. C. Wu, W. T. Nickell, Dave Brewer, Mark Shafer, and WGRL support personnel. Results of these tests are presented in the following pages.

A. PHYSICAL EXAMINATION

I. External Dimensions (LxWxH): 18.2 cm x 11.4 cm x 5.08 cm
Weight (kg): 1.173 kg Batteries (kg): 0.114 kg

II. Connectors. Are all external connectors:

a. Sufficiently secure to ensure reliable electrical contact? Yes

Comment:

A marker is needed on the female connector to facilitate correct insertion.

b. Rapidly disconnected in an emergency? X

Comment:

Connection appears to be tight. It should be verified by NASA.

III. Are there sharp edges on the case? X

Comment:

When cassette door is opened, sharp edges are exposed on the door and the locking mechanism.

IV. Check rigidity and security of indicated parts:

a. Case O.K.

b. Batteries X

Comment:

1. Banana jack needed tightening.
2. Not easy to change batteries.
3. Needs a cover to prevent accidental operation of the switch on the cartridge. Recommend a supply of spare cartridges be provided with the unit.

c. LCD Assembly O.K.

d. Electronic Cards X

Comments:

1. PC board need cleaning.
2. Unused switch on the tape recorder needs to be covered.
3. Battery and tape recorder power supply wires need to be harnessed or secured.
4. The real time clock battery holder spring needs to be modified so as to prevent short circuit of the battery.

V. Shake the unit. Are any unusual sounds produced? Yes

Comment:

Cassette is not securely mounted. Cassette strap ring should be removed.

VI. Is the LCD display readable? Yes

VII. Tape Drive

- a. Does the tape drive motor produce an abnormal noise level? No
- b. Operate the tape removal and insertion mechanism. Is performance satisfactory? Yes
- c. Is 'rewind' switch operation satisfactory? See comments

Comments:

1. The door does not provide easy access to the rewind switch. Suggest additional clearance when door is opened (modify hinges).
2. When the door is closed, movement of the recorder switch to "Stop" position should be prevented.
3. Operation of door closing mechanism is difficult.

IIIX. Check materials included in prototype against materials list.

Mechanical Listing

1. Toggle switch movement shown in drawing ED-14843 is 90° off prototype position - Change the drawing.
2. Prototype fitted with Phillip screws. Drawing ED-14843 shows straight screws.
3. Items in the drawings should specify all parts. For example, Item 7 in ED-14843 should specify both push button switches.

Needs electrical parts listing and materials used list.

IX. Can all indicator lights be seen under normal ambient light levels? Yes

Color as required? Yes

Comment:

When the tape is full, there is a warning sound. This sound should be approved by NASA for operational convenience. Audibility of this sound under Spacelab condition should be checked by NASA.

B. ELECTRONIC TESTS

I. Circuit diagram review. Carefully review the units circuit diagram.

- a. Is item complete? Yes
- b. Is circuit satisfactory? See comments

Comments:

- i. Symbols not consistent - example LED
- ii. Core and size of transmit transformer not defined.
- iii. Receiver transformer ratio not defined. Suggest using the receiver transformer for impedance matching between transducer and amplifier input stage.
- iv. Pin 16 of hybrid ED-15236-2 is not defined.
- v. The signal quality test light is amber instead of red as shown in drawing.
- vi. In EC-15033 and ED14401, a bigger DIP package than needed is used.(!)
- vii. Size and type of plug should be defined for DRS power control jack and DRS "MIC" jack (EC-14402).
- viii. Capacitor on pin 7 of power supply hybrid not labeled (EC-14402).
- ix. Pin 17 test point not identified in the drawing EC15019.

II. Functional Test. Place a transducer set in a water bath. Verify that instrument works, using LCD display as output.

- a. Stability O.K.
- b. Accuracy O.K.

Comments:

- a. Up to 1 mm fluctuation in display.
- b. 24 \pm 1 counts/2 mm

III. Quality of output signals. Conduct these measurements with power supply voltage at lowest specified value. Photograph signals using oscilloscope and camera.

- a. Output pulse. Measure with 50 ohm termination.

Amplitude? 5V.P-P

Rise Time? 35 nS

- b. Frequency content. Determine power spectrum of pulse.

See Attached Drawing

Amplitude? _____

Rise Time? _____

- c. Output pulse. With transducer attached.

Amplitude? 67V.P-P

Rise Time? 50 nS

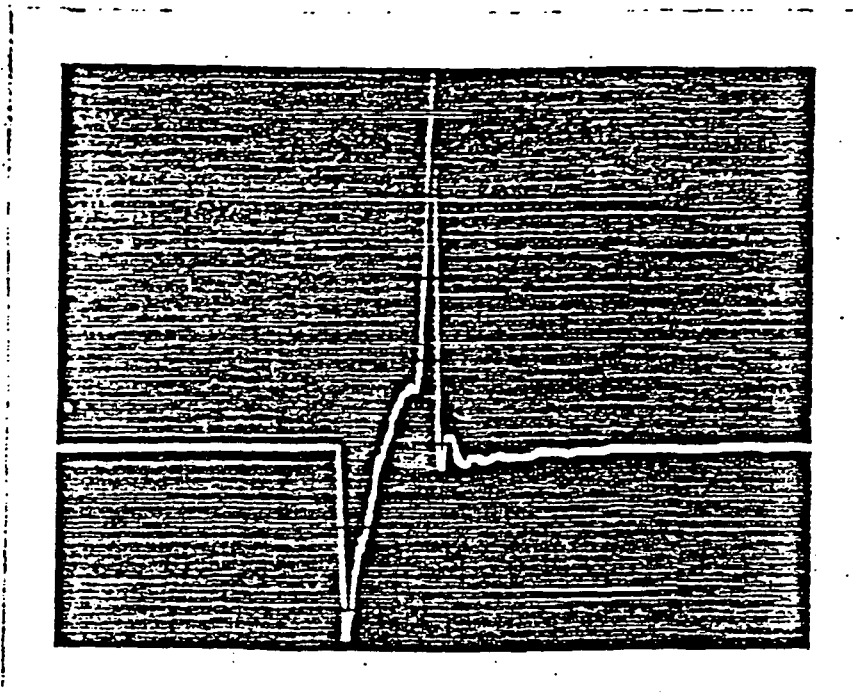
- d. Digital output. Measure using expected logic termination.

Amplitude? 5V.P-P

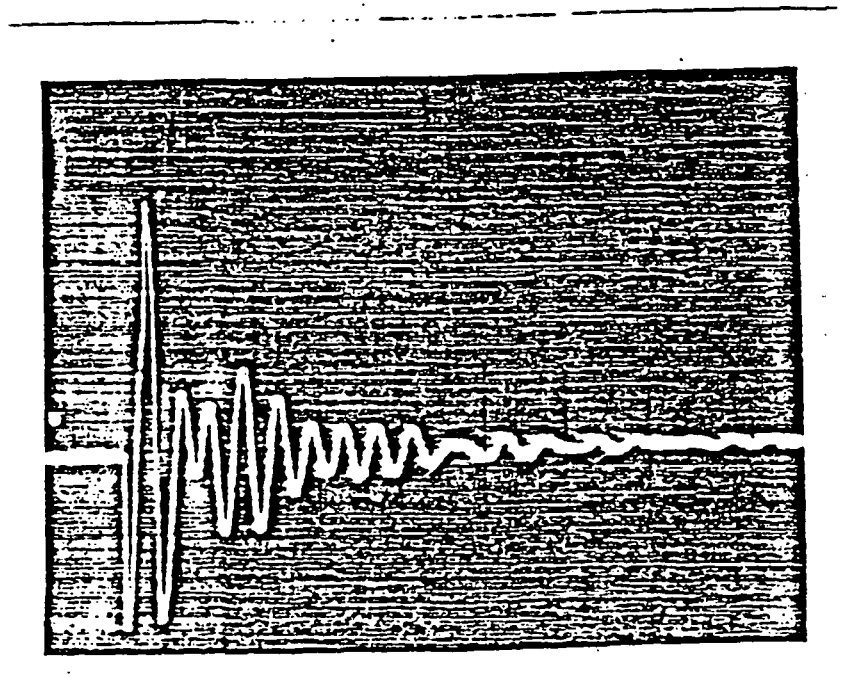
Pulse Shape? O.K.

Noise? O.K.

See next pages for graphs and pictures.



Transmit Transformer output with 50 Ω (using Biomation)



With Transmitter (Captured on Biomation)

FIGURE 31: ULP Transducer Output Pulse Shape

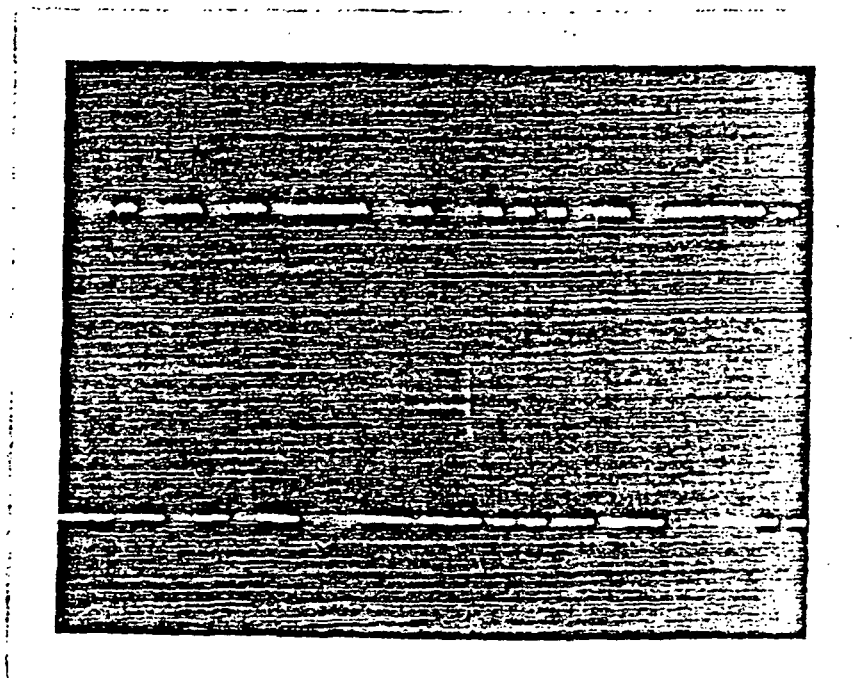


FIGURE 32. Digital Output in EDI Mode (2400 Baud)

OUTPUT PULSE WITH 50 OHM TERMINATION

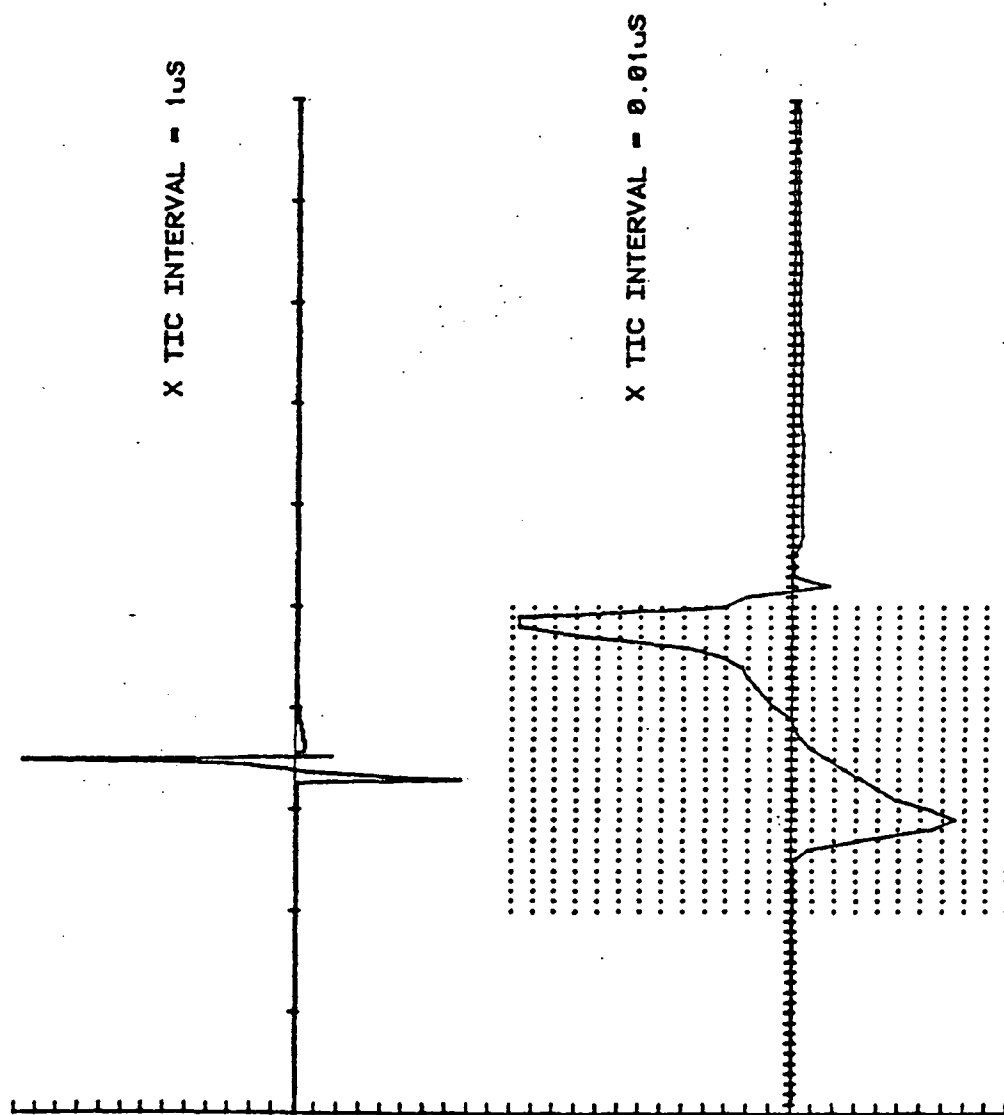


FIGURE 33. Output Pulse with 50 Ω Termination

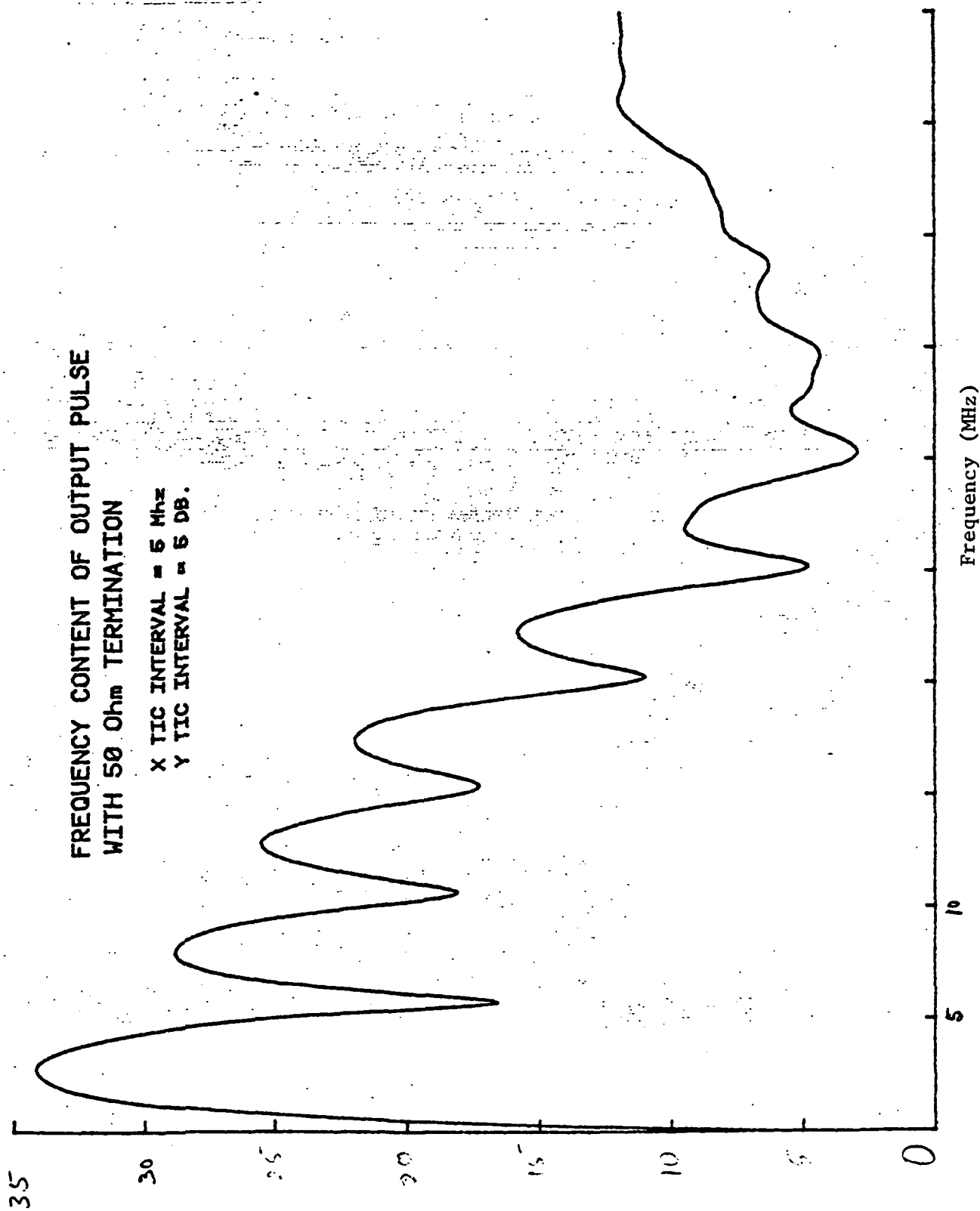


FIGURE 34. Amplitude Spectrum of the Output Pulse

OUTPUT PULSE WITH TRANSDUCER ATTACHED

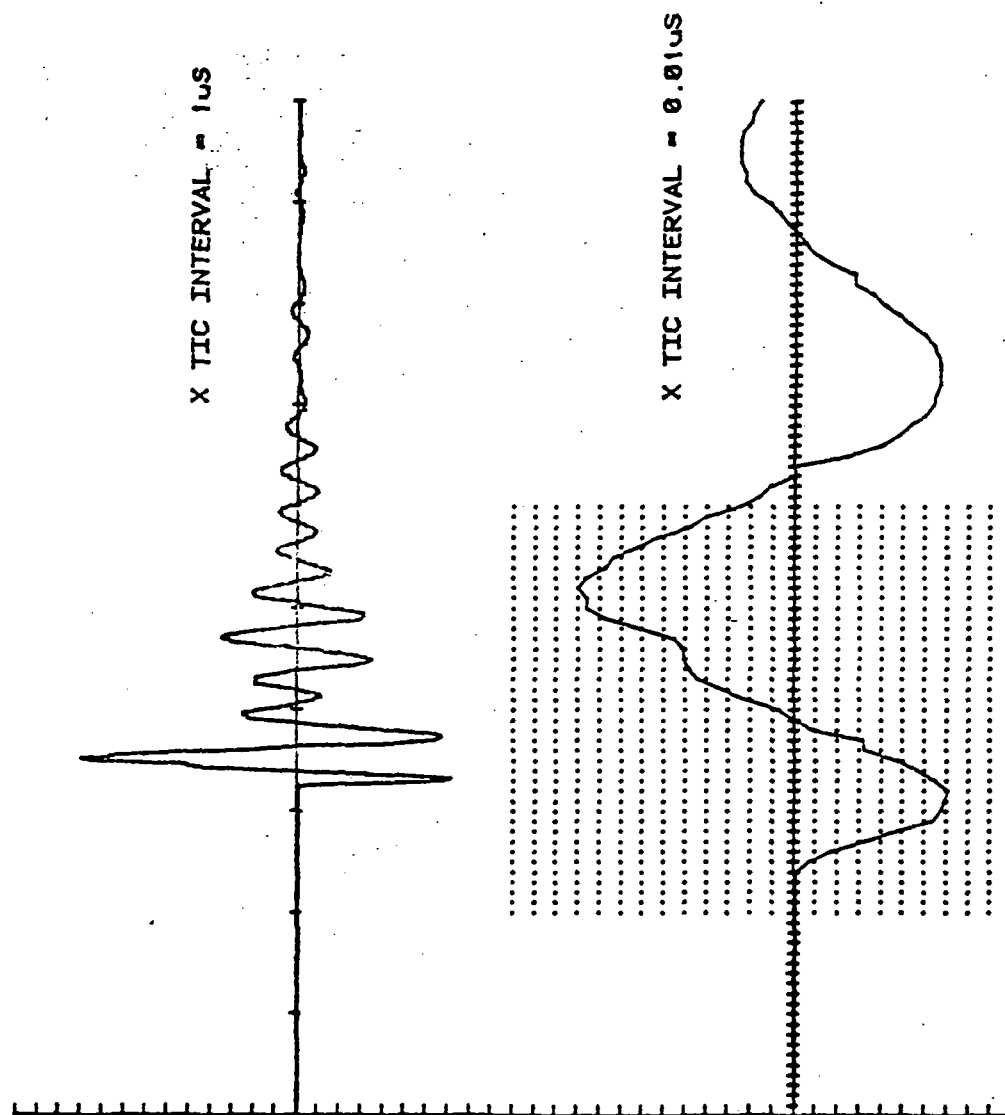


FIGURE 35. Pulse Shape with Transducer Load

IV. Receiver and Trigger. Conduct these tests with lowest permitted supply voltage.

a. Receiver amplifier Gain 53db

Acceptable? _____

b. Noise level of receiver. 50mVRms

Acceptable? _____

c. CMRR of Receiver >20dB

Acceptable? >20dB

d. Threshold stability of trigger.

Acceptable? Yes

e. Input Impedance of receiver. Measure input impedance of receiver between 450 kHz and 10MHz.

Data enclosed. Resonance occurs between 1.5 and 2 MHz (Phase Change) - Measured using vector impedance meter.

f. Frequency response of receiver. Determine 3dB point.

50kHz and -5.5MHz

Comment:

Measured using differential sine wave input.

g. Determine range of transmitter - receiver combination, as compared with original ULVS unit.

Minimum - 6.1 cms, Maximum - 24 cms

Comparable? Yes, but the minimum is higher than the original ULVS unit.

ULP RECEIVER IMPEDANCE

FREQ. (MHz)	IMPEDANCE (Ohms)		PHASE ANGLE	
	INPUT 1	INPUT 2	INPUT 1	INPUT 2
0.5	370	380	+90°	+90°
1.0	1.05K	1.05K	+86°	+86°
1.5	3.0K	4.3K	+60°	+56°
2.0	3.0K	2.9K	-62°	-65°
2.5	1.4K	1.35K	-76°	-77°
3.0	950	920	-80°	-81°
3.5	720	710	-82°	-82°
4.0	600	580	-82°	-83°
4.5	500	480	-82°	-83°
5.0	430	420	-82°	-83°
5.5	380	370	-82°	-83°
6.0	340	335	-82°	-83°
6.5	310	300	-82°	-83°
7.0	280	280	-82°	-83°
7.5	260	260	-82°	-83°
8.0	240	235	-82°	-83°
8.5	220	215	-82°	-83°
9.0	200	200	-80°	-82°
9.5	195	195	-80°	-82°
10.0	185	180	-80°	-82°

Comment:

1. Due to the design of the testing pad additional noise is introduced into the receiver output. For this reason, the numbers listed above do not reflect actual values.
2. The actual receiver gain is lower than that specified in the end item specification. However, operation appears to be satisfactory.

V. Function switches. Check function of switches.

- | | |
|--------------------|-------------|
| a. Time Set | <u>O.K.</u> |
| b. Time on/off | <u>O.K.</u> |
| c. Fast/slow | <u>O.K.</u> |
| d. Self-test/Reset | <u>O.K.</u> |
| e. Power | <u>O.K.</u> |

Comment:

- i. Operation of 2 or 4 chord switch has no effect until 'Reset' is operated.
- ii. Access to function switches is difficult due to their location under the tape recorder. Suggest vertical mounting of the switches for ease of operation.

VI. Automatic signal quality check.

Does automatic signal quality check system perform properly? Yes

Describe measurements made to verify operation of this function:

Transducers 100 mm apart were placed in a water bath.

- a. One of the transducers was rotated until poor signal quality was apparent. The warning light indicated this condition correctly.
- b. Keeping one of the transducers fixed, the other was given sinusoidal displacement at varying rates. When the amplitudes and frequencies of 5 mm, 0.5Hz; 2.5 mm, 0.7Hz and 1.0 mm, 1.6 Hz were exceeded the warning light was 'ON' even though the signal quality was good.

The warning light sometimes is 'on' during physiological tests even though the quality of signal is good. Suggest changing the test range of signal quality.

VII. Power Consumption. Measure average steady state power consumption using series ammeter and volt meter.

- | | |
|---------------------|------------------------|
| a. Slow Mode | 179-182 ma, 7V 2 chord |
| | 182-186 ma, 7V 4 chord |
| b. Fast Mode | 172 ma, 7V 2 chord |
| | 176-180 ma, 7V 4 chord |
| c. Recorder Running | 167 ma, 7V 2 chord |
| | 120 ma, 3.5V 2 chord |

For 4 chords, the numbers are essentially the same.

- d. Battery Life Under Normal Operation from full charge. 33 hrs.

Comment:

Out of spec conditions on voltage were observed on two occasions. Suggest recheck of power supply hybrid.

II. Time Base Accuracy

- a. Clock Frequency 18.0042 MHz, 60.0014 Hz
- b. Determine clock Accuracy by test against official standard.

Drift was 6 seconds for four days and 37 seconds for twenty days when tested against WWV.

	Initial Readings	Standard	ULP
1 week	_____	_____	_____
1 month	_____	_____	_____

IX. Tape Operation

- a. Quality of Recorded Signal

Amplitude	<u>O.K.</u>
Noise Level	<u>O.K.</u>

Stability

O.K.

See attached data on page .

- b. Interface to LSLE computer. Comment on any problems encountered:

Interference between EDI data output and receiver input was observed, however, rearrangement of external wire eliminated this problem. We feel that EDI output sometimes feeds signals to the receiver amplifier during data transmission.

- c. Data Reliability. Record a string of at least 5,000 data points. Play recorded data into LSLE computer. Determine number of transmission errors which occur.

Slow Mode Error Rate

1 error

Fast Mode Error Rate

NONE

Comments:

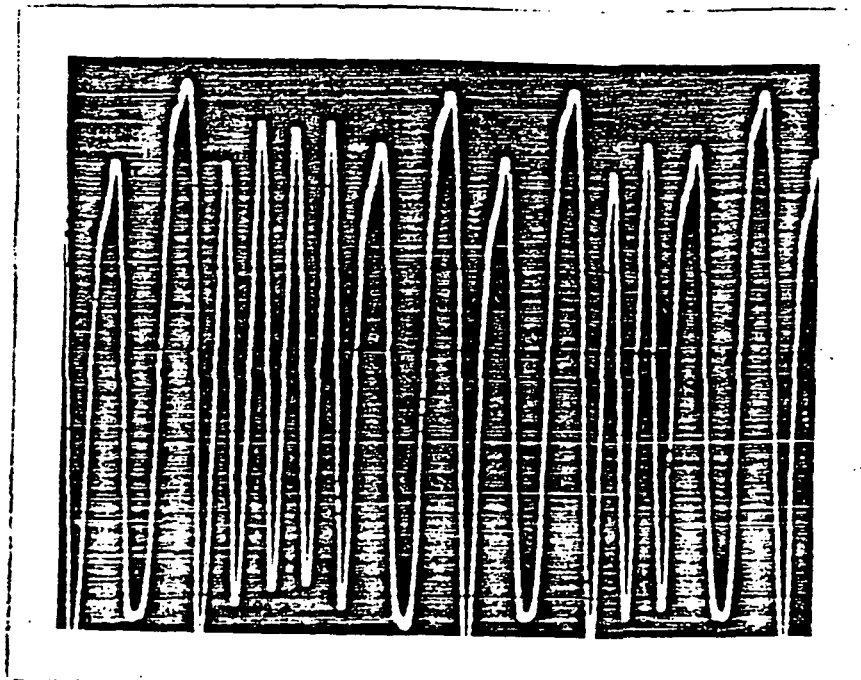


FIGURE 36. Tape Recorded Signal Played Back with 1K Load and Capture by Biomation A/D Converter.

C. USE TESTS

- I. Ease of use. Attach the unit to an experimental subject. Instruct subject to operate controls, change tapes, conduct simple exercises, and remove and reattach the unit.

a. Accessibility of Controls O.K.

b. Visibility of Indicator Lights O.K.

c. Ease of Changing Tape and Battery

See section A, IV b of this report.

d. Difficulty in detaching or reattaching cables and connectors

See section A, II of this report.

e. Comfort _____

Comments:

Need 'pouch' to comment on comfort.

- II. Provocative Tests. Conduct Venous Occlusion and tilt-table tests to produce changes in limb volume.

a. Transmit data directly into LSLE microcomputer

Quality of Data O.K.

Interpretation of Data O.K.

Comments:

More noise spikes on 2nd chord. Does not seem to be on transducer. The problem is intermittent. Data enclosed.

b. Record data on tape.

Quality of Data O.K.

Interpretation of Data O.K.

Comments:

Data enclosed on pages 99, 100 and 101.

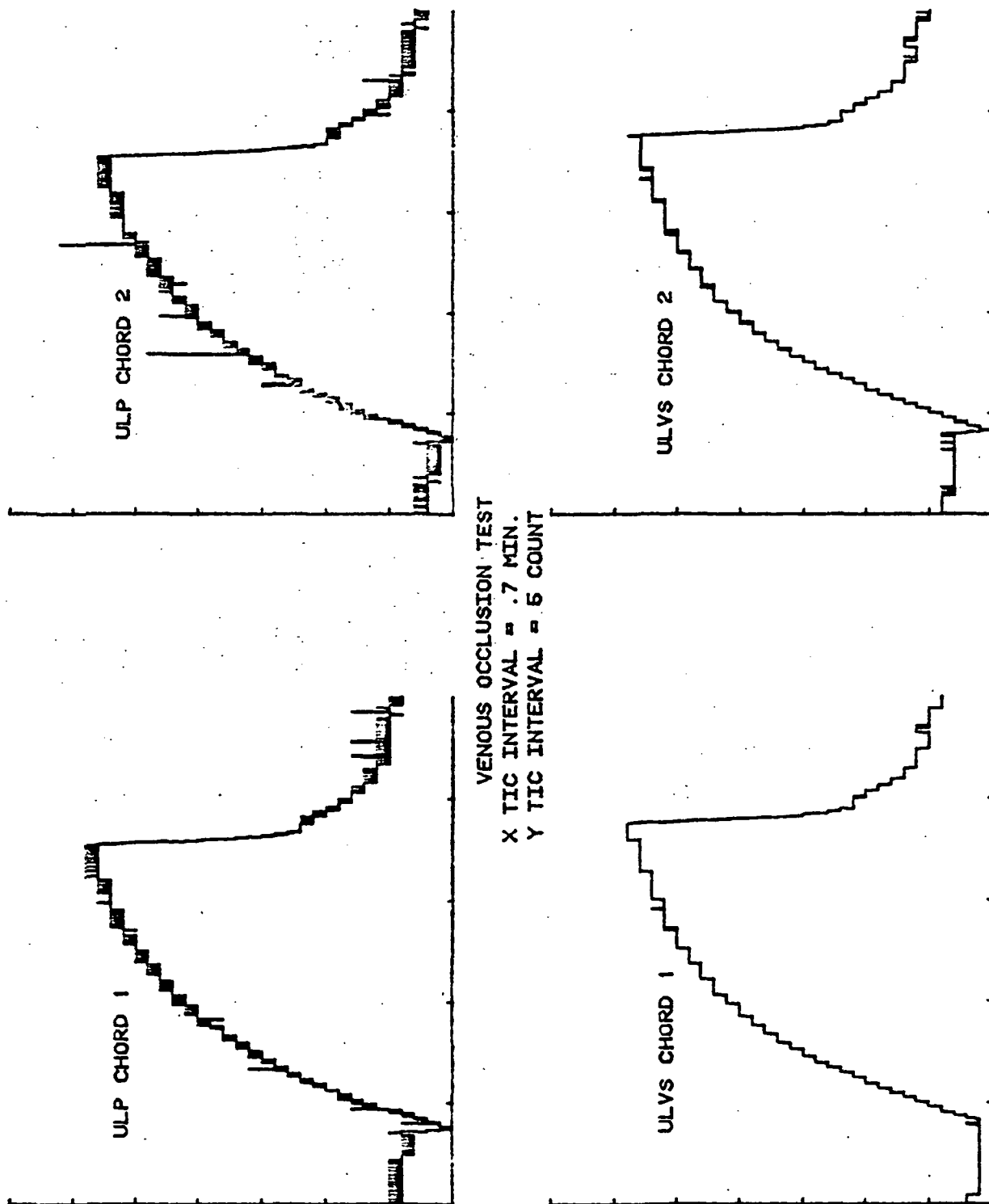


FIGURE 37. Time Course of Dimension Changes Under 50 mm Hg Venous Occlusion Procedure

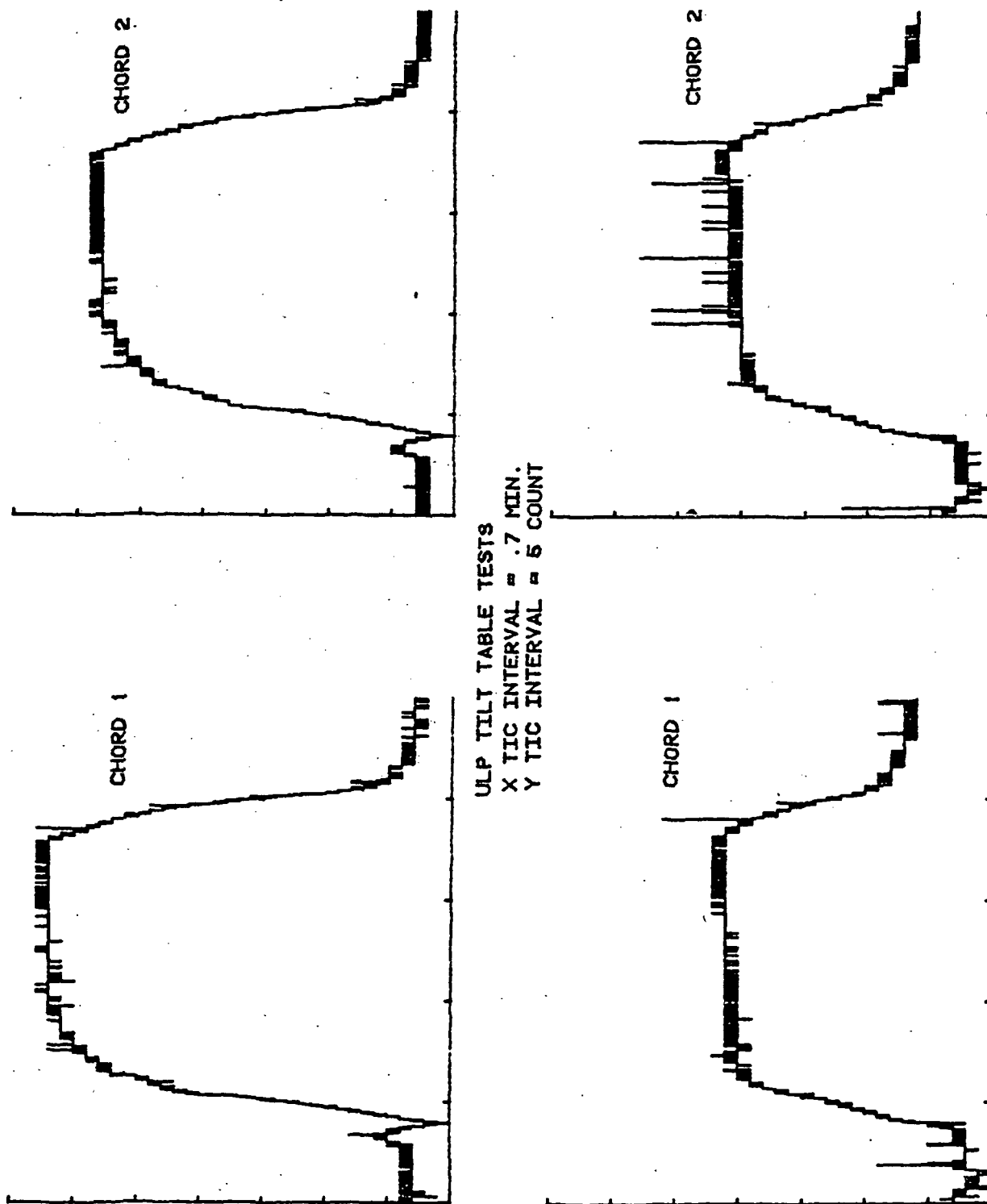


FIGURE 38. Time Course of Limb Dimension Changes Under 50° Head Up Tilt

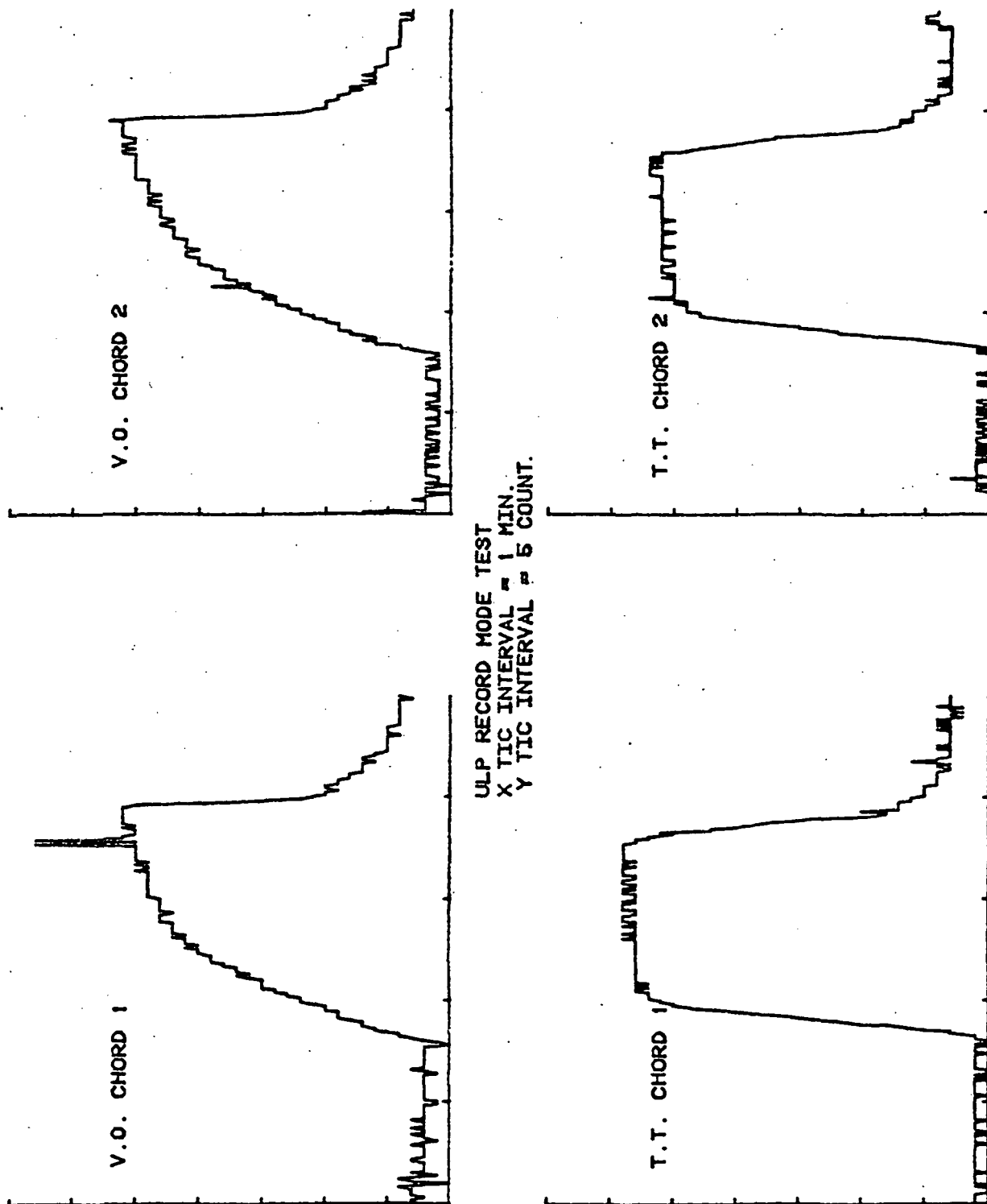


FIGURE 39. ULP Data Played Back From the Recorded Venous Occlusion (50 mmHg) Data

III. Routine Monitoring. Use tilt-table to produce leg volume data over a 30 minute period.

Quality of Data

O.K.

Ease of Interpretation

O.K.

Comments:

Data enclosed on page 103 .

IV. Automatic signal check. Use automatic signal check feature to place transducers on subjects leg. Verify quality of signal using oscilloscope.

trials/# correct

O.K.

Comments:

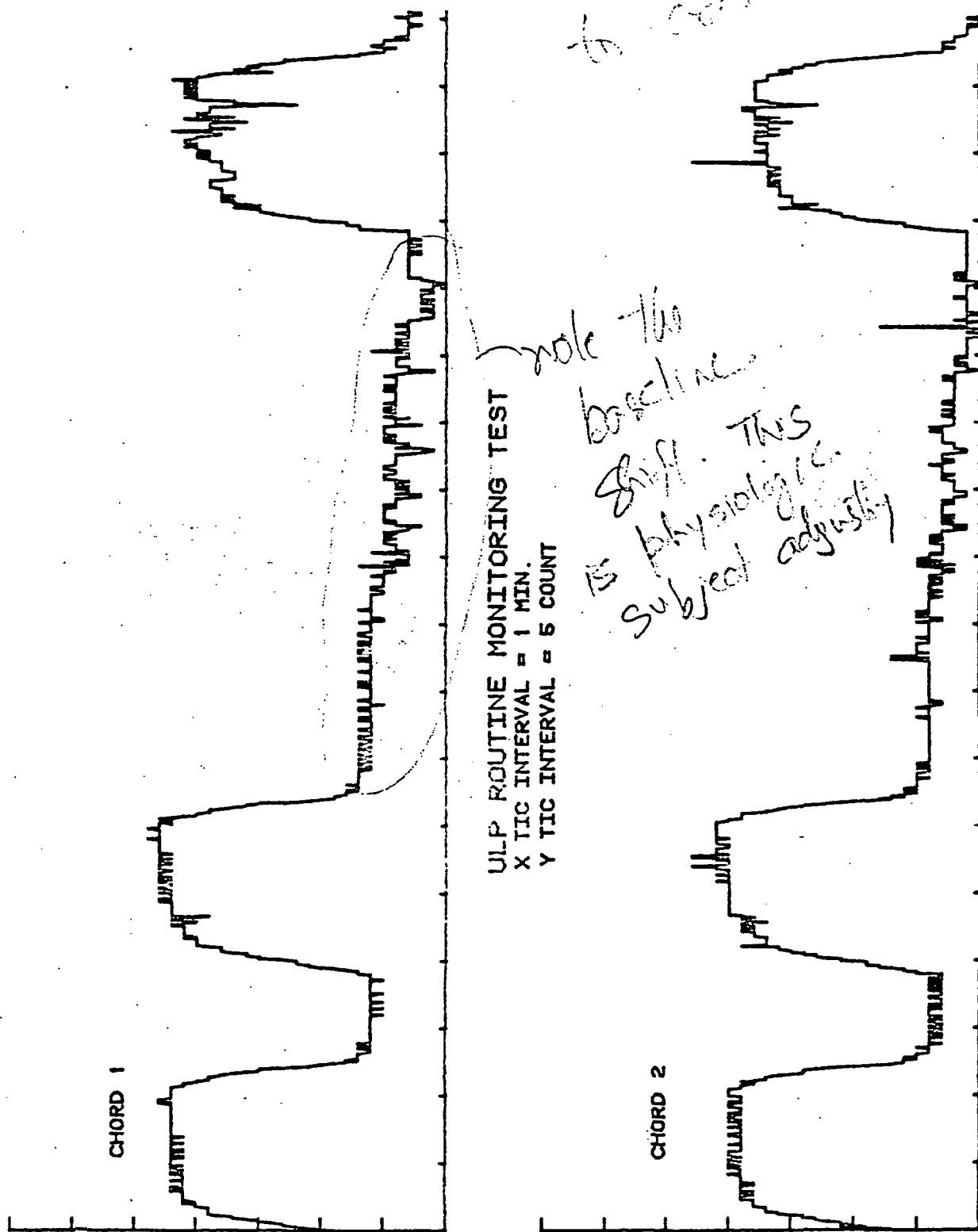
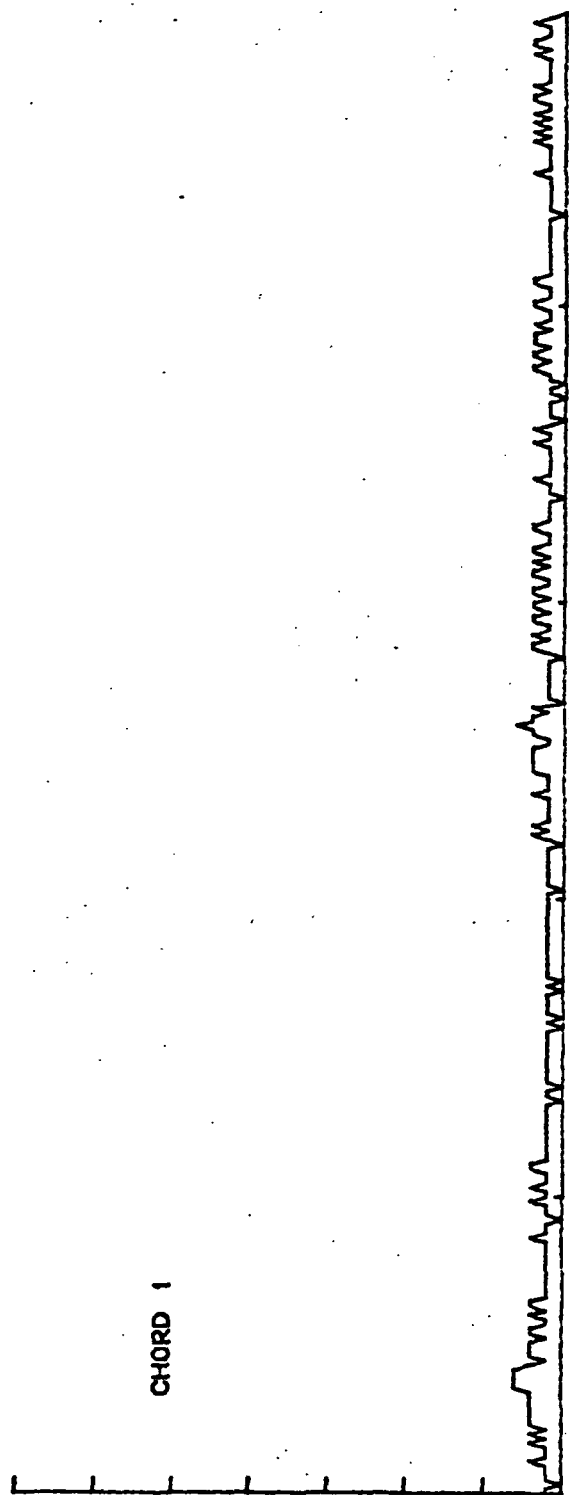


FIGURE 40. Passive Monitoring of Data Through a Tilt Table Experiment



ULP ROUTINE MONITORING TEST

X TIC INTERVAL = 1 MIN.

Y TIC INTERVAL = 5 COUNT

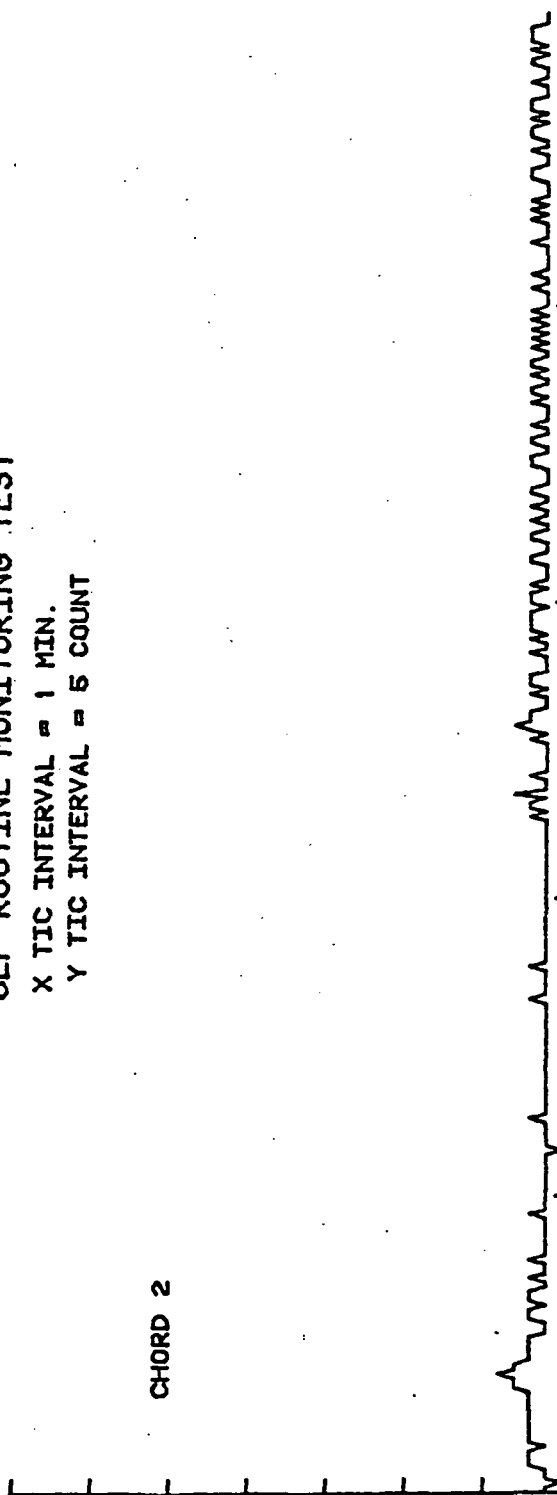


FIGURE 40. (Continued)

TEST EQUIPMENT USED IN EVALUATION OF ULP

1. Biomation, Model 8100, Transient Recorder
2. Tektronix, 604, Monitor
3. Tektronix, SC 502, Oscilloscope
4. Hewlett-Packard, 7402A, Strip Chart Recorder
5. Fluke, D802 Multimeter
6. Fluke, 8020A Multimeter
7. ULVS, Wenner-Gren Research Laboratory
8. OHAUS, Harvard Trip Balance
9. Wavetek, HF Sweep Generator, Model 144
10. Tektronix, 7633 Multimode Storage Oscilloscope, with plug-in units, 7A26 Dual Time Trace Amplifier, 7D15 225 MHz Universal Counter/Timer and 7B53A Dual Time Base
11. Hewlett-Packard, 4815A RF Vector Impedance Meter
12. Tektronix, 4051 Graphics System With 4051E01 Rom Expander
13. Tektronix, 4662 Interactive Digital Plotter
14. Tektronix, P6202 Probe
15. Tektronix, C-5B Oscilloscope Camera
16. Hewlett-Packard, 5303B Frequency Counter
17. Velmex, Series B2500, Positioning System
18. Velmex, Model 311, Control Unit
19. La Berne Tilt Table
20. MTS 442 Controller
21. Cromemco, System Three, Computer
22. MTS Servoram
23. LAMBDA LH-124 FM, D.C. Power Supply
24. RCA WP-702A, Dual D.C. Power Supply

Conclusions and Recommendations

The basic design of the ULP unit is sound. Most problems encountered in our testing program were operational difficulties which can be fixed by either modifications of software and/or development of proper procedures. The following specific recommendations are made:

1. RF signal cannot be seen on a conventional oscilloscope because of the low repetition rate. This makes transducer placement very difficult without the original ULVS. Software fix is needed to provide at least 100 sweeps/sec.
2. We have had some problems with the automatic signal quality check. It is sometimes 'ON' when the signal is good and 'OFF' when the signal is bad. Resetting the levels might cure the problem. We suggest calculation of power requirement of the Automatic Signal check. The signal quality check could be made only once every 10 sec., for example if this would save power. In addition, the maximum sampling rate could be increased.
3. Polarity of the leads is a problem. The first 1/2 cycle of a "good" signal is normally small. It is desirable to trigger on the the 2nd half cycle. With the ULVS this problem is handling by reversing polarity. The leads should be designed so that the polarity can be set using an oscilloscope and recovered when leads are reattached.
4. The receiver transformer needs further work. The turns ratio should be set to match transducer impedance to receiver impedance. The transformer does not behave in an ideal manner over the important frequency range. There is a resonance between 1.5 and 2.0 MHz. We suggest consultation with WGRL or purchase of

commercial units. Improvement of the transformer design will probably improve the receiver gain significantly.

5. Transmitter pulse width is long compared with the natural period of the transducer; the pulse is bipolar. This might cause problems if a higher frequency transducer were to be used.

6. The size and weight of the unit are slightly above specifications. We offer the following suggestions for reducing these values:

a. The present case is made of very thick material. Size and weight could be reduced significantly by using a less substantial case.

b. The tape recorder case, the replay electronics, and the speaker are superfluous. Space and weight could be saved by removing these components.

c. A more compact shape might be produced by careful arrangements of parts. Unfortunately, the length and width of the unit are set by the size of the PC board. Placement of the circuit on two PC boards would allow a more compact shape to be produced.

7. The gain of the receive amplifiers is slightly lower than that of the original ULVS. Increasing the gain by a factor of two would improve device performance.

8. Turning the unit 'OFF' causes loss of data back to the last tape recorder dump. This will be an operational inconvenience in some cases. The software should be written so that the ULP stops recording data when the transducers are disconnected. This would allow the power switch to remain 'ON' for long periods without draining the batteries significantly.

APPENDIX C

Description of Individual Circuit Blocks of Two Transmitter ULVS

A. Processor, Memory and Display

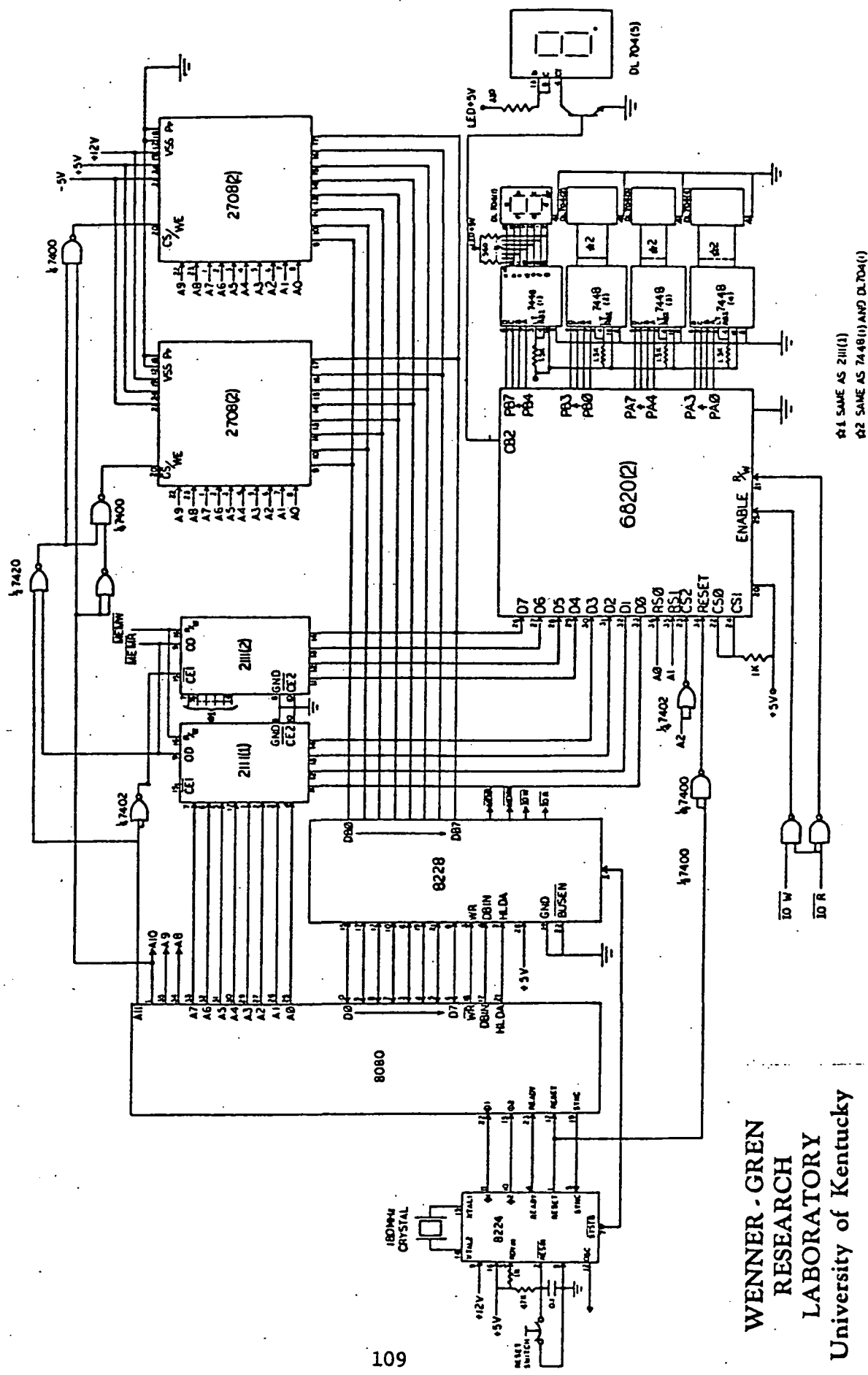
This block (Fig. 41) consists of one Intel 8080 CPU, two 2708 EPROMs for storage of instruction codes and constants, two 2111 RAM chips for storage of generated data, one 8228 data bus and status controller, and an 8224 clock generator which provides the working clock at 2 MHz for the CPU and also supplies the clock frequency for the counter at 18 MHz. It also contains a 6820 Motorola PIA which drives four BCD to seven segment decoders/drivers 7448, which in turn drive 4 DL-704 common cathode LED's where the results are displayed. The 5th digit of the LED display is wired so that it will show blank or "1" only; this digit is driven by an npn-transistor which is controlled by line CB2 of the 6820 PIA. Two 7400 NAND and one 7402 NOR gates are used to provide the required address decoding. They also provide suitable enabling signals. Because the 8080 has both memory reference and I/O reference instructions, the circuit is arranged so that the 6820 occupies I/O addresses 04 to 07 of the CPU (address 00 to 03 is reserved for the use of the other 6820 which will be discussed later). The two 2708 ROM chips use memory addresses from 000 to 7FF Hex. Two 2111 RAM chips then occupy memory addresses from 800 Hex to 8FF Hex. The decoding and enabling logic of each peripheral chip is implemented as follows:

Chip Select of 2708 (1) = $\overline{\text{All}} + \text{MEMR} \quad . \quad \overline{\text{A10}}$

Chip Select of 2708 (2) = $\overline{\text{All}} + \text{MEMR} \quad . \quad \text{A10}$

Chip disable of 2111 (1), 2111 (2) = $\overline{\text{All}}$

Output disable of 2111 (1), 2111 (2) = $\overline{\text{MEMR}}$



Read/Write of 2111 (1), 2111 (2) = $\overline{\text{MEMW}}$

Chip Select 0 and 1 (CS0 and CS1) of 6820's = 1

Chip Select 2 (CS2) of 6820 (2) = A2

Chip Select 2 (CS2) of 6801 (1) = $\overline{\text{A2}}$

Enable of 6820's = IOW + IOR

Read/Write of 6820's = IOR

Where A0 to A11 are address lines from the CPU, and MEMR, MEMW, IOR, and IOW are signals from the 8228. These signals represent memory-read, memory-write, input/output read, and input/output write respectively. Note that in order to simplify the decoding circuit, non-fully-decoded addressing is used.

The Intel 8080 microprocessor serves as the CPU of the system. The two clocks, ϕ_1 and ϕ_2 , the reset, ready, and synchronizing signals are all provided by the 8224 clock, which controls the timing for the entire system. An 18 MHz crystal is connected at pins 14 and 15 of the clock and the resulting oscillatory output is available at pin 12 to run the counter in the next block (see Figure 42). An external reset button is connected between the Reset Input ($\overline{\text{Resin}}$), Ready Input (Rdyin), and ground to allow manual reset of the system. The status strobe ($\overline{\text{STSTB}}$) is connected to the 8228 Data Bus (Pin 1, $\overline{\text{STSTB}}$) to synchronize its operation.

The 8228 Data Bus and Status Controller is used to increase the driving capacity of the CPU. It generates all signals required to directly interface RAM, ROM, and I/O components. It also provides isolation of the 8080 data bus from memory and I/O which allows for the optimization of control signals. The isolation of the bus driver also provides for enhanced system noise immunity. Data lines D0 to D7 of the 8080 are tied to D0 to D7 respectively of the 8228. The Write

(WR), Data Bus in (DBIN) and the Hold Acknowledge (HLDA) lines of the 8080 are tied to the corresponding lines, WR, DBIN, and HLDA of the 8228. The DBIN signal indicates to external circuits that the data bus is in the input mode. The HLDA appears in response to the Hold signal and indicates that the data and address bus will go to the high impedance state. Line 22, BUSEN, is the bus enable input. It is tied to ground to keep the data bus always enabled. The output of the 8228 are lines DBO to DB7, the extension of 8080's data lines. These data lines are then available to the peripheral components. This provides a two-way data path with high fan-out between CPU and external components. Four other output lines of the 8228, Memory Read ($\overline{\text{MEMR}}$), Memory Write ($\overline{\text{MEMW}}$), I/O Read ($\overline{\text{IOR}}$), and I/O Write ($\overline{\text{IOW}}$) are available to control read/write operations in other components.

Memory capabilities of the system include two 256 x 4 RAM and two 1k x 8 ROM chips. Input/output data lines of the two RAMs (pins 11 - 14 of both chips) are tied to the Data lines DBO-DB7 of the 8228 to allow data transfer between the CPU and RAM. Each RAM has its address line AO-A7 tied to AO-A7 of the 8080 to enable the CPU to store and read data at specific addresses in RAM. Read and Write enabling signals come from the MEMR and MEMW lines of the 8228. Input/output data lines of each ROM (pins 9-11, 13-17 of each chip) are also tied to the Data lines DBO-DB7 of the 8228 to allow data transfer between the CPU and ROM. Each ROM has its address lines AO-A9 tied to AO-A9 of the 8080 to enable the CPU to read data from specific addresses in the ROM. Each memory chip is located at the addressable location stated above.

A 6820 Peripheral Interface Adaptor (PIA) is included to

facilitate efficient data transfer of the computed limb cross-sectional area to the display. Data lines of the 8228 are tied to the corresponding data lines to the PIA and when the area has been computed, the PIA reads in the data. The data is then output from lines PA0-PA7 to the 7448 BCD-to-seven segment decoders, whose output goes to the seven segment displays. Read and write signals for the PIA are supplied by the IOR and IOW lines of the 8228 respectively. A Reset signal is supplied by 8224 clock. The PIA is located at the addressable memory locations stated above. Switching in all circuits is controlled by the program in 8080.

B. Controller Logic, Transmitter Select, and Counter

The function of this block (Fig. 42) is to control the flow of information throughout the system, to select a transmitter for chord length measurement and to provide a count proportional to measured ultrasonic transit time for further computation. It contains a 6820 PIA which drives three cascaded 4-bit 7493 binary counters, a CD4052 analog switch, a 7474 D-type flip-flop, a 74121 one shot, and 7400 NAND chip for logic level converting and gating between the binary counters, flip-flop, one shot and the analog switch.

The PIA in this block is used to interface the binary counters with the CPU, and it is connected almost in an identical manner to the previous PIA (Fig. 41). Data line DO-D7 (pins 26-33) as well as reset, enable, read/write, RSO, and RSI (pins 34, 25, 21, 36, and 35) are all connected as described earlier. The only difference is the chip select 2 (CS2) pin. This allows the CPU to select one or the other of the PIA's. Lines PA0-PA7 and PBO-PB3 are connected to the output of the 7493 binary counters as shown in Fig. 42, in order to allow the CPU access the binary count. The three counters are

connected in cascade such that the least significant bit of the count is output at pin 12 of the 7493 #1 and the most significant bit is output at pin 11 of the 7493 #3. The counting frequency is supplied by the 8224 clock (Fig. 41) and is connected to pin 14 of the 7493 #1. Counting frequency is 18 MHz, hence the accuracy of time measurements is 55 nsec. The counters are enabled by a 7474 D-type flip-flop.

The 7474 is set by the transmitter enabling pulse from the CPU through the PIA at line PB7. Pin 4 of the flip-flop is the reset. Initialization of the counters is provided by the output, Q, of the flip-flop. Q and the 18 MHz pulse from the 8224 clock are input to a 7400 NAND gate, and the output is used to enable the counter and control its counting frequency. Pin 1 of 7474 is the clear input, and it is connected to the receiver's comparator output in order to stop the counters when the signal is received.

Since the receiver amplifier has high gain, the possibility of false output from the comparator due to the presence of low level interference may exist during the activation phase of the transmitted signal. This possibility is avoided through use of a 74121 one shot which inhibits the receiver comparator output during this period. This one shot is enabled by the transmitter enabling pulse from the CPU through the 6820 at line PB7. The output of the 74121 is set at about 10 usec. This time period is of sufficient length to prevent false firing of the comparator (set as a threshold detector).

A CD4052 analog switch is used for selection of either one of the two transmitters for activation. The transmitter enabling pulse from line PB7 of the 6820 (1) is input to the 4052 where it is multiplexed

to output at either X_0 (pin 12) or X_1 (pin 14). Two transistors (2N222) at the output are used to convert the logic levels from the analog switch to a 15 V pulse to activate the ultrasonic transmitting circuit (pinger). S1 (pin 9) and S0 (pin 10) of the 4052 are the multiplexer select lines. S1 is grounded (Logic Level "0") since only two of the outputs are used and S0 is connected to the mode switch.

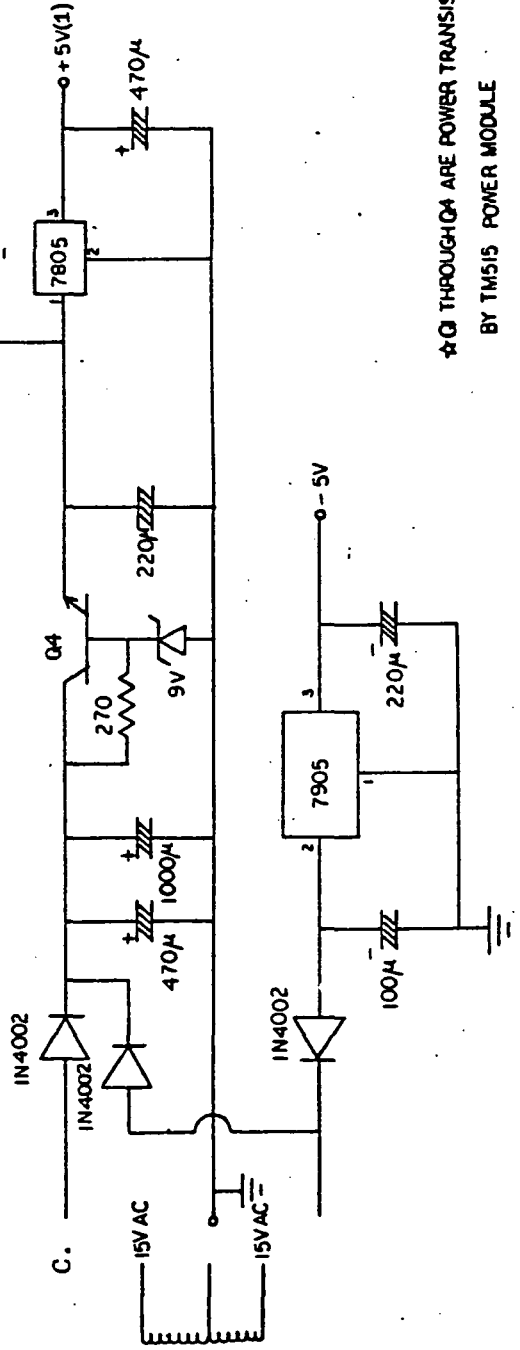
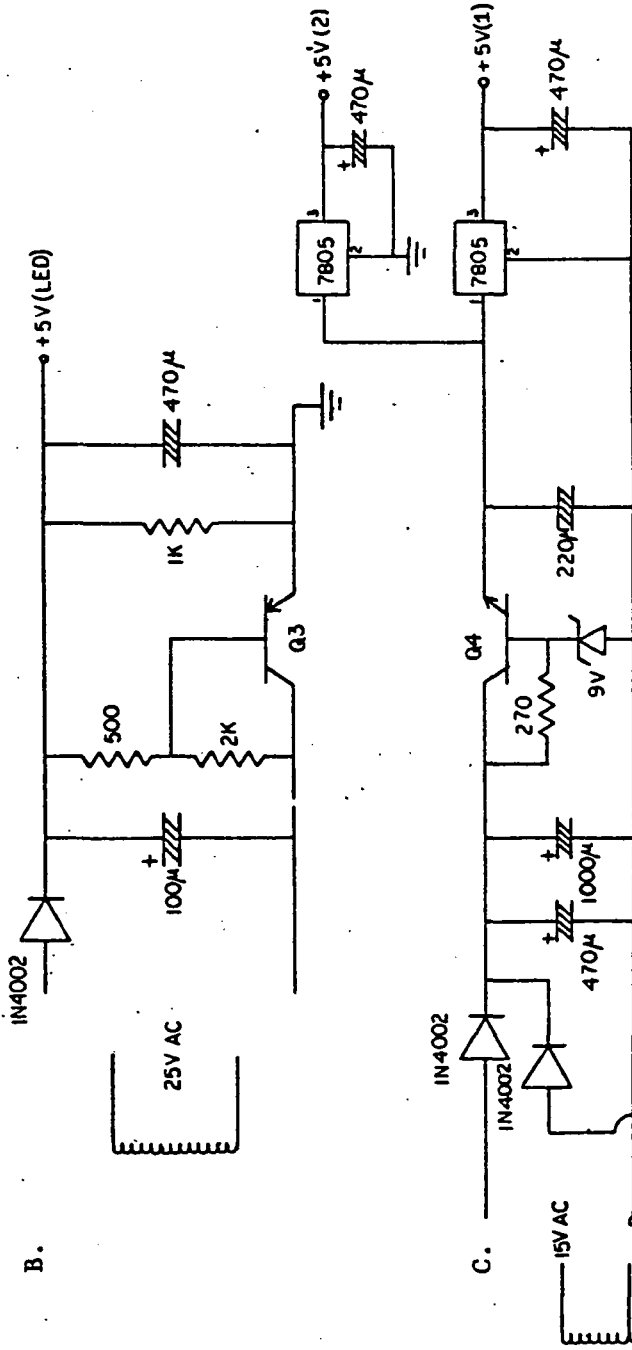
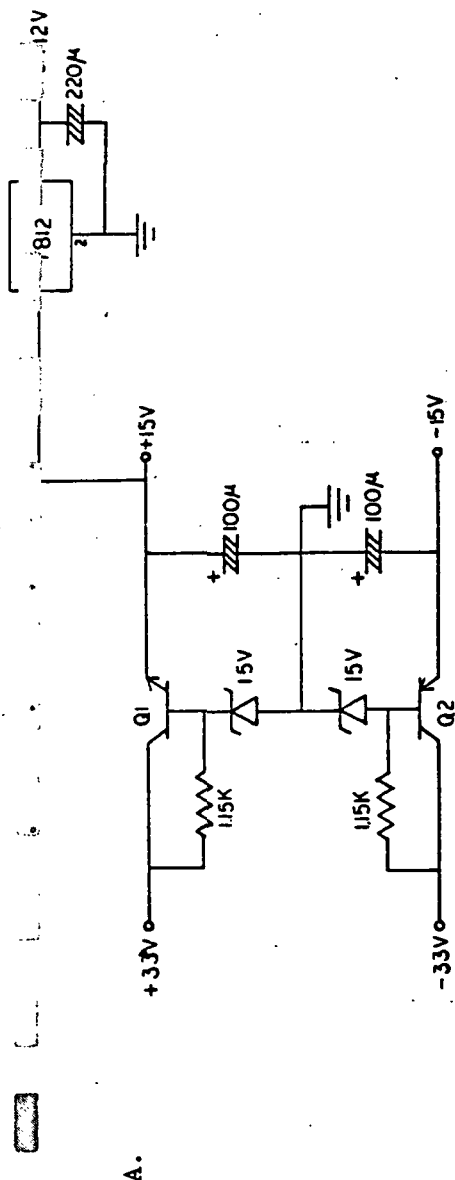
A two-pole three position slide switch is used as a mode selector. In the first two positions a ground level is sensed by line PB4 of the 6820 and notifies the CPU to send out approximately a 2 KHz pulse test signal to either one of the transducer enabling inputs of the transmitting "pinger", depending on the position of the switch. This in turn will provide a continuous pulsed ultrasound output so that the operator can place the receiver transducer at a proper position. In position 3, the run mode, the CPU takes over and selection of the transmitter is controlled by the stored program.

Power Supply Circuits

Power for all clocks of the system is supplied by the TM515 power module. Fig. 43 shows the designed voltage regulator circuits to convert this power source into the required 5V, 12V, and 15V required by the system. The three circuits operate as follows:

Figure 43A produces +15V and +12V. A regulated voltage source provided by a 15V Zener diode and a pnp power transistor produces the -15V supply. A second similar voltage source using a npn transistor produces the +15V supply. The +15V supply is also used as the input to an LM 7812 +12V precision voltage regulator which produces the 12V supply. Capacitors are used to filter out any AC ripple.

Since the LED displays do not require a precise voltage source, a simple voltage dividing network, shown in Fig. 43B, is used to



Q1 THROUGH Q4 ARE POWER TRANSISTORS SUPPLIED
BY TM515 POWER MODULE
☆ ALL THE RESISTOR USED HERE IS 1W

WENNER - GREN
RESEARCH
LABORATORY
University of Kentucky
NAS 9 - 15452
Principal Investigator:
P. K. Bhagat
June 27, 1979

FIGURE 43- Schematic of power supply circuits used in two transmitter ULVS

produce its 5V supply. Line voltage is stepped down to 25V through a transformer. A pnp power transistor and three resistors are used to produce the voltage divider which produces 5V at the output of Fig. 43 B. In order to prevent the 100 mf capacitor from discharging back into the transformer, a diode is included at the input. Capacitors are used at the input and output to filter out any AC ripple.

Two +5V precision voltage regulators (LM 7805) and one -5V precision voltage regulator (LM 7905) are used in Fig. 43B to produce the 5V supplied. Line voltage is stepped down to 15V through a center tapped transformer. The center tap is grounded. Full wave rectification of the secondary voltage across the end terminals of the top portion of Fig. 43C is accomplished by two diodes. A regulated voltage source, provided by an npn transistor and a 9V Zener diode with input and output capacitors for filtering out ac ripple, is used as an input to the two 7805's. Half wave rectification of the secondary voltage across the end terminals of the lower portion of Fig. 43C is accomplished by one reverse-biased diode to allow only negative voltages to pass. This is used as the input to 7905, which produces the -5V supply. Transistors Q_1 through Q_2 are power transistors supplied by the TM 515 power module. All resistors are 1 watt.

SOFTWARE IMPLEMENTATION

The operation of the Ultrasonic Plethysmograph is controlled by the 8080 microprocessor and the program implemented in the 8080 provides the process for determining limb cross-sectional area. To fully understand the operation of this device it is necessary to understand the software implementation. A flow graph of the program is shown in Fig. 44.

The program counter within the 8080 microprocessor chip is initialized through a SPST pushbutton switch located on the front panel. Automatic power-on-reset of the program counter is provided through an R-c charging network. The program begins with initialization of the 6820 PIA. The stack pointer is then set up followed by the choice of operating mode. In the testing mode a 2 KHz pulse repetition frequency (prf) is used to excite one of the transducers based on the position of the selector switch. This feature enables one to observe the received signals on the oscilloscope screen and adjust the transducer locations for optimum results. Once the optimum transducer sites have been located, the selector switch is moved to position 3, run mode, indicating that limb area computations may now be carried out. It begins by resetting the binary counters upon activation of transducer 1. The program then calls subroutine "NOTYET" shown in Fig. 45. This subroutine takes the binary count, which is the time required for the ultrasonic pulse to traverse from transmitter to receiver, and converts it into a corresponding chord length, d1. This information is stored in the RAM. In a similar manner the second chord length data, d2, is obtained and stored. The limb cross-sectional area is computed and

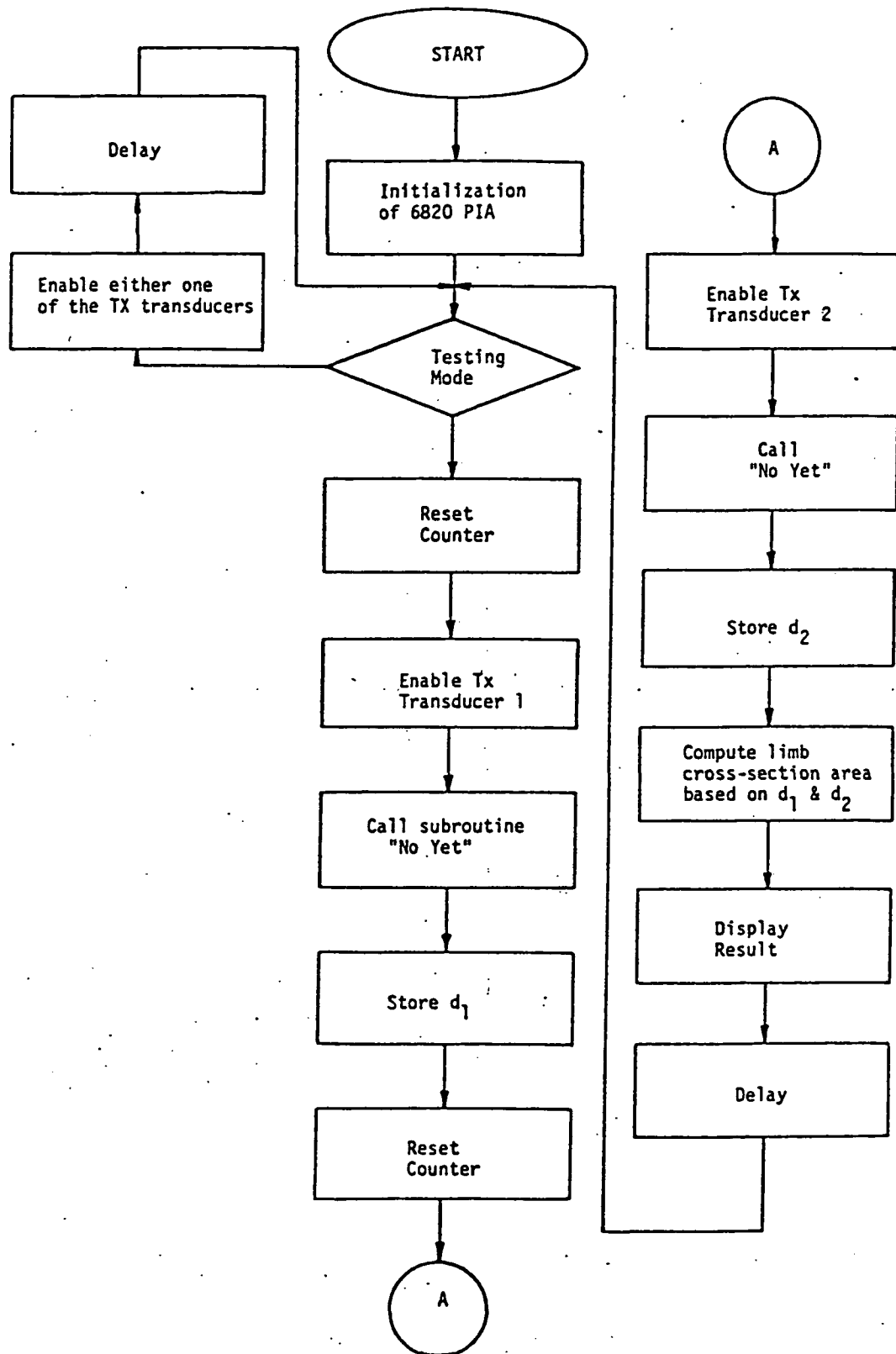


FIGURE 44. Flow Graph of Software Implementation

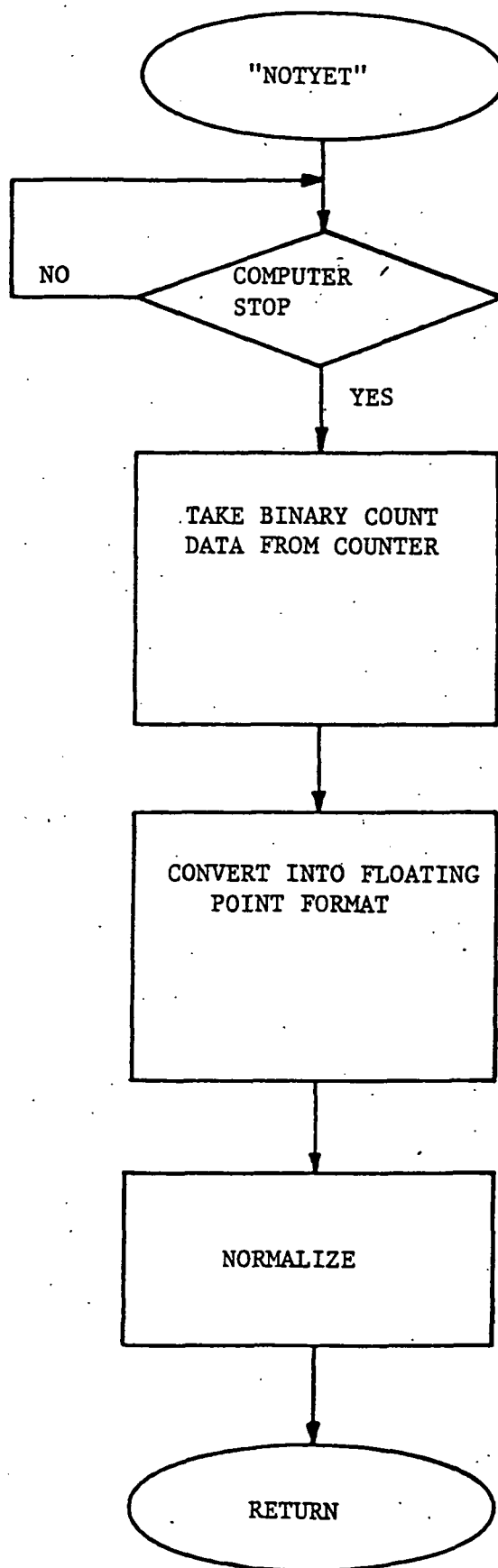


FIGURE 45. Subroutine "NOTYET"

displayed on the front panel LED readout. After a delay (firmware adjustable, normally set a 1 sec), the program returns to the testing mode and a second sequence of events begins, unless the selector switch is moved to positions 1 or 2.

A complete listing of software is included in the following pages.

SOFTWARE PROGRAM LISTING

```

; *****
; ULTRASONIC LOWER LIMB AREA COMPUTATION.
; *****
;
; THIS IS A PROGRAM TO COMPUTE AREA OF
; A SEGMENT OF THE LOWER LIMB UNDER MEASUREMENT.
; COMPUTATIONS ARE DONE BY UTILIZING FLOATING
; POINT ROUTINES WHICH ARE ADOPTED AND
; MODIFIED FROM THE INITIAL VERSION OF IMSAI
; 8K BASIC SOURCE LISTING. THESE ROUTINES ARE
; LISTED FOR REFERENCE.
;
;
; PARAMETERS ARE DEFINED AS FOLLOWS:
;
; D1= DISTANCE BETWEEN 1ST TRANSMITTING TRANSDUCER
;     AND THE RECEIVING TRANSDUCER.
; D2= DISTANCE BETWEEN 2ND TRANSMITTING TRANSDUCER
;     AND THE RECEIVING TRANSDUCER.
; D= DISTANCE BETWEEN TWO TRANSMITTING TRANSDUCERS.
;   WHICH IS PRESETED AS 2.5( CM).
; PROGRAM IS STORED IN TWO 2708 EPROMS AND
; STRAT AT LOCATION 0.
; GENERATED AND TEMPERARY DATAS ARE STORED IN
; TWO 4 BY 256 RAM WHICH ARE LOCATED AT 800H.
; FLOATING POINT DATAS ARE STORED IN 4 CONSEQUITIVE
; BYTES WITH THE 1ST BIT OF THE 1ST BYTE
; BE THE SIGN OF THE MANTISA AND 2ND BIT OF THE 1ST
; BYTE BE THE SIGN OF EXPONENT. THE REST
; OF THE 1ST BYTE IS EXPONENT AND THE FOLLOWED
; 3 BYTES ARE MANTISA.
;
; *****
;      ORG      0
;
; *****
; SET THE STACK POINTER AT 4300Q(980H).
; LOCATIONS 800H TO 97FH ARE SAVED TO
; STORE GENERATED AND TEMPERARY DATAS.
;      LXI      SP,4300Q
;
; *****
; INITIALIZE PIAS(MOTOROLA 6820).
; PIA(1) CHANNEL A IS SET AS INPUT.
; PIA(1) FIRST 2 BITS OF CHANNEL B
; IS SET AS OUTPUT OTHERS AS INPUT.

```

```
; INPUT ARE FROM BINARY COUNTER, OUT.
; PUT ARE TO THE CONTROLLING LOGIC.
; PIA(2) CHANNEL A AND B ARE SET AS
; OUTPUT ONLY.
; REFER TO CHAPTER 4 FOR DETAILS.
;
```

```
    XRA    A        ;CLEAR A.
    OUT    1        ;ACCESS DATA DIRECTION
```

```
0003 AF          XRA    A        ;CLEAR A.
0004 D301        OUT    1        ;ACCESS DATA DIRECTION
0006 D303        OUT    3        ;REGISTERS.
0008 D305        OUT    5
000A D307        OUT    7
000C D300        OUT    0        ;SET AS INPUT.
000E 3EC0        MVI    A,300H
0010 D302        OUT    2
0012 3EFF        MVI    A,377H
0014 D304        OUT    4        ;SET AS OUTPUT.
0016 D306        OUT    6
0018 3E34        MVI    A,64H
001A D301        OUT    1        ;ACCESS DATA REGISTERS.
001C D301        OUT    1
001E D303        OUT    3
0020 D305        OUT    5
0022 D307        OUT    7
```

```
;
;*****
```

```
; IN THE FOLLOWING THE STATUS OF THE
; THE MODE SELECTION SWITCH IS DETECTED.
; IF THE MODE IS SELECTED AS TESTING, A
; 2KHZ PULSE IS SENT TO EITHER ONE OF THE
; TRANSMITTING TRANSDUCERS. OTHERWISE
; COMPUTATION SEQUENCE IS RESUMED.
```

```
0024 DB02        SNP     IN      2        ;CHECK TESTING?
0026 E610        ANI     020H
0028 C24000      JNZ     FREE    ;JUMP IF NOT TESTING.
002B 3E80        MVI     A,200H ;OTHERWISE TURN ON PULSE.
002D D302        OUT     2
002F 3E00        MVI     A,0      ;TURN OFF PULSE.
0031 D302        OUT     2
0033 210000      LXI     H,0
0036 7D          DL      MOV     A,L    ;DELAY FOR 1/2 MSEC.
0037 23          INX     H
0038 FE22        CPI     42H
003A C23600      JNZ     DL
003D C32400      JMP     SNP
```

```
;
;*****
```

```
; START COMPUTATION SEQUENCE.
; ROUTINES ARE SPECIFIED AS FOLLOWING,
```

; RST6= STORE (A) INTO <H,L>
 ; RST5= RESTORE <H,L> INTO (A)
 ; FACC= FLOATING POINT ACCUMULATOR.
 ; FMUL= FLOATING POINT MULTIPLICATION.
 ; FSUB= FLOATING POINT SUBTRACTION
 ; FDIV= FLOATING POINT DIVISION.
 ; FADD= FLOATING POINT ADDITION.
 ; FOUT= CONVERT FLOATING POINT NUMBERS INTO BCD.
 ; WHERE (A) IS CONTENTS OF A REGISTER.
 ; <H,L> IS LOCATION DEFINED BY REGISTER H AND L.

0040 3E3C	FREE	MVI	A,740	;CLEAR COUNTER.
0042 D303		OUT	3	
0044 3E34		MVI	A,648	
0046 D303		OUT	3	
0048 3E80		MVI	A,2008	;SEND PULSE TO
004A D302		OUT	2	;ULTRASONIC PINGER.
004C AF		XRA	A	
004D D302		OUT	2	
004F CD8205		CALL	NOTYET	;GO CONVERTING ROUTINE.
0052 210A08		LXI	H,D1	;STORE 1ST CHORD.
0055 CDCF03		CALL	RST6	
0058 3E3C		MVI	A,740	;CLEAR COUNTER.
005A D303		OUT	3	
005C 3E34		MVI	A,640	
005E D303		OUT	3	
0060 3EC0		MVI	A,3008	;SEND 2ND PULSE.
0062 D302		OUT	2	
0064 AF		XRA	A	
0065 D302		OUT	2	
0067 CD8205		CALL	NOTYET	
006A 210E08		LXI	H,D2	;STORE 2ND CHORD.
006D CDCF03		CALL	RST6	
0070 210A08		LXI	H,D1	;RESTORE D1.
0073 CD8803		CALL	RST5	
0076 213108		LXI	H,FACC	
0079 CD8001		CALL	FMUL	;GET D1 SQUARE.
007C 210A08		LXI	H,D1	
007F CDCF03		CALL	RST6	;STORE D1 SQUARE.
0082 210E08		LXI	H,D2	
0085 CD8803		CALL	RST5	
0088 213108		LXI	H,FACC	
008B CD8001		CALL	FMUL	;GET D2 SQUARE.
008E 210E08		LXI	H,D2	
0091 CDCF03		CALL	RST6	;STORE D2 SQUARE.
0094 210A08		LXI	H,D1	
0097 CD9C04		CALL	FADD	;ADD D1 ² AND D2 ² .
009A 218004		LXI	H,DC	
009D CD6005		CALL	FSUB	;SUBTRACT BY D ² .
00A0 211908		LXI	H,VA	
00A3 CDCF03		CALL	RST6	;STORE IT.
00A6 213108		LXI	H,FACC	

00A9 CD8001	CALL	FMUL	;SQUARE IT.
00AC 218804	LXI	H,F4	;GET 4.
00AF CDEF03	CALL	FDIV	;DIVIDED BY 4.
00B2 210A08	LXI	H,D1	
00B5 CDEF03	CALL	FDIV	;DIVIDED BY D1^2.
00B8 210E08	LXI	H,D2	
00BB CDEF03	CALL	FDIV	;DIVIDED BY D2^2.
00BE 211D08	LXI	H,VASQ	
00C1 CDCF03	CALL	RST6	;STORE IT.
00C4 218C04	LXI	H,F1	
00C7 CD8803	CALL	RST5	;1 TO FACC
00CA 211D08	LXI	H,VASQ	
00CD CD6005	CALL	FSUB	;GET 1-(VASQ).
00D0 210E08	LXI	H,D2	
00D3 CD8001	CALL	FMUL	;MULTIPLIED BY D2^2.
<hr/>			
00D6 212508	LXI	H,Y2SQ	
00D9 CDCF03	CALL	RST6	;STORE IT.
00DC 211908	LXI	H,VA	;TO RESTORE VA.
00DF CD8803	CALL	RST5	
00E2 219004	LXI	H,F2	;GET 2.
00E5 CDEF03	CALL	FDIV	;GET VA/2.
00E8 212108	LXI	H,VAHF	
00EB CDCF03	CALL	RST6	;STORE IT.
00EE 210E08	LXI	H,D2	
00F1 CD8803	CALL	RST5	;RESTORE D2^2.
00F4 212108	LXI	H,VAHF	
00F7 CD6005	CALL	FSUB	;GET D2^2-VAHF.
00FA 213108	LXI	H,FACC	
00FD CD8001	CALL	FMUL	;SQUARE IT.
0100 218804	LXI	H,F4	
0103 CDEF03	CALL	FDIV	;DIVIDED BY 4.
0106 212508	LXI	H,Y2SQ	
0109 CDEF03	CALL	FDIV	;DIVIDED BY Y2SQ.
010C 212908	LXI	H,YCSQ	
010F CDCF03	CALL	RST6	;STORE IT.
0112 210A08	LXI	H,D1	
0115 CD8803	CALL	RST5	;RESTORE D1^2.
0118 218804	LXI	H,F4	
011B CDEF03	CALL	FDIV	;DIVIDED BY 4.
011E 212908	LXI	H,YCSQ	
0121 CD9C04	CALL	FADD	;ADD IT WITH YCSQ.
0124 219404	LXI	H,PHI	
0127 CD8001	CALL	FMUL	;MULTIPLIED BY PHI.
012A 214508	LXI	H,STRIN	
012D CDF701	CALL	FOUT	;CONVERT RESULT INTO BCD.
0130 CD3601	CALL	DISP	;DISPLAY RESULT ON LEDS.
0133 C32400	JMP	SNP	;GO BACK FOR NEXT.

```

;
;*****
; THIS SUBROUTINE DISPLAY THE BCD RESULTS
; FROM FOUT ROUTINE ONTO FRONT PANEL LED DISPLAY.

```

; THE RESULTS FROM FOUT IS ASSUMED TO BE LESS THAN
; 200 CM SQUARE AND GREATER THAN 20 CM SQUARE.

```

0136 =      DISP      EQU      $
0136 3E34      MVI      A,640
0138 D307      OUT      7      ;CLEAR 1ST DIGIT.
013A 0E05      MVI      C,5      ;NUMER OF DIGIT INTO C.
013C 111208     LXI      D,OUTSTR      ;SET DISPLAY BUFFER.
013F 214508     LXI      H,STRIN ;LOCATE BCD RESULT.
0142 7E      REPT      MOV      A,M
0143 23      INX      H
0144 FE0A      CPI      10      ;CHECK IF IS A BCD.
0146 F24201     JP      REPT      ;IF NOT SKIP IT.
0149 12      STAX      D      ;OTHERWISE INTO BUFFER.
014A 13      INX      D      ;INCREMENT BUFFER.
014B 0D      DCR      C      ;LESS ONE DIGIT.
014C C24201     JNZ      REPT      ;GO REPEAT IF MORE DIGIT.
014F 211208     LXI      H,OUTSTR      ;LOCATE BUFFER.
0152 7E      MOV      A,M
0153 FE02      CPI      2      ;CHECK IF >100.0
0155 F25E01     JP      SKIP      ;SKIP IF NOT.
0158 3E3C      MVI      A,740      ;OTHERWISE GO LIT
015A D307      OUT      7      ;1ST DIGIT TO 1.
015C 23      INX      H
015D 7E      MOV      A,M      ;GET NEXT.
015E 23      SKIP      INX      H
015F 07      RLC      ;ROTATE TO LEFT.
0160 07      RLC
0161 07      RLC
0162 07      RLC
0163 E6F0      ANI      0F0H      ;STRIP TO 4 BITS.
0165 86      ADD      H      ;MERGE WITH NEXT BCD.
0166 D306      OUT      6      ;DISPLAY IT(2 DIGITS).
0168 23      INX      H
0169 7E      MOV      A,M      ;GET 3RD BCD.
016A 07      RLC      ;ROTATE IT.
016B 07      RLC
016C 07      RLC
016D 07      RLC
016E 07      RLC
016F E6F0      ANI      0F0H
0171 23      INX      H
0172 86      ADD      H      ;MERGE WITH LAST BCD.
0173 D304      OUT      4      ;DISPLAY AT LAST 2 DIGITS.
0175 210000     LXI      H,0      ;DELAY FOR 1 SEC.
0178 7C      DL1      MOV      A,H
0179 23      INX      H
017A FE7F      CPI      1770
017C C27801     JNZ      DL1
017F C9      RET      ;RETURN.

```

```

;*****
; FLOATING POINT MULTIPLICATION SUBROUTINE.
; FLOATING POINT MULTIPLY THE NUMBER AT (H,L) TO
; THE FACC.
;

```

0180 =	FMUL	EQU	\$
0180 CD6303		CALL	FTEST
0183 C8		RZ	
0184 23		INX	H
0185 7E		MOV	A,M
0186 2B		DCX	H
0187 B7		ORA	A
0188 CA8803		JZ	RST5
018B 113108	FMUL1	LXI	D,FACC
018E 1A		LDAX	D
018F CD7103		CALL	FEXP
0192 47		MOV	B,A
0193 7E		MOV	A,M
0194 CD7103		CALL	FEXP
0197 80		ADD	B
0198 CDD703		CALL	FOVUN
019B E67F		ANI	127
019D 47		MOV	B,A
019E 1A		LDAX	D
019F AE		XRA	H
01A0 E680		ANI	128
01A2 B0		ORA	B
01A3 12		STAX	D
01A4 113E08		LXI	D,FTEMP+9
01A7 0603		MVI	B,3
01A9 23		INX	H
01AA CD7803		CALL	COPYH
01AD 213508		LXI	H,FTEMP
01B0 0606		MVI	B,6
01B2 CDE703		CALL	ZEROM
01B5 113208		LXI	D,FACC+1
01B8 0603		MVI	B,3
01BA 1A	FMUL5	LDAX	D
01BB 77		MOV	H,A
01BC AF		XRA	A
01BD 12		STAX	D
01BE 13		INX	D
01BF 23		INX	H
01C0 05		DCR	B
01C1 C2BA01		JNZ	FMUL5
01C4 0E18		MVI	C,24
01C6 0603	FMUL6	MVI	B,3
01C8 213E08		LXI	H,FTEMP+9
01CB AF		XRA	A
01CC 7E	FMUL7	MOV	A,M
01CD 1F		RAR	
01CE 77		MOV	H,A

01CF 23		INX	H
01D0 05		DCR	B
01D1 C2CC01		JNZ	FMUL7
01D4 D2E201		JNC	FMUL8
01D7 113708		LXI	D, FTEMP+2
01DA 213D08		LXI	H, FTEMP+8
01DD 0606		MVI	B, 6
01DF CD7D03		CALL	FADDT
01E2 0606	FMUL8	MVI	B, 6
01E4 213D08		LXI	H, FTEMP+8
01E7 AF		XRA	A
01E8 7E	FMUL9	MOV	A, M
01E9 17		RAL	
01EA 77		MOV	M, A
01EB 2B		DCX	H
01EC 05		DCR	B
01ED C2E801		JNZ	FMUL9
01F0 0D		DCR	C
01F1 C2C601		JNZ	FMUL6
01F4 C39003		JMP	FNORM

; *****
; FLOATING POINT OUTPUT ROUTINE.

; THIS SUBROUTINE CONVERTS A NUMBERS IN THE FLOATING
; POINT ACCUMULATOR TO A BCD STRING SUITABLE FOR DISPLAY.

01F7 =	FOUT	EQU	\$
01F7 113408		LXI	D, FACC+3
01FA 1A		LDAX	D
01FB F607		ORI	7
01FD 12		STAX	D
01FE CD6303		CALL	FTEST
0201 3620		MVI	M, ' '
0203 E20802		JP	FOUT0
0206 362D		MVI	M, ' - '
0208 23	FOUT0	INX	H
0209 C21202		JNZ	FOUT2
020C 3630		MVI	M, ' 0 '
020E 23		INX	H
020F 3620	FOUT1	MVI	M, ' '
0211 C9		RET	
0212 3A3108	FOUT2	LDA	FACC
0215 CD7103		CALL	FEXP
0218 C21D02		JNZ	FOUTV
021B 3E80		MVI	A, 128
021D E680	FOUTV	ANI	128
021F 320908		STA	DEXP
0222 E5		PUSH	H
0223 3A3108	FOUT3	LDA	FACC
0226 CD7103		CALL	FEXP
0229 FE01		CPI	1
022B F24402		JP	FOUT6

022E 210908	FOUT4	LXI	H,DEXP
0231 34		INR	M
0232 217C04		LXI	H,TEN
0235 F23E02		JP	FOUT5
0238 CD8001		CALL	FXUL
023B C32302		JMP	FOUT3
023E CDEF03	FOUT5	CALL	FDIV
0241 C32302		JMP	FOUT3
0244 FE05	FOUT6	CPI	5
0246 F22E02		JP	FOUT4
0249 213508		LXI	H,FTEMP
024C CDCF03		CALL	RST6
024F 3A3108		LDA	FACC
0252 CD7103		CALL	FEXP
0255 0E06		MVI	C,6
0257 CDAE02		CALL	FOUTB
025A FE0A		CPI	10
025C FA6802		JM	FOUTU
025F 213508		LXI	H,FTEMP
0262 CD8803		CALL	RST5
0265 C32E02		JMP	FOUT4
0268 CD9C02	FOUTU	CALL	FOUT9
026B AF	FOUT7	XRA	A
026C 323108		STA	FACC
026F CD9202		CALL	FOUT8
0272 213508		LXI	H,FTEMP
0275 CDCF03		CALL	RST6
0278 CD9202		CALL	FOUT8
027B CD9202		CALL	FOUT8
027E 113408		LXI	D,FACC+3
0281 213808		LXI	H,FTEMP+3
0284 0604		MVI	B,4
0286 CD7D03		CALL	FADDT
0289 CD9C02		CALL	FOUT9
028C C26B02		JNZ	FOUT7
028F C3C502		JMP	FOUTh
0292 213408	FOUT8	LXI	H,FACC+3
0295 54		MOV	D,H
0296 5D		MOV	E,L
0297 0604		MVI	B,4
0299 C37D03		JMP	FADDT
029C F600	FOUT9	ORI	0
029E E1		POP	H
029F E3		XTHL	
02A0 77		MOV	H,A
02A1 23		INX	H
02A2 79		MOV	A,C
02A3 FE06		CPI	6
02A5 C2AB02		JNZ	FOUTA
02A8 362E		MVI	H,'.'
02AA 23		INX	H
02AB E3	FOUTA	XTHL	

02AC 0D		DCR	C
02AD E9		PCHL	
02AE 5F	FOUTB	MOV	E,A
02AF AF		XRA	A
02B0 323108		STA	FACC
02B3 213408	FOUTC	LXI	H,FACC+3
02B6 0604		MVI	B,4
02B8 7E	FOUTD	MOV	A,M
02B9 17		RAL	
02BA 77		MOV	H,A
02BB 2B		DCX	H
02BC 05		DCR	B
02BD C2B802		JNZ	FOUTD
02C0 1D		DCR	E
02C1 C2B302		JNZ	FOUTC
02C4 C9		RET	
02C5 E1	FOUTH	POP	H
02C6 3645		MVI	H,'E'
02C8 23		INX	H
02C9 3A0908		LDA	DEXP
02CC 362B		MVI	H,'+'
02CE 57		MOV	D,A
02CF B7		ORA	A
02D0 F2DC02		JP	FOUTI
02D3 362D		MVI	H,'--'
02D5 E67F		ANI	127
02D7 2F		CMA	
02D8 3C		INR	A
02D9 57		MOV	D,A
02DA 2F		CMA	
02DB 3C		INR	A
02DC 23	FOUTI	INX	H
02DD E5		PUSH	H
02DE 1EFF		MVI	E,OFFH
02E0 1C	FOUTJ	INR	E
02E1 D60A		SUI	10
02E3 F2E002		JP	FOUTJ
02E6 C60A		ADI	10
02E8 47		MOV	B,A
02E9 7B		MOV	A,E
02EA CD9C02		CALL	FOUT9
02ED 78		MOV	A,B
02EE CD9C02		CALL	FOUT9
02F1 E1		POP	H
02F2 3620		MVI	H,' '
02F4 7A		MOV	A,D
02F5 B7		ORA	A
02F6 F2FF02		JP	FOUTK
02F9 FEFE		CPI	OFEH ; -2
02FB D8		RC	
02FC C30203		JMP	FOUTL

02FF FE06	FOUTK	CPI	6
0301 D0		RNC	
0302 4F	FOUTL	MOV	C,A
0303 0605		MVI	B,5
0305 3620	FOUTM	MVI	M,' '
0307 2B		DCX	H
0308 05		DCR	B
0309 C20503		JNZ	FOUTM
030C EB		XCHG	
030D 2B		MOV	A,E
030E D605		SUI	5
0310 6F		MOV	L,A
0311 7A		MOV	A,D
0312 DE00		SBI	0
0314 67		MOV	H,A
0315 79		MOV	A,C
0316 B7		ORA	A
0317 CA2803		JZ	FOUTO
031A FA3D03		JN	FOUTR
031D 46	FOUTN	MOV	B,H
031E 23		INX	H
031F 7E		MOV	A,M
0320 70		MOV	M,B
0321 2B		DCX	H
0322 77		MOV	M,A
0323 23		INX	H
0324 0D		DCR	C
0325 C21D03		JNZ	FOUTN
0328 EB	FOUTO	XCHG	
0329 7E	FOUTP	MOV	A,M
032A FE30		CPI	'0'
032C C33503		JMP	FOUTQ
032F 3620		MVI	M,' '
0331 2B		DCX	H
0332 C32903		JMP	FOUTP
0335 FE2E	FOUTQ	CPI	'.'
0337 23		INX	H
0338 C0		RNZ	
0339 2B		DCX	H
033A 3630		MVI	M,'0'
033C C9		RET	
033D FEFF	FOUTR	CPI	255
033F C24B03		JNZ	FOUTS
0342 2B		DCX	H
0343 7E		MOV	A,M
0344 362E		MVI	M,'.'
0346 23		INX	H
0347 77		MOV	M,A
0348 C32803		JMP	FOUTO
034B 2B	FOUTS	DCX	H
034C 7E		MOV	A,M
034D 3630		MVI	M,'0'

```

034F 23      INX      H
0350 77      MOV      M,A
0351 62      MOV      H,D
0352 6B      MOV      L,E
0353 0606    MVI      B,6
0355 2B      FOUTT    DCX      H
0356 7E      MOV      A,M
0357 23      INX      H
0358 77      MOV      M,A
0359 2B      DCX      H
035A 05      DCR      B
035B C25503  JNZ      FOUTT
035E 362E    MVI      M,'.'
0360 C32803  JMP      FOUTO

```

```

;
;*****
; TEST THE SIGN OF THE NUMBER IN THE FACC.
;

```

```

0363 =      FTEST    EQU      $
0363 3A3208  LDA      FACC+1
0366 B7      ORA      A
0367 C8      RZ
0368 3A3108  LDA      FACC
036B F67F    ORI      127
036D 3A3108  LDA      FACC
0370 C9      RET

```

```

;
;*****
; EXPAND EXPONENT INTO 8 BINARY BITS.
;

```

```

0371 =      FEXP     EQU      $
0371 E67F    ANI      127
0373 C640    ADI      64
0375 EE40    XRI      64
0377 C9      RET

```

```

;
;*****
; MOVE THE STRING FROM (H,L) TO (D,E) COUNT IN B.
;

```

```

0378 =      COPYH    EQU      $
0378 EB      XCHG
0379 CDC603  CALL     COPYD
           EXHG
037C C9      RET

```

```

;
;*****
; ADD TWO MULTIPRECISION NUMBERS (D,E) & (H,L).
;

```

```

037D =      FADDT    EQU      $
037D AF      XRA      A
037E 1A      FAD1     LDAX    D
037F 8E      ADC      M
0380 12      STAX     D
0381 1B      DCX      D
0382 2B      DCX      H

```

```

0383 05          DCR      B
0384 C27E03      JNZ      FAD1
0387 C9          RET

```

```

;
;*****

```

```

; LOAD THE FLOATING POINT ACCUMULATOR WITH THE 4 BYTES
; AT (H,L).

```

```

0388 =          RST5     EQU      $
0388 113108      LXI      D,FACC
038B 0604        MVI      B,4
038D C37803      JMP      COPYH

```

```

;
;*****

```

```

; NORMALIZE THE FLOATING ACCUMULATOR. THAT IS,
; THE FIRST BIT MUST BE SIGNIFICANT.

```

```

0390 =          FNORM    EQU      $
0390 213408      LXI      H,FACC+3
0393 7E          MOV      A,M
0394 2B          DCX      H
0395 B6          ORA      M
0396 2B          DCX      H
0397 B6          ORA      M
0398 C29E03      JNZ      FNRM1
039B 2B          DCX      H
039C 77          MOV      M,A
039D C9          RET
039E 7E          FNRM1    MOV      A,M
039F B7          ORA      A
03A0 FA6303      JM       FTEST
03A3 23          INX      H
03A4 23          INX      H
03A5 0603        MVI      B,3
03A7 AF          XRA      A
03A8 7E          FNRM2    MOV      A,M
03A9 17          RAL
03AA 77          MOV      M,A
03AB 2B          DCX      H
03AC 05          DCR      B
03AD C2A803      JNZ      FNRM2
03B0 7E          MOV      A,M
03B1 CD7103      CALL     FEXP
03B4 3D          DCR      A
03B5 FE80        CPI      128
03B7 CA0000      JZ       OVERR
03BA E67F        ANI      127
03BC 47          MOV      B,A
03BD 7E          MOV      A,M
03BE E680        ANI      128
03C0 80          ORA      B
03C1 77          MOV      M,A
03C2 23          INX      H

```

```

03C3 C39E03          JMP      FNRN1
;
;*****
; MOVE THE STRING FROM (D,E) TO (H,L) COUNT IN B.
03C6 =      COPYD      EQU      $
03C6 1A          LDAX     D
03C7 77          MOV      M,A
03C8 23          INX      H
03C9 13          INX      D
03CA 05          DCR      B
03CB C2C603      JNZ      COPYD
03CE C9          RET
0000 =      OVERR      EQU      0
;
;*****
; STORE THE FLOATING POINT ACCUMULATOR AT (H,L)
03CF =      RST6      EQU      $
03CF 113108      LXI      D,FACC
03D2 0604      MVI      B,4
03D4 C3C603      JMP      COPYD
;
;*****
; TEST EXPONENT FOR OVERFLOW OR UNDERFLOW.
03D7 =      FOVUN      EQU      $
03D7 B7          ORA      A
03D8 F2F103      JP      FOU1
03DB FEC1      CPI      193
03DD D0          RNC
03DE C30000      JMP      OVERR
03E1 FE40      FOU1      CPI      64
03E3 D8          RC
03E4 C30000      JMP      OVERR
;
;*****
; MOVES A STRING OF BINARY NZEROS,COUNT IN B.
03E7 =      ZEROM      EQU      $
03E7 3600      MVI      M,0
03E9 23          INX      H
03EA 05          DCR      B
03EB C2E703      JNZ      ZEROM
03EE C9          RET
;
;*****
; FLOATING POINT DIVISION SUBROUTINE.
;
; FLOATING POINT DIVIDE THE NUMBER AT (H,L) INTO
;THE FACC.
03EF =      FDIV      EQU      $
03EF CD6303      CALL     FTEST
03F2 C8          RZ
03F3 23          INX      H
03F4 7E          MOV      A,M

```

03F5 2B		DCX	H
03F6 B7		ORA	A
03F7 CA0000		JZ	OVERR
03FA 7E		MOV	A,M
03FB CD7103		CALL	FEXP
03FE 47		MOV	B,A
03FF 113108		LXI	D,FACC
0402 1A		LDAX	D
0403 CD7103		CALL	FEXP
0406 90		SUB	B
0407 3C		INR	A
0408 CDD703		CALL	FOVUN
040B E67F		ANI	127
040D 47		MOV	B,A
040E 1A		LDAX	D
040F AE		XRA	H
0410 E680		ANI	128
0412 B0		ORA	B
0413 12		STAX	D
0414 E5		PUSH	H
0415 13		INX	D
0416 213508		LXI	H,FTEMP
0419 3600		MVI	M,0
041B 23		INX	H
041C 0603		MVI	B,3
041E 1A	FDIV3	LDAX	D
041F 77		MOV	M,A
0420 AF		XRA	A
0421 12		STAX	D
0422 23		INX	H
0423 13		INX	D
0424 05		DCP	B
0425 C21E04		JNZ	FDIV3
0428 D1		POP	D
0429 0603		MVI	B,3
042B 13		INX	D
042C 3600		MVI	M,0
042E 23		INX	H
042F CDC603		CALL	COPYD
0432 0E18		MVI	C,24
0434 113808	FDIV5	LXI	D,FTEMP+3
0437 213C08		LXI	H,FTEMP+7
043A 0604		MVI	B,4
043C CD7104		CALL	FSUBT
043F D24E04		JNC	FDIV6
0442 113808		LXI	D,FTEMP+3
0445 213C08		LXI	H,FTEMP+7
0448 0604		MVI	B,4
044A CD7D03		CALL	FADDT
044D 37		STC	
044E 3F	FDIV6	CMC	

```

044F 0603      MVI      B,3
0451 213408    LXI      H,FACC+3
0454 7E        FDIIV7  MOV      A,M
0455 17        RAL
0456 77        MOV      M,A
0457 2B        DCX      H
0458 05        DCR      B
0459 C25404    JNZ      FDIIV7
045C AF        XRA      A
045D 0604      MVI      B,4
045F 213808    LXI      H,FTEMP+3
0462 7E        FDIIV8  MOV      A,M
0463 17        RAL
0464 77        MOV      M,A
0465 2B        DCX      H
0466 05        DCR      B
0467 C26204    JNZ      FDIIV8
046A 0D        DCR      C
046B C23404    JNZ      FDIIV5
046E C39003    JMP      FNORM

```

```

;
;*****
; SUBTRACT THE TWO MULTIPRESION NUMBERS (D,E) & (H,L)
0471 =         FSUBT   EQU      $
0471 AF        XRA      A
0472 1A        FSB1    LDAX    D
0473 9E        SBB      M
0474 12        STAX     D
0475 1B        DCX      D
0476 2B        DCX      H
0477 05        DCR      B
0478 C27204    JNZ      FSB1
047B C9        RET

```

```

;
;*****
; FOLLOWING ARE CONSTANTS TO BE USED IN THE COMPUTATION
; SEQUENCES. ALL THE CONSTANTS ARE ARRANGED IN FLOATING
; POINT FORMAT.
;
047C 04        TEN     DB      04H      ;INTEGER 10.
047D A0        DB      0A0H
047E 00        DB      0
047F 00        DB      0
0480 03        DC      DB      03H      ;SQUARE OF 2.5(CM).
0481 C8        DB      0C8H
0482 00        DB      00H
0483 00        DB      00H
0484 02        TWO     DB      02H      ;INTEGER 2.
0485 80        DB      80H
0486 00        DB      0
0487 00        DB      0
0488 03        F4      DB      03H      ;INTEGER 4.
0489 80        DB      80H

```


048A 00		DB	0	
048B 00		DB	0	
048C 01	F1	DB	1	;INTEGER 1.
048D 80		DB	80H	
048E 00		DB	00	
048F 00		DB	00	
0490 02	F2	DB	2	;2.
0491 80		DB	80H	
0492 00		DB	0	
0493 00		DB	0	
0494 02	PHI	DB	2	;PHI=3.1415926
0495 C9		DB	0C9H	
0496 0F		DB	0FH	
0497 D7		DB	0D7H	
0498 7A	SPEED	DB	7AH	;SPEED OF ULTRASOUND.
0499 8C		DB	8CH	;=0.15CM/USEC.
049A A4		DB	0A4H	
049B 9C		DB	9CH	

; FLOATING POINT ADDITION SUBROUTINE.

; FLOATING POINT ADD THE NUMBER AT (H,L) TO FACC

049C =	FADD	EQU	\$
049C 23		INX	H
049D 7E		MOV	A,H
049E B7		ORA	A
049F CA6303		JZ	FTEST
04A2 2B		DCX	H
04A3 CD6303		CALL	FTEST
04A6 CA8803		JZ	RST5
04A9 113108		LXI	D,FACC
04AC 1A		LDAX	D
04AD CD7103		CALL	FEXP
04B0 47		MOV	B,A
04B1 7E		MOV	A,H
04B2 CD7103		CALL	FEXP
04B5 4F		MOV	C,A
04B6 90		SUB	B
04B7 CACC04		JZ	FADD4
04BA F2BE04		JP	FADD3
<hr/>			
04BD 2F		CMA	
04BE 3C		INR	A
04BF FE18	FADD3	CPI	24
04C1 DACC04		JC	FADD4
04C4 78		MOV	A,B
04C5 91		SUB	C
04C6 F26303		JP	FTEST
04C9 C38803		JMP	RST5
04CC F5	FADD4	PUSH	PSW
04CD C5		PUSH	B
04CE 113508		LXI	D,FTEMP

04D1 0604		MVI	B,4
04D3 CD7803		CALL	COPYH
04D6 C1		POP	B
04D7 F1		POP	PSW
04D8 CAFF04		JZ	FADD9
04DB 213608		LXI	H,FTMP+1
04DE F5		PUSH	PSW
04DF 78		MOV	A,B
04E0 91		SUB	C
04E1 F2F104		JP	FADD6
04E4 213108		LXI	H,FACC
04E7 79		MOV	A,C
04E8 E67F		ANI	127
04EA 4F		MOV	C,A
04EB 7E		MOV	A,M
04EC E680		ANI	128
04EE B1		ORA	C
04EF 77		MOV	M,A
04F0 23		INX	H
04F1 F1	FADD6	POP	PSW
04F2 4F		MOV	C,A
04F3 0603	FADD7	MVI	B,3
04F5 AF		XRA	A
04F6 E5		PUSH	H
04F7 CD7905		CALL	FSHFT
04FA E1		POP	H
04FB 0D		DCR	C
04FC C2F304		JNZ	FADD7
04FF =	FADD9	EQU	5
04FF 113108		LXI	D,FACC
0502 213508		LXI	H,FTMP
0505 1A		LDAX	D
0506 AE		XRA	M
0507 FA3205		JM	FADDA
050A 113408		LXI	D,FACC+3
050D 213808		LXI	H,FTMP+3
0510 0603		MVI	B,3
0512 CD7D03		CALL	FADDT
0515 D26303		JNC	FTEST
0518 213108		LXI	H,FACC
051B 7E		MOV	A,M
051C E680		ANI	128
051E 47		MOV	B,A
051F 7E		MOV	A,M
0520 CD7103		CALL	FEXP
0523 3C		INR	A
0524 E67F		ANI	127
0526 80		ORA	B
0527 77		MOV	M,A
0528 23		INX	H

```

0529 37          STC
052A 0603        MVI      B,3
052C CD7905      CALL     FSHFT
052F C36303      JMP      FTEST
0532 =          FADDA     EQU      $
0532 213908      LXI      H,FTEMP+4
0535 0604        MVI      B,4
0537 CDC603      CALL     COPYD
053A 113408      FADDB     LXI      D,FACC+3
053D 213808      LXI      H,FTEMP+3
0540 0603        MVI      B,3
0542 CD7104      CALL     FSUBT
0545 D29003      JNC      FNORM
0548 113108      LXI      D,FACC
054B 213508      LXI      H,FTEMP
054E 0608        MVI      B,8
0550 CD7803      CALL     COPYH
0553 113108      LXI      D,FACC
0556 213508      LXI      H,FTEMP
0559 7E          MOV      A,M
055A EE80        XRI      128
055C 12          STAX     D
055D C33A05      JMP      FADDB

```

```

;
;*****
; FLOATING POINT SUBTRACTION SUBROUTINE.
;
; FLOATING POINT SUBTRACT THE NUMBER AT (H,L)
; FROM THE FACC.

```

```

0560 =          FSUB     EQU      $
0560 23          INX      H
0561 7E          MOV      A,M
0562 B7          ORA      A
0563 CA6303      JZ       FTEST
0566 2B          DCX      H
0567 113508      LXI      D,FTEMP
056A 0605        MVI      B,5
056C CD7803      CALL     COPYH
056F 213508      LXI      H,FTEMP
0572 7E          MOV      A,M
0573 EE80        XRI      128
0575 77          MOV      M,A
0576 C39C04      JMP      FADD

```

```

;
;*****
; INCREMENTING SHIFT RIGHT.
;

```

```

0579 =          FSHFT     EQU      $
0579 7E          MOV      A,M
057A 1F          RAR
057B 77          MOV      M,A

```

```

057C 23      INX      H
057D 05      DCR      B
057E C27905  JNZ      FSHFT
0581 C9      RET

```

```

;
;*****
; SUBROUTINE "NOTYET".
;
; THIS ROUTINE TAKES A BINARY NUMBER
; FROM THE COUNTER (THE COUNTER WHICH
; HAS THE TRAVERSE TIME INFORMATION)
; AND CONVERT IT INTO CORRESPONDING
; CHORD LENGTH.
; THE RESULT IS IN FLOATING POINT
; FORMAT AND IS NORMALIZED.
;

```

```

0582 =      NOTYET EQU      $
0582 DB02      IN      2
0584 E620      ANI      0400      ;CHECK IF COUNTER READY?
0586 C28205     JNZ      NOTYET    ;GO BACK IF NOT.
0589 DB00      IN      0          ;OTHERWISE TAKE 1ST BYTE.
058B 5F        MOV      E,A        ;STORE IT.
058C 07        RLC                ;ROTATE IT.
058D 07        RLC
058E 07        RLC
058F 07        RLC
0590 E6F0      ANI      0F0H      ;STRIP INTO 4 BITS.
0592 323308     STA      FACC+2    ;STORE INTO 3RD BYTE OF FACC.
0595 7B        MOV      A,E        ;RESTORE 1ST BYTE.
0596 0F        RRC                ;ROTATE IT.
0597 0F        RRC
0598 0F        RRC
0599 0F        RRC
059A E60F      ANI      0FH       ;STRIP TO 4 BITS.
059C 5F        MOV      E,A        ;STORE IN E.
059D DB02      IN      2          ;GET NEXT HIGHER BYTE.
059F 07        RLC                ;ROTATE.
05A0 07        RLC
05A1 07        RLC
05A2 07        RLC
05A3 E6F0      ANI      0F0H      ;STRIP TO 4.
05A5 83        ADD      E          ;MERGE.
05A6 323208     STA      FACC+1    ;STORE INTO FACC.
05A9 3E0C      MVI      A,0CH      ;MOVE '12' INTO EXPONENT
05AB 323108     STA      FACC      ;OF FACC.
05AE 3E00      MVI      A,0        ;CLEAR LAST BYTE OF
05B0 323408     STA      FACC+3    ;FACC.
05B3 CD9003     CALL     FNORM      ;NORMALIZED IT.
05B6 219804     LXI      H,SPEED   ;MULTIPLIED COUNTS BY SPEED
05B9 CD8001     CALL     FMUL      ;TO GET CHORD LENGTH.
05BC C9        RET                ;RETURN.

```

```

;
;*****
; FOLLOWING ARE DEFINED RAM AREAS.
;

```

		ORG	4000Q
0800			
0800	TEMP1	DS	4
0804	TEMP2	DS	4
0808	TEM	DS	1
0809	DEXP	DS	1
080A	D1	DS	4
080E	D2	DS	4
0812	OUTSTR	DS	7
0819	VA	DS	4
081D	VASQ	DS	4
0821	VAHF	DS	4
0825	Y2SQ	DS	4
0829	YCSQ	DS	4
082D	VB	DS	4
0831	FACC	DS	4
0835	FTEMP	DS	12
0841	MULPR	DS	4
0845	STRIN	DS	20
0859		END	

REFERENCES:

1. Paulev, P. E., F. Neumann, S. L. Nielson and N. Keiding. "Strain gage versus water plethysmography; Description of simplified system and analysis of differences and accuracy." Med. Biol. Eng. 12, pp 437-445, 1974.
2. Whitney, R. J. "The measurement of volume changes in human limbs." J. Physiol. 12, pp. 1-27, 1953.
3. Sigdell, J. E., "Venous occlusion plethysmography." Biomedical Engineering, August and September 1973.
4. Lafferty, J. F., "A feasibility study of limb volume measuring system. Final report NAS9-12749, September 1974 and Final report NAS9-14392, October 1977.
5. Berry, C. A. and A. D. Catterson. "Pre-Gemini medical prediction versus Gemini flight results." Gemini Summary Conference, NASA SP-138, 1967.
6. Dietlein, L. F. and W. V. Judy. "Cardiovascular Conditioning." A Review of Medical Results of Gemini 7 and Related Flights, NASA TM X-60589, pp. 1-35, 1966.
7. Hoffler, G. W. and R. L. Johnson. "Apollo flight crew cardiovascular evaluations." In Biomedical Results of Apollo, NASA, 1975, pp. 227-264.
8. Hoffler, G. W., R. L. Johnson and R. A. Wolthuis. "Apollo space crew cardiovascular evaluations." Aerospace Medicine, 45: pp. 807-820, 1974.
9. Johnson, R. L., G. W. Hoffler, A. E. Nicogossian, S. A. Bergman, Jr. and M. M. Jackson. "Lower body negative pressure: Third Manual Skylab Mission." NASA, SP-377, pp. 284-312, 1977.
10. Thornton, W. E. and G. W. Hoffler. "Hemodynamic studies of the legs under weightlessness." NASA, SP-377, pp. 324-329, 1977.
11. Barnett, R. D., R. J. Gowen, F. L. Zaebst and D. R. Carrol. "A Capacitance Plethysmograph." Seventh Annual Rocky Mountain Bio-Engineering Symposium, 1970.
12. Bhagat, P., M. Kadaba, R. Ware and W. Cockerill. "Frequency dependence of acoustic parameters of freshly excised tissues of sprague dawley rats." Ultrasonics, pp. 179-182, July, 1977.
13. Kadaba, M. P. "Tissue characterization using ultrasonic transmission and scattering parameters." Ph.D. Dissertation, University of Kentucky, 1978.
14. Rushmer, R. F., D. L. Franklin and E. M. Ellis. "Left ventricular dimensions recorded by sonocardiometry." Circulation Research, Volume 4, pp. 684-688, 1956.

15. Stegall, H. F., M. B. Kardon, H. L. Stone and V. S. Bishop. "A portable, simple sonomicrometer." J. Appl. Physiol., 23, 289-293, 1967.
16. Horwitz, L. D., V. S. Bishop, H. L. Stone and H. F. Stegall. "Continuous measurement of internal left ventricular diameter." J. Appl. Physiol., 24, 738-740.
17. Stegall, H. F., J. M. Ofstad, V. E. Simmons and R. F. Rushmer. "An integrated facility for peripheral vascular studies in man." Volume 6, p. 75, Proceeding 17th ACEMB, Cleveland, 1964.
18. Bhagat, P. K., J. F. Lafferty and M. P. Kadaba. "An ultrasonic plethysmograph." Aerospace Medical Association Meeting, Washington, D. C., Reprint, 73-74, May 1979.
19. Kadaba, M. P., P. K. Bhagat and V. Wu. "Attenuation and backscattering of ultrasound in freshly excised animal tissues." IEEE Trans. BioMed Eng., BME-27(2), 76-83, 1980.
20. Bhagat, P. K., J. F. Lafferty, D. Bowman and M. P. Kadaba. "An ultrasonic plethysmograph for space flight applications." Aviat. Space Environ. Med. 51(2), 185-188, 1980.
21. Wu, V. C. "A microprocessor based ultrasonic lower limb volume measurement system." M. S. Thesis, University of Kentucky, 1980.
22. Levitan, B. M. "Evaluation of plethysmographic systems proposed for use on the space shuttle." Special Report NAS9-14880, 1980 and Aviat. Space Environ. Med. 53(1), 6-10, 1983.
23. Bhagat, P. K., M. P. Kadaba, V. N. Gupta and V. Wu. "Microprocessor based system for ultrasonic tissue characterization." Med. Instrum. 14(4), 220-224, 1980.
24. Dekker, A. J. "Solid state physics", Prentice-Hall, Sixth Edition, 184-209, 1962.
25. Mason, W. P., "Piezoelectric crystals and their application to ultrasonics." D. Van Nostrand Co., pp. 234-288, 1950.
26. Hueter, T. F. and Bolt, Ultrasonics, 59-85 and 401-415, John Wiley, 1955.
27. Van Trigt, P., B. J. Bauer, C. O. Olsen, J. S. Rankin and A. S. Wechsler. "An improved transducer for measurement of cardiac dimensions with sonomicrometry." Am. J. Physiol., 240 (Heart Circ. Physiol. 9), H664-H669, 1981.
28. DeSilets, C. S., J. D. Fraser and G. S. Kino. "The design of efficient broadband piezoelectric transducers." IEEE Trans. Sonics Ultrason., SU25, 115-125, 1978.